

Univerzita Hradec Králové

Přírodovědecká fakulta

Katedra fyziky

Disertační práce

2021

František Šeba

Univerzita Hradec Králové
Přírodovědecká fakulta
Katedra fyziky

Cellular automata and their potential in didactics of physics

Disertační práce

Autor: RNDr. František Šeba
Studijní program: Fyzika
Studijní obor: Didaktika fyziky
Školitel: Doc. Mgr. Milan Krbálek, Ph.D.

Prohlášení:

Prohlašuji, že jsem tuto disertační práci vypracoval pod vedením školitele samostatně a uvedl jsem všechny použité zdroje.

V Hradci Králové dne 20. 03. 2021

Poděkování:

Na tomto místě bych chtěl poděkovat svému školiteli doc. Mgr. Milanu Krbálkovi, Ph.D. za jeho podporu, vedení při studiu a cenné rady. Také bych chtěl velmi poděkovat své rodině a zejména své manželce Lence Šebové za nesmírnou trpělivost, kterou projevovala po celou dobu mého studia.

Anotace

ŠEBA, František. *Celulární automaty a jejich přínos v didaktice fyziky*. Hradec Králové: Přírodovědecká fakulta Univerzity Hradec Králové, 2021. 158 p. Disertační práce.

Disertační práce se zabývá celulárními automaty, zejména jejich schopností modelovat fyzikální systémy, a zkoumá možnost jejich aplikace v didaktice fyziky. Nejprve byla provedena rešerše na dané téma, na jejíž základě jsou v práci prezentovány informace o historii, vlastnostech a klasifikaci celulárních automatů. Pozornost byla věnována zejména vlastnosti celulárních automatů generovat extrémně komplexní chování, na základě velmi jednoduchých pravidel. Této velmi zajímavé vlastnosti celulárních automatů je využito k modelování některých složitých přírodních systémů, zatímco vlastní popis těchto systémů je realizován popisem jednoduchých zákonitostí, kterými se celulární automat řídí. Možnost za pomoci celulárních automatů studovat i nejsložitější systémy bez nutnosti použít komplexní matematický aparát byla rozpoznána jako přínosem pro didaktiku fyziky a tvoří vlastní základ této práce. Za účelem podpořit a demonstrovat tento koncept byla vytvořena celá řada modelů přírodních fyzikálních systémů, jejichž popis je vždy dán pouze jednoduchými pravidly souvisejícího celulárního automatu. Nakonec, za účelem dále demonstrovat potenciál celulárních automatů v didaktice fyziky, jsou v práci představeny výsledky současného výzkumu v oblasti fyziky dopravy, v jehož kontextu je v práci zdůrazněna schopnost celulárních automatů jednoduše popsat systém, který ještě nebyl do detailu poznán, a jež je v současnosti předmětem výzkumu.

Klíčová slova,

Cellular automata, didactics of physics, complex system modeling, system dynamics, freeway traffic, traffic gas models, Excel based modeling, number variance, super-chaotic statistics.

Annotation

ŠEBA, František. *Cellular automata and their potential in didactics of physics*. Hradec Králové: Faculty of science Univerzity Hradec Králové, 2021. 158 p. Dissertation thesis.

This thesis deals with the problem of cellular automata, especially with their ability to model physical systems, and explores their potential in didactics of physics. In order to understand the concept in detail, research on the topic was conducted, and based on this research, compiled information about the history, classification, function and typology of cellular automata is presented. Special focus was given to study the remarkable property of cellular automata to exhibit even the most complex behavior, while following only very basic and simple rules. This very special property of cellular automata is utilized to model some of the most complex systems occurring in nature, while the description of the system itself is still being given only by the basic rule set of the underlying cellular automaton. The ability to study such complex systems, while not having to rely on complex mathematics is understood to have a great potential in didactics of physics and is the fundament of this thesis. To support the presented concept, several models of highly complex physical systems are presented in this thesis while their rule-based description is always delivered in a simple sentence, or by utilizing only elementary visual schematics. Finally, to further highlight the potential of cellular automata in didactics of physics, some of the very recent research on physics of traffic is presented to highlight the remarkable ability of cellular automata to describe even not yet fully understood systems where scientific research is still ongoing.

Keywords

Cellular automata, didactics of physics, complex system modeling, system dynamics, freeway traffic, traffic gas models, Excel based modeling, number variance, super-chaotic statistics.

Contents

Introduction	7
1. Cellular automata description and history.....	8
1.1 Description of cellular automata.....	9
1.2 History of cellular automata	15
1.3 Classification, types and application of cellular automata.....	21
1.3.1 Classification of cellular automata	21
1.3.2 Types and application of cellular automata.....	23
2. Modelling of physical systems using cellular automata	28
2.1 Randomness in nature and cellular automata	29
2.1.1 Environment induced randomness.....	31
2.1.2 Randomness induced by initial conditions	32
2.1.3 Randomness intrinsically generated by a system	34
2.2 Continuity and discreteness in nature and cellular automata.....	37
2.3 Computational equivalence of natural and artificial systems.....	44
3. Potential of cellular automata in didactics of physics	50
3.1 Cellular automaton approach to model fluid flow	53
3.1.1 Introduction to fluid flow.....	53
3.1.2 Fluid flow simulation cellular automaton	55
4. Pilot didactical purpose cellular automaton models	59
4.1 Microsoft Excel as a cellular automaton programming interface	59
4.2 Ant simulator	61
4.2.1 Introduction to ants	61
4.2.2 Ant simulation cellular automaton	63
4.2.3 Examples of interesting ant simulator dynamics patterns.....	67
4.3 Flocking simulator	73

4.3.1	Introduction to flocking and swarm formation.....	74
4.3.2	Flocking simulation cellular automaton	74
4.3.3	Examples of interesting flocking simulator dynamics patterns	77
4.4	Freeway traffic simulator.....	80
4.4.1	Introduction to traffic flow modelling	80
4.4.2	Nagel-Schreckenberg model cellular automaton	81
4.4.3	Examples of interesting freeway traffic simulator dynamics patterns	83
4.5	Further simulator ideas and potential in didactics of other school subjects	88
4.5.1	Nuclear reaction simulation	88
4.5.2	Lightning strike simulator	90
4.5.3	Simulation of water boiling.....	92
4.5.4	Crystallization of water and snowflake formation.....	93
4.5.5	Fur pattern formation	95
4.5.6	Diffusion-limited aggregation	96
4.5.7	Cellular automata in didactics of computer science.....	97
5.	Cellular automata and the physics of traffic.....	99
5.1	Quantitative analysis of probabilistic dependencies in a thermal balanced traffic gas	100
5.1.1	Model description	101
5.1.2	Mathematical tools for quantitative analysis of probabilistic dependencies.....	105
5.1.2.1	Pearson's correlation coefficient.....	106
5.1.2.2	Number variance	108
5.1.2.3	Convolution perturbation	109
5.1.3	Potential in didactics of physics	111

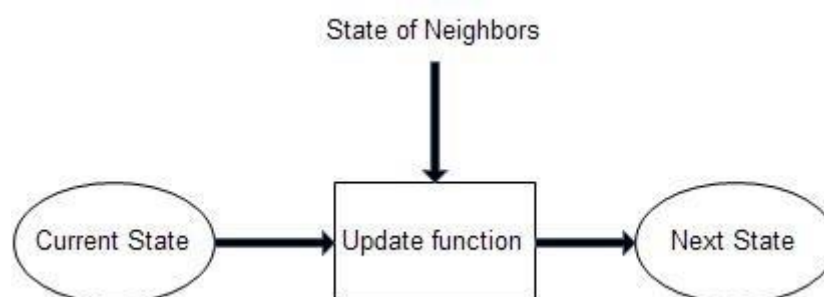
5.2	Traffic Flow Merging – Statistical and Numerical modeling of microstructure.....	113
5.2.1	Classical approach to traffic merging.....	114
5.2.2	Empirical observations of traffic merging and their statistical interpretations.....	115
5.2.2.1	Origin of the data.....	115
5.2.2.2	Macroscopic characteristics of a traffic merging systems.....	117
5.2.2.3	Microscopic characteristics of a traffic merging systems.....	119
5.2.2.4	Modeling traffic merging by utilizing a cellular automaton	124
5.3	Super-chaotic statistics in traffic flow.....	130
5.3.1	Origin of the data.....	130
5.3.2	The difference between the fast and the slow lane	133
5.3.3	Number variance of traffic flow	138
	Conclusion.....	142
	Bibliography.....	143

Introduction

The ability to teach well has been a challenge ever since John Amos Comenius and Wolfgang Ratke placed the very first fundamentals of what we today call didactics. This is especially true when one is concerned with teaching natural science, physics in particular. Traditionally, a mathematical approach to didactics of physics has been adopted for many years with great success. However successful this approach might be if applied in general, there still are systems in physics, which can't be easily addressed with this current approach, as the related mathematics is simply too complex. The aim of this thesis is to introduce a new kind of description mechanism for these systems, which could serve as a complementary didactical tool to the currently adopted mathematical approach. This description mechanism is based on cellular automata, especially their property to generate or mimic complex behavior. First of all, a general description of cellular automata will be given and a simple example of how a cellular automaton works will be presented. A brief history of the concept will be discussed to introduce how cellular automata were invented. After that, the potential of cellular automata in didactics of physics will be discussed in detail and several cellular-automaton-based models of physical systems will be explored. Each of these physical systems which will be modeled are especially difficult to educationally address through the standard mathematical approach to highlight the potential benefits of the cellular automaton approach. Finally, several models from current research on physics of traffic will be discussed to highlight, that the very same tools that can be utilized for the description of standard school subjects in didactics of physics can be in fact used to address not yet known and understood physical phenomena, further highlighting the potential of cellular automata in didactics of physics.

1. Cellular automata description and history

A cellular automaton is a mathematical idealization of a physical system, where space and time are discrete, and where all physical quantities can take only a finite set of discrete values [1]. It represents a discrete model of computation. A cellular automaton consists of a regular uniform grid (or array) of cells (usually infinite in extent), each of which have a finite number of possible states described by a discrete variable. The grid itself, can have any non-infinite number of dimensions. For each of the cells, a set of cells called “neighborhood” exists (typically, the neighborhood is the cell itself together with cells directly adjacent to it). The state of the cellular automaton at any point in time is defined by the individual discrete values of each cell. An initial state (the state of the cellular automaton at time zero) is created by assigning a discrete variable to each cell. A cellular automaton evolves in discrete time steps, where a new configuration of the cells is acquired by a simultaneous update of all cell states based on the values of variables of cells in their neighborhood, and based on a definite set of rules (typically mathematical functions) [1], [2]. Cellular automata can simulate a variety of real-world systems. They have found application in biology, physics, mathematics, social science, philosophy, computer science, art, technology, artificial intelligence and artificial life, catastrophe theory, chaos theory, complexity theory, cybernetics, dynamical system theory, evolution theory, nanotechnology, nonlinear dynamics, self-organization, statistical mechanics, traffic modeling and many others.



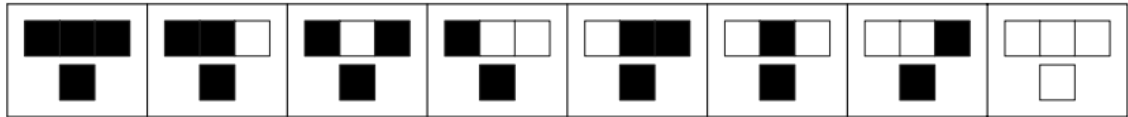
Picture 1. State transition chart of a general cellular automaton [2].

1.1 Description of cellular automata

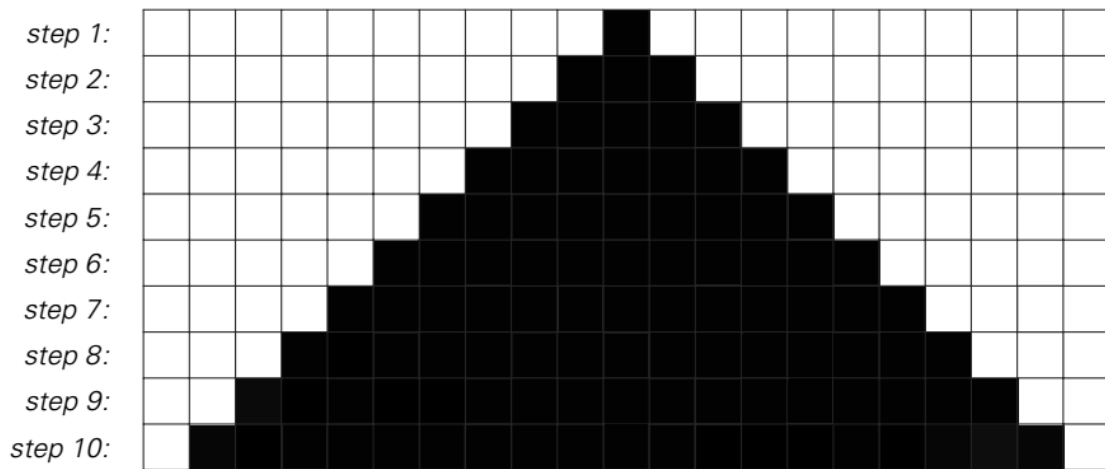
Before moving to a more detailed discussion about cellular automata, their classification and their properties, let us describe and demonstrate on a simple cellular automaton example what basic terms apply and what properties and behavior a cellular automaton may exhibit. For this purpose, we have chosen a one dimensional, two states cellular automaton (the rule 254 automaton described in [3]). This automaton lives in a universe represented by a line of cells, which stretches indefinitely in both directions (left and right). Each cell can have only one of two possible states (discrete numeric state represented by either “1” or “0”, or for better imagination by black and white color). Each cell has a neighborhood (simply the directly adjacent left and right cell, see picture 2). At time ($t = 0$), a state is assigned to each cell in the universe (in our example, only one cell will be black, all the others will be white). A set of definite rules describe, how a cell state can change with each step (what the new color of the cell will be) based on the colors of the cell’s neighborhood. For this specific case, the rule specifies (see picture 3) that a cell should be black in the next step, if the cell itself, or either of its neighbors is black in the previous step. In total, there are 8 different rules (8 possible transition possibilities) which can be listed in a look up table (this applies in general - all rules for each possible cellular automaton, no matter the complexity can be listed in a look up table, it is just more compact to define a sentence or a mathematical function, which can describe many possible states at once). A general feature of cellular automata is, that for most of them their evolution can be displayed in a visual way. In fact, for simple cellular automata (like the one in this example), not even a computer is necessary and a sheet of graph paper is sufficient. The graphical representation of the behavior of the first example cellular automaton (rule 254) can be seen in picture 4. As you can see, starting from a single black cell and applying rule 254 results in a simple growing pattern.



Picture 2. Graphical example a cells (visualized black) “neighborhood” (red colored cells) [3].



Picture 3. Graphical representation of the rule set (rule 254) used in the first example. A cell will have a black color in its next generation, if and only if it is black in the previous generation or at least one of its neighbors is black in the previous generation [3].

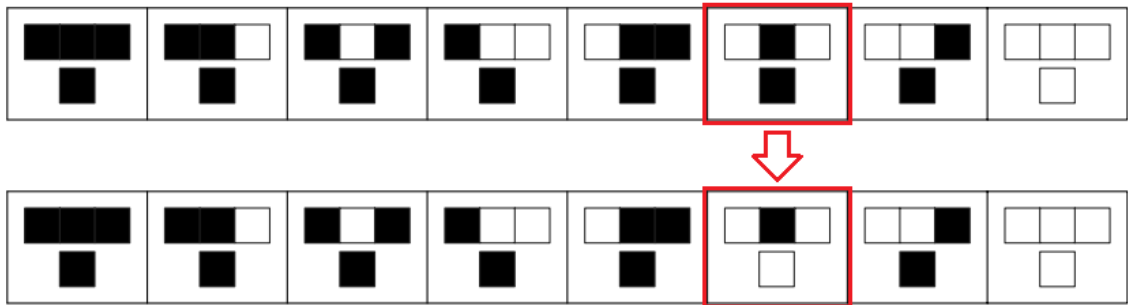


Picture 4. The first 10 steps of evolution of the first example cellular automaton (rule 254). The evolution exhibits a simple growth pattern. [3].

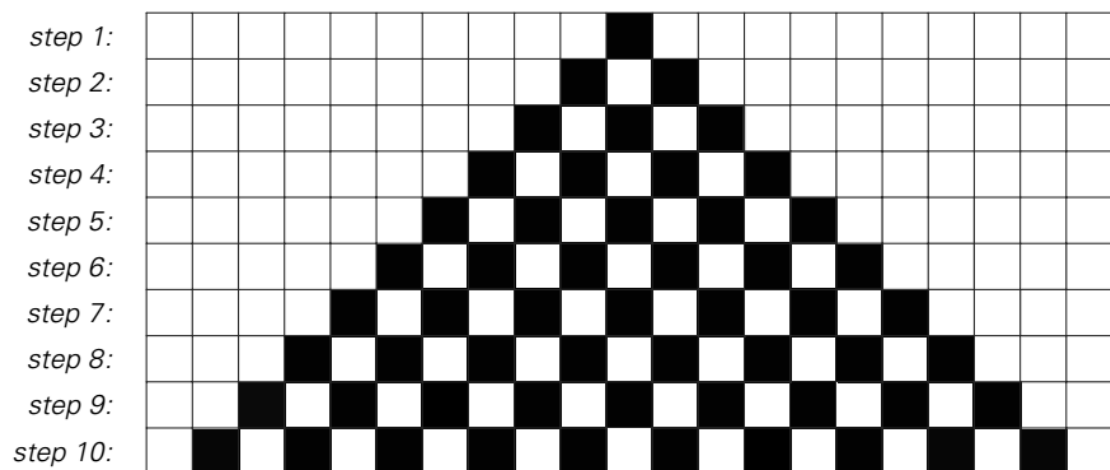
As a next example, let us investigate what happens, if we slightly modify the rule set. Let's say as a new rule, black cells for which both neighborhood cells have white color, will now be white instead of black in the next generation. The graphical representation of the rule modification can be seen in picture 5. As can be seen, even the initial conditions remained the same (still starting from a single black cell), just a slight modification of the cellular automaton rule results into a completely different pattern. Instead of a growing pattern, the new rule leads to a checkboard pattern, although the pattern again is very simple (see picture 6). One could come to the conclusion, that for such an easy automaton (only one dimensional and a maximum of 8 rules), all possible patterns which can be generated will be very simple, but surprisingly this is not the case. Let us consider yet another example. The rule set for this third example states, that a cell should be

black in the next generation if and only if one of the neighbor cells (but not both) is black in the previous generation. Again, the rule set is very simple, but the pattern the automaton now exhibits is not simple anymore (see picture 7 and picture 8). It seems, that the new rule (rule 90 as described in [3]) generates a pattern containing self-similar nested structures, with the overall pattern being much like a fractal. But even the pattern is not as simple as patterns from rule 254 and 250, it still is highly regular when observed on a larger scale. As a last example, let us explore, whether it is possible to generate even a more complex pattern, containing no, or only limited regularities. One could assume, that due to the simplicity of the underlying rules, the cellular automaton could never exhibit complex behavior, however this can be proven wrong. Some of the rules (rule 30 in particular), show very complex behavior. Rule 30 can be summarized as follows. If a cell and its right neighbor are white in the previous step, the cell will have the same color as the left neighbor in the previous step. Otherwise, it will have the opposite color. For better imagination, see picture 8 where rule 30 is visualized. The pattern generated by rule 30 can be observed in picture 10 (small scale) and picture 11 large scale. The remarkable complexity of the emerging pattern is fascinating. Also, it is unclear where such an irregularity and complexity comes from. The automaton started, as all the other examples, from a single black cell, and the underlying rules were also very simple. Yet, it could produce this extremely complex pattern. This is a fundamental phenomenon common to all cellular automata and is both strange as well as fascinating. The fact that even the underlying rules of a system (doesn't matter whether it is a cellular automaton or a natural system) are very simple and even though the starting conditions of that system are very simple, the system is still capable of producing behavior of extreme complexity. Nobody knows where this complexity comes from. I believe that it is possible to take advantage of this fact (without going deeper into detail of origin of the complexity) and utilize it to describe some of the most complex systems occurring in nature just by finding the underlying rules, without having to rely on complex mathematical descriptions. This possibility to describe a system without having to apply hard mathematical rigor can be advantageous in didactics, as it can open a completely new universe to students which do not have deep

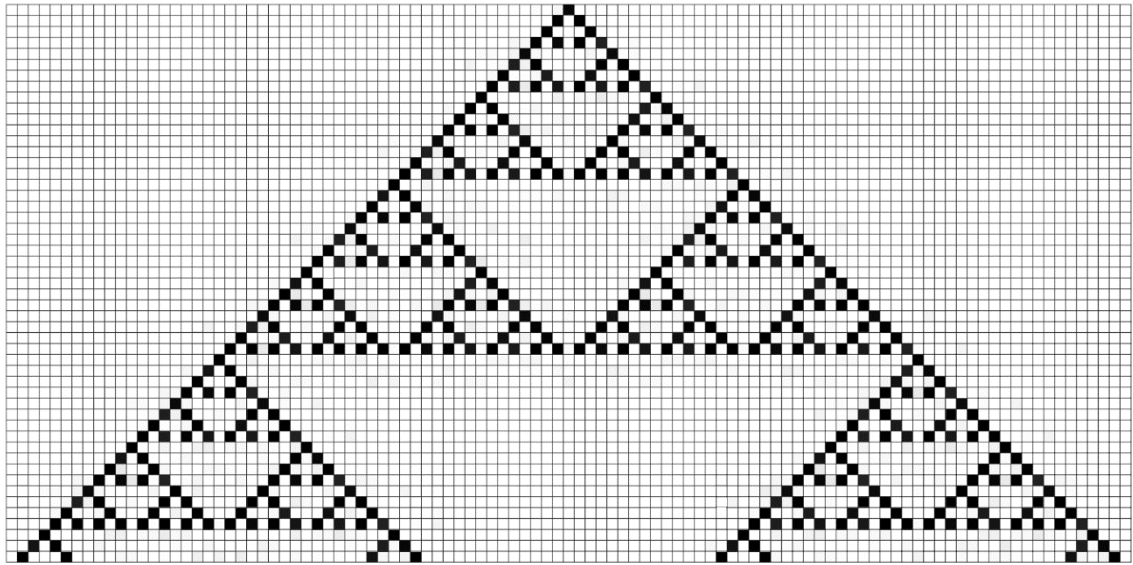
knowledge of mathematics, but yet would like to investigate the fascinating beauty of these complex natural systems.



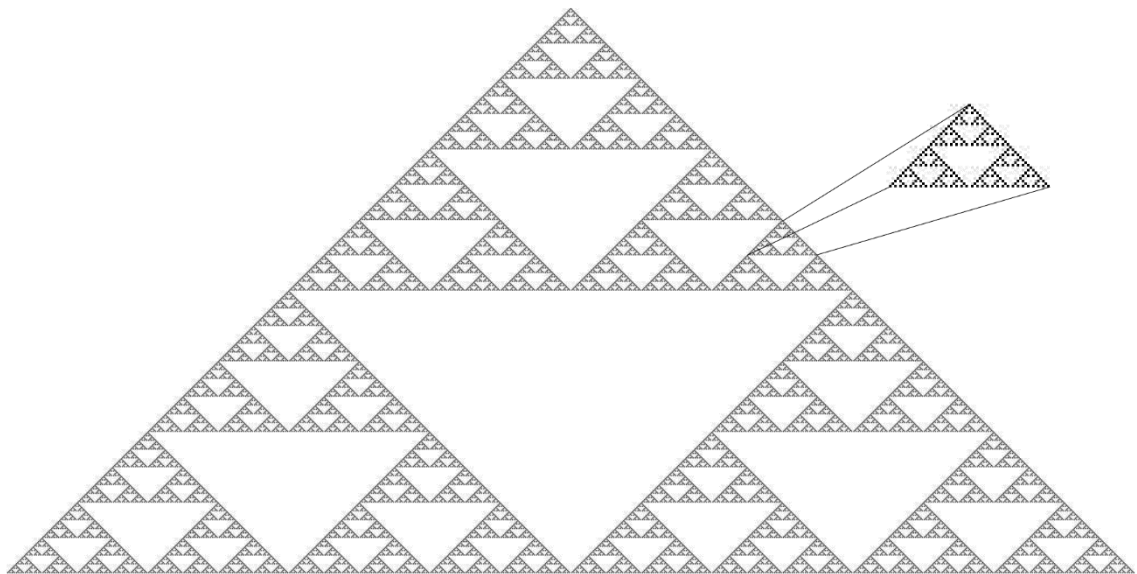
Picture 5. Graphical representation of the updated rule set (rule 250). The difference between the original rule set (rule 254 top row) and the new rule set (250 bottom row) is highlighted in red [3].



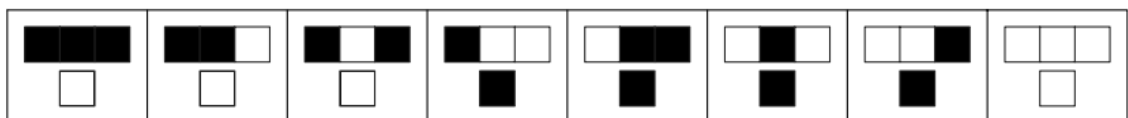
Picture 6. The first 10 steps of evolution of the modified rule example cellular automaton (rule 250). The evolution exhibits a checkboard pattern [3].



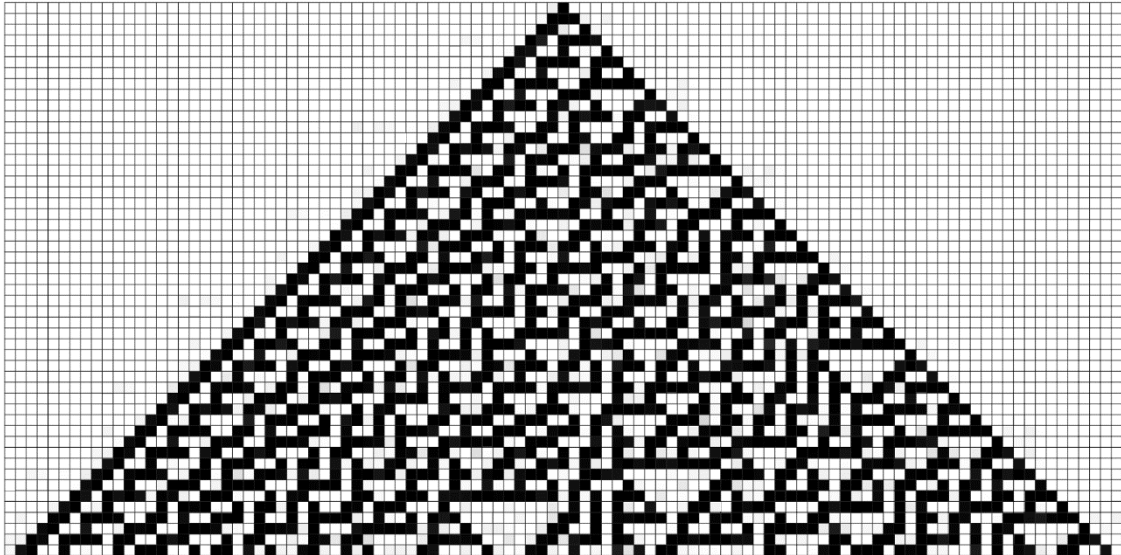
Picture 7. The result pattern of the rule 90 automaton displayed on a small-scale grid. The pattern is no longer simple and contains interesting triangle like nested structures [3].



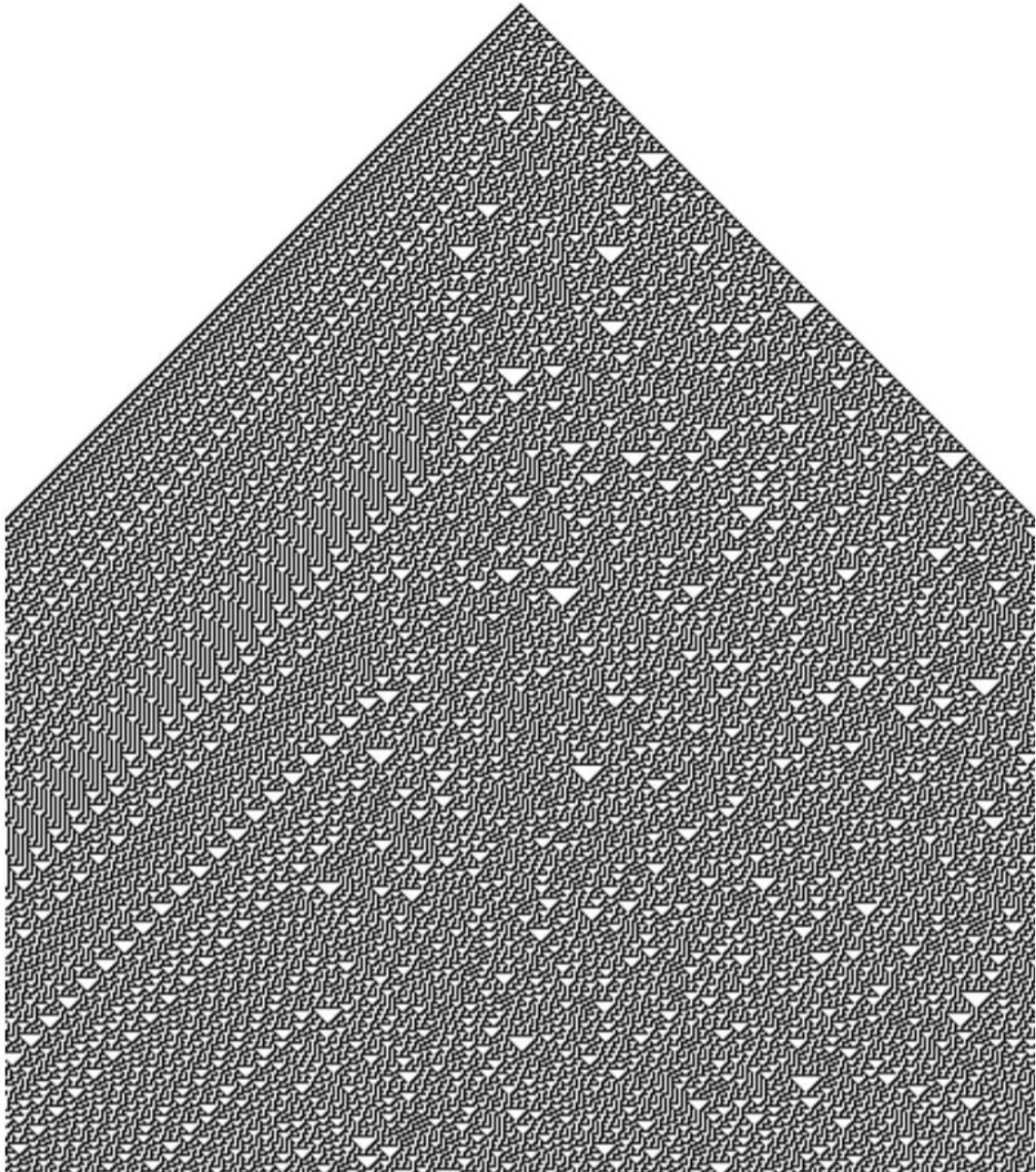
Picture 8. The result pattern of the rule 90 automaton displayed on a larger scale grid. The automaton exhibits a regular fractal like pattern [3].



Picture 9. Graphical representation of the final rule set (rule 30) [3].



Picture 10. The result pattern of the rule 30 automaton displayed on a small-scale grid. The pattern shows almost no overall regularity and seems random.



Picture 11. The result pattern of the rule 30 automaton displayed on a larger scale grid. The pattern is a result of five hundred automaton steps. The asymmetry of the left and right side of the pattern is a direct consequence of the asymmetry of the underlying rule set.

1.2 History of cellular automata

The history of cellular automata began at the Los Alamos National Laboratory (famous laboratory in the US, well known for its role in the Manhattan Project and World War II) in the late 1940's, and is closely related to the names Stanislaw Ulam

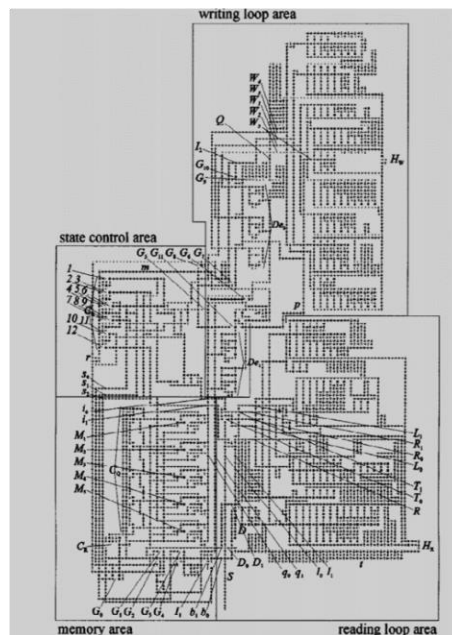
(1909-1984) and John von Neumann (1903-1957). Ulam was a mathematician, especially known for his contribution to pure and applied mathematics (set theory, topology, projective algebra, graph theory and combinatorics), famous for inventing the Monte Carlo computation method as well as co-inventing the hydrogen bomb (together with Edward Teller). Von Neumann was a physicist, computer scientist and mathematician (probably one of the best mathematicians of his time, who integrated both pure and applied science [4]). He made extensive contributions in many fields, including physics (quantum mechanics, hydrodynamics, statistical mechanics), economics (game theory), computer science (Von Neuman architecture, stochastic computing) and mathematics (operator algebra, geometry, topology, set theory). Together with Herman Goldstein he designed the architecture of first electronic computers.

In the late 1940's, one of the questions that John von Neumann was concerned with was the "*concept of complication*". In one of his papers [5] he pointed out, that while it is tempting to expect that when an automaton performs a certain operation, this operation must have a lower degree of complication than the automaton itself, thus if an automaton would have the ability of constructing another automaton, which again could construct another automaton, this construction sequence would show a complexity degeneration tendency. This however is in contradiction to what can be seen in nature. Living organisms can reproduce themselves without any decrease in complexity. On the top of that, enduring evolution makes the complexity of living organisms even grow. Could it be possible for a machine to produce another machine as complicated as itself? To answer this question, von Neuman suggested an automat consisting of a relatively low number of standardized parts, each of which has a specific function. This "catalogue" of parts is defined to be able to permit construction of wide variety of functions and mechanisms, to have sufficient axiomatic rigor to answer the question. Von Neuman was wondering, whether there exists an aggregate out of such parts, which, placed in a reservoir full of parts, could build other aggregates out of these parts, which are exactly same as the original one. Through applying Turing's theory of computing automata (Turing was a famous English logician, who could prove that a completely general description of any automata can be given in a finite number of words [6]), von Neumann was able to prove that building of

such an aggregate is feasible, the same way as it is feasible to build a completely general computation automat [5]. However, as much as it was theoretically possible to build such an aggregate of parts, the difficulty to actually build the aggregate, and the complexity and costs of a reservoir full of floating parts hindered von Neumann from actually building such an aggregate and reservoir to make his proof convincing [7]. Here is, where Ulam (who was working with von Neuman at the Los Alamos National Laboratory, and who may have already considered independently the same problem) suggested in 1951 to use a discrete system of cells, each of which could hold a finite number of states (representing individual machine parts), and each of which would have a finite number of connections to its neighbor cells. The state of the neighbors at time $t(n)$ would induce in a certain way the state of the cell in time $t(n + 1)$. Utilizing this concept, von Neuman was able to introduce in 1952 a description of the first self-reproducing cellular automaton. It was based on a two-dimensional lattice of cells, each of which had only a small neighborhood (only cell which touch are considered neighbors) and which could hold 29 different states. Von Neumann gave a proof, that a certain configuration could self-reproduce by designing a 200000-cell automat that could do so [3], [8]. This design is called von Neumann's universal constructor (see picture 13).



Picture 12. John von Neumann's and Stanislaw Ulam's photos from their Los Alamos ID batch. [9], [10]



Picture 13. John von Neumann’s universal constructor on a sheet of paper. [11]

Interesting is, that John von Neumann never published his findings. It seems, that once he solved the problem, he moved on to other things. Considering Ulam’s and von Neumann’s contribution to the invention of cellular automata, one can say, that the “cellular” portion comes from Ulam, and the “automata” portion from von Neumann [7].

In the 1960s, most of the scientific research on cellular automata was related to capturing the essence of self-reproduction by studying mathematical properties of cellular automata, and even more simple self-reproducing cellular automata were found. Also, it was found out, that cellular automata could be considered parallel computers, and detailed research (often similar to research on Turing machines) was conducted in this field [3]. At the end of 1960s, cellular automata were studied as a certain type of dynamic systems [12]. Although at that point in time, even though general-purpose computers could have been used to run cellular automata, they were mostly used for studying more traditional systems like partial differential equations. However, there were exceptions. Stanislaw Ulam used computers to produce what he called “recursively defined geometrical objects”, which were in fact objects evolving from black cells of simple 2D cellular automata. Ulam discovered, that very simple rules could generate a very complex pattern, and mentioned that this could have implications relevant to biology [3]. Another








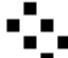






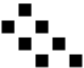


exception, and also a big event in the history of cellular automata was the discovery of a simple set of rules by John Conway, which he called “The Game of Life” and which can exhibit a wide range of complex behavior. The Game of Life went widely known in the early computing community thanks to Martin Gardner, which published its rules in a Scientific American article [13]. The rules of the game are remarkably simple. There is a universe consisting of a two-dimensional grid of square cells, which can have only one of two possible states – life or dead (or present and non-present). Every cell has its so called “neighborhood”, which consists of cells which are directly adjacent to it (vertically, horizontally or diagonally). The game evolves in discrete steps in time following 3 simple rules (which Conway called “genetic laws”):

- 1) **Survivals.** Every alive cell with two or three alive neighbors survives for the next generation.
- 2) **Deaths.** Every alive cell with four or more neighbors dies from overpopulation, every alive cell with one or zero neighbors dies from isolation.
- 3) **Births.** Every dead cell which has exactly three alive neighbors comes into life.

Very important is, that all the births and deaths need to happen simultaneously. They form a single generation, a single “move” in the game of life [13].

Even though the rules are quite simple, the possible evolution of individual patterns can be extremely complex. Some initial configurations, lead to emergence of complicated macroscopic patterns, other lead to spontaneous self-organization. There are configurations which will evolve chaotic behavior. Some configurations lead to formation of a universal constructor. Theoretically, any Turing machine can be formed through the game of life, as it is computationally universal [14], [15]. As an example, game of life can simulate a counter, it is possible to construct logic gates (like OR, AND, NOT, XOR). In fact, several programable computer architectures were implemented in the game of life [16]. It is even possible to

implement the famous Tetris game in game of life [17]. As can be seen, the game attracted a lot of attention through popularization by Martin Gardener, and extensive effort was put in finding specific initial conditions, that could show interesting behavior, however no real systematic scientific research was conducted, as the topic was more or less treated as recreation [3]. There was, however, also a completely opposite direction of thinking, taking cellular automata far more seriously.

<p>3P2.1 Blinker</p> 	<p>4.1 Block</p> 	<p>4.2 Tub</p> 	<p>5.1 Boat</p> 	<p>5P4H1Y1.1 Glider</p> 	<p>6.2 Ship</p> 
<p>6.4 Beehive</p> 	<p>6.5 Barge</p> 	<p>6P2.1 Toad</p> 	<p>6P2.2 Beacon</p> 	<p>7.2 Long Boat</p> 	<p>7.4 Loaf</p> 
<p>8.7 Pond</p> 	<p>8.8 Mango</p> 	<p>8.9 Long Barge</p> 	<p>12.41 Half-Fleet</p> 	<p>14.533 Half-Bakery</p> 	

Picture 14. Example of some basic patterns from Conway's Game of Life. Some patterns just stay still, others move or blink. A combination of multiple patterns may behave extremely complex [18].

Starting in 1969 with Konrad Suze (inventor of the first working computer – the Z3), who published his book *Calculating Space* [19], [20]. In his book he suggested, that the physical laws of the universe are discrete, and that basically all processes in the universe and even the universe itself could be an output of a deterministic computation of a giant cellular automaton [21]. Independently of Suze, Edward Fredkin also suggested that the Universe itself could be some sort of a highly parallel computational device, similar to a cellular automaton [22]. This was the foundation of a view today known as the simulation hypothesis, pancomputationalism and digital physics, which states that the whole universe,

inclusive earth and everything else, could in fact be a computer simulation [23], [21].

In 1981, Steven Wolfram began working on cellular automata. Wolfram was asking himself, why is it that complex patterns could arise in nature – apparently violating the second law of thermodynamics [3]. Wolfram published his first paper investigating cellular automata (rule 30 in particular) in 1983 [1]. In this paper, he already discussed in raw form several core ideas, that later lead to formulation of what Wolfram himself called “a new kind of science”, especially the idea that instead of using mathematical equations (a traditional approach to science), complex phenomena can be reproduced by simple cellular automata models. Twenty years later, Steven Wolfram published his life work in a book. Wolfram argues, that cellular automata have significance in all disciplines of science inclusive physics, and that sufficiently complicated automata could be capable of simulating any physical system, supposing there is an appropriate input and sufficient computational time. And exactly this approach (to use a cellular automaton instead of mathematical equations) to describe a physical system is the very fundament of this thesis. The approach to describe a (sometimes very) complex system, just by a simple set of rules of a cellular automaton, instead of hard mathematical rigor is of indisputable value in the didactics of physics, as it makes these systems available for study even for first grade and second grade students.

1.3 Classification, types and application of cellular automata

1.3.1 Classification of cellular automata

Even though the behavior and properties of cellular automata vary significantly (based on their underlying rules and initial configuration conditions), and the individual patterns yield by individual cellular automata always differ one from another, still the number of essentially different types of patterns is limited [3]. This was discovered by Steven Wolfram after he observed thousands and thousands of unique cellular automaton pattern evolutions. Wolfram argues, that based on the behavior and complexity of the observed patterns, almost all cellular

automata can be assigned to one of four basic classes. These classes are numbered 1-4, based on their growing complexity [3]:

- Class 1 – The cellular automaton behavior is very simple, and almost all initial configurations lead to a stable uniform final configuration, even if the initial configuration is random.
- Class 2 – The cellular automaton behavior is simple. Initial configurations may evolve into many different final configurations, but all of them are built just from a set of simple structures which either last forever, or repeat itself after only a small number of steps.
- Class 3 – The cellular automaton behavior is complicated. Initial configurations seem to evolve randomly or chaotically. Although small-scale structures always seem to form at certain steps, they later are consumed by the surrounding chaos.
- Class 4 – The cellular automaton behavior is complex. Initial configurations evolve in a mix of order and chaos. Simple local structures emerge and move around to interact with other local structures in a very complex way. Cellular automaton may be capable of universal computation.

Although there are some cellular automata, which can't be classified by this system (based on their properties, they may fall into several of the above-mentioned classes and are not clearly distinguishable), they remain more or less a quite unusual specialty as most of the cellular automata behavior falls into one of the four mentioned classes [3]. Interesting is to consider the overall activity of individual cellular automata classes. One would assume, that the activity of the cellular automaton is proportional to its complexity. However, this is not always the case. It is no surprise, that for class 1 and class 2 automata, the activity quickly slows down to states, where activity is no longer present. Highest activity is (counterintuitively) present in class 3 automata, and not in class 4. The reason for this is, that class 3 automata seem to have a lot of cells changing at every step. This

allows for maintaining a high degree of activity forever. Class 4 cellular automata, in contrast, are somewhere in the middle. They do not settle down like class 2 automata, so the activity does not cease to exist, but they also cannot maintain the high level of activity seen in class 3. This seems to be a general characteristic, seen for example also in other types of cellular automata [3].

1.3.2 Types and application of cellular automata

Cellular automata can be also categorized according to the rule logic they follow [2]. This of course makes it possible to define many custom categories - based on which subset of rule features the cellular automata share. Therefore, it is difficult to obtain a complete list of cellular automata types. The most famous types include [2]:

- **Linear cellular automata** - these automata utilize XOR logic. If cellular automaton rules contain only XOR logic (in general an affine transform of the type $x \rightarrow x \oplus c$ where \oplus represents the exclusive or as a generalization of addition in vector space or cellular automaton state space), and if these rules apply to every cell of the cellular automaton, then the automaton can be considered a linear cellular automaton. Typical applications of linear cellular automata include studies in graph theory, cryptographic applications and VLSI design and test [2], [24], [25].
- **Complement cellular automata** - these automata utilize XNOR logic (inversion of the above mentioned modulo-2 logic). The rule needs to apply to all cells of the automaton. Typically, it is utilized in cryptography [26].
- **Additive cellular automata** - these automata utilize a combination of the above mentioned XOR and XNOR logic. Their typical applications include VLSI design and testing, bit error correction, fault diagnosis, data encryption, image processing, and in many other real-life problems like. [2], [26], [27], [28].

- **Non-linear cellular automata** – in general utilize the AND/OR/NOT logic and are usually powerful pattern recognizers [2].
- **Uniform cellular automata** – If all cells follow the same rule, the automaton is considered uniform [2].
- **Hybrid cellular automata** – these automata are the opposite of uniform automata. If the automaton cells obey different rules, the automaton is considered hybrid. Typically, they are utilized in cryptography, but have many other applications including idealization of real physical systems like fluid dynamics, plasma physics, crystal growth, chemical systems, economics or traffic flow systems [29].
- **Null boundary and periodic boundary cellular automata** – If in a one-dimensional cellular automaton both first and last cell are considered neighbors, the automaton is considered a periodic boundary automaton. In the opposite case is considered a null boundary automaton. It needs to be mentioned, that this condition applies in any finite number of dimensions. Typical applications include pattern recognition, pattern generation and fault diagnosis [30].
- **Programmable cellular automata** – If a cellular automation contains some control logic, or some control signals, it is considered programmable. Based on the control signal state (which can dynamically change during the automations runtime), the automaton behavior can be directly controlled. Typically, such an automaton is utilized in parallel computing and parallel computer design [2].
- **Reversible cellular automata** – A cellular automation is considered reversible, if it can at any state return to its initial conditions. In these types of automata also reverse iteration is possible. Typically, the automaton has a rule for a standard step $t = t + 1$, and it has also a reverse rule to that rule

used for a backward step $t = t - 1$. In such a case, the automaton can eventually reach its initial state $t = 0$. Usual applications are related to cryptography [31].

- **Fuzzy cellular automata** – These automata utilize fuzzy logic. They are capable of pattern recognition and pattern classification. Their fundamental advantage is their ability to handle not only binary patterns, but also multi-cell state patterns including any rational number in $(0,1)$ [32].

As can be seen, the typology of cellular automata is wide, and so is the range of application, ranging from physics and mathematics through computer science and cryptography up to biology, material technology and traffic modeling and even up to philosophy and social science. The most famous and most utilized applications however can be summarized into the following four categories [3], [2]:

a) Parallel computing application category of cellular automata

In machine and computer design, after initial proof of concept prototypes, utilization of cellular automata was standardized already from the early 1980s. Typical application in computer and machine design include sorting machines, parallel multipliers, prime number sieves and parallel processors. Other applications consider cellular automata as fault resistant computing machines. For pattern recognition and image processing, two-dimensional cellular automata were put to a good use as well. A very interesting utilization of cellular automata are complex system simulators, which are based on high degree parallelism capability, which can lead to several orders magnitude higher simulation performance than standard computational systems, while still working at comparable costs. Also, cellular automaton based self-replicating structures can be used to solve NP-complete problems [2].

b) Physical, biological and chemical system modeling

A second major category of cellular automata utilization is the modeling of physical or biological systems, as an alternative approach to standard differential equations which are traditionally used for this purpose. Physical systems, where this approach was especially successful were all sort of systems where pattern formation occurs. The most prominent systems among them include modeling of hydrodynamical systems, diffusion systems, spin systems, and diverse forms of regular, dendritic or random growth pattern systems. Cellular automata are also utilized heavily in chemical system modeling, for example investigation on absorption and desorption phenomena, heterogenous catalysis, various diffusion systems modeling, solidification process and also phase transformation and alloy formation processes [2]. Although the modeling capabilities of cellular automata are undisputed (a throughout investigation on how deep cellular automation models can reflect physical reality will be delivered in the next chapter), no rigorous attempts were ever made to investigate their capabilities in didactics, as cellular automata themselves always remained a topic of scientific investigation, or were utilized as a scientific modeling or engineering application tools.

c) VLSI design and testing

A major application category of cellular automata is also VLSI design (very large-scale integration design – integrated circuit design). Typical use cases of cellular automata in VLSI design include implementation of multi-stage noise shaping cascades utilized in various VLSI application (whenever a parallel generation of random analog vectors is required), including analog encryption, secure communication, self-tests, stochastic neural networks and simulated annealing optimalization in machine learning [2].

d) Pattern recognition

The fourth and last major category of cellular automata application is related to pattern recognition. The solution is based on a syntactic evaluation approach,

where a finite cellular automaton works as a so called "*language acceptor*", where the initial configuration of the automaton is defined by an input string, and the acceptance of the input string is represented by a machine halt in a specific condition (specific automaton state). By acceptance or rejection of certain input strings, the automaton can be trained to recognize patterns. It is a fundamental approach in machine learning and now popularized in neural-network-approach-based pattern recognizers [2].

2. Modelling of physical systems using cellular automata

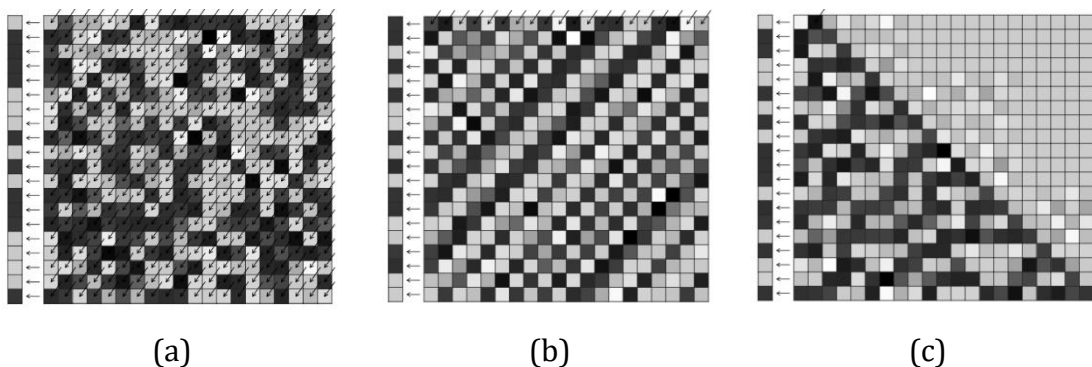
In the previous chapters a brief description and classification of cellular automata was given. It was shown that cellular automata found application in many fields. For a complete picture, also a historical context was provided. It was as well proven on a simple example, that such an elementary algorithm indeed can produce behavior of great complexity. But is the simple fact that cellular automata can produce complex behavior enough to make the conclusion they can also model physical systems or physical reality? This chapter will explore to what extend the behavior of cellular automata is similar to the behavior seen in nature, and will show that the very same fundamental concepts, that make natural systems behave as they do can in fact be found also in cellular automata. To see that there might be a common principle working in nature and in cellular automata, one can just have a look on the pictures of natural systems and pictures of simple program outputs described in [3]. When the detailed level structure is compared, there are obviously differences, but once both systems are observed from an overall level it is immediately visible that there are surprising similarities. As highlighted in [3], it is astonishing how often cellular automata show behavior that is almost identical to what can be seen in nature. That can't be a coincidence. It is suspected [3] that there might be a deep correspondence between cellular automata and natural systems, much deeper than a plain visual similarity. That is not only the case when natural systems and cellular automata are compared. The similarities apply also when two independent natural systems are compared. And although individual systems may be (and usually are) build up from completely different physical, biological or chemical components, their overall behavioral patterns are remarkably similar. This suggests, that a certain universality exists which is independent on the underlying rules, and that principally it does not matter whether the components of a system are real molecules or idealized cells [3]. It is this universality that makes cellular automata so much suitable as a tool in didactics of physics, as they do not merely reproduce natural patterns without a deeper context to the studied system. Instead, it directly touches the (highly

abstract) fundamentals of the system itself, but in a neat sandbox-like framework of simple rules, easily explainable to a student by plain words and traditional sentences. In its essence it is similar to mathematics heavily utilized in didactics of physics. Both tools (from didactical perspective) utilize a certain language as the building block of the interface between the student and the studied matter. But while mathematics uses formal language, the cellular automaton concept can utilize natural language, which I believe is (especially for basic or secondary school education) a major benefit. Obviously, when not considering the didactical aspect, the formal language of mathematics (besides some of its known issues [33]) is in many respects superior to almost all known tools to scientifically address a studied topic, however when the didactical aspect is taken into consideration, most of the students will not appreciate the high level of abstraction the mathematical axiomatic system is able to provide and in most cases in our current approach in didactics of physics, equation and formulas are memorized in a repetitive learning ritual rather than throughout studied to establish a deeper understanding of the fundamental underlying principles in the universe on the most abstract level. This chapter intends to highlight some of the basic phenomena seen in nature and show that they have a counterpart in cellular automata, to highlight the immense potential of cellular automata in modeling physical systems.

2.1 Randomness in nature and cellular automata

One of the fundamental phenomena seen in nature is randomness. There are many systems in nature exhibiting at least at some degree randomness and as seen in one of the examples in the previous chapters, cellular automata are perfectly capable of exhibiting such randomness too. Essentially, there are three main mechanisms how to introduce randomness to a system. First of all, randomness can be introduced to a system as part of its underlying rules. In case of a cellular automaton, this would correspond to an automaton rule choosing a cell color by random, in case of a natural system it would correspond to a random external environment continuously affecting the system [3]. A schematic representation in form of a cellular automaton can be found in picture 15 (a). A second possibility how

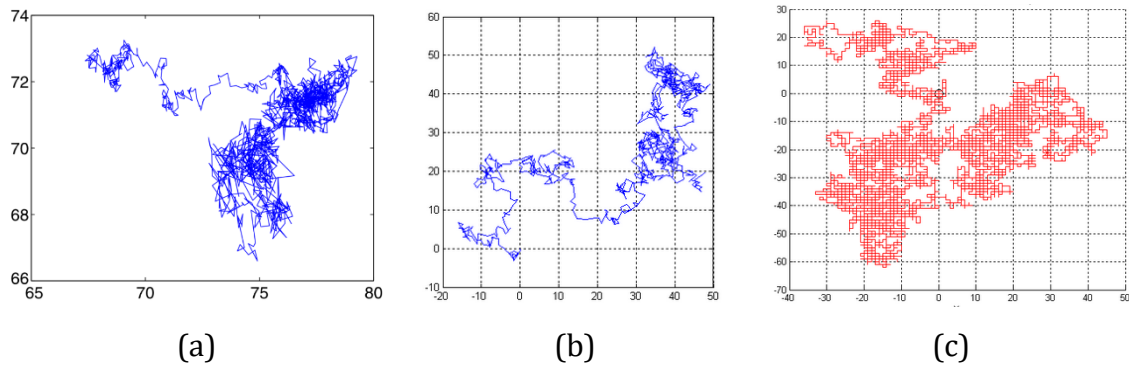
to introduce randomness to a system is to set it up in the initial configuration of the system. For a cellular automaton this could mean that the initial cell states of such an automaton are chosen randomly, but the rules the automaton will later follow do not involve randomness anymore. A similar concept applies also for a natural system. In this case, all the randomness in the system is a function of the randomness already present in the systems initial configuration. The concept is presented in picture 15 (b). Both the first and the second mechanism assume, that initially there is no randomness present in the system and that it is introduced from the outside of the system (either initially, or continuously). In both cases, no conclusion can be made about the real origin of the randomness. There is a third possible mechanism of how randomness can enter a system, and it is in fact responsible for the majority of randomness seen in natural systems. The randomness can simply emerge as a product of individual system parts interaction as shown in picture 15 (c). This emergence is a fundamental property of complex systems and both natural systems as well as cellular automata are known to show emergence occurrence as their inherent aspect [34]. This shows a deep correspondence between natural systems and cellular automata, which reaches far beyond simple visual similarity. All three sources of randomness in a system will be studied deeper in the corresponding chapters.



Picture 15. Schematic examples of how randomness may occur in a system. The randomness can be a result of external environmental influence where each cell (or component) of a system is continuously influenced by an external random input (a), it can be a result of initial random configuration of a system (b) or it can emerge as a property of the system itself from individual system part interaction (c) [3].

2.1.1 Environment induced randomness

As discussed in the previous chapter, randomness of any specific system may be a result of continuous interaction of that particular system with its environment. A classic example of such a system is the notoriously known Brownian motion. It is a natural phenomenon occurring in a system where particles are submerged in a certain medium (for example gas or liquid) which causes these particles to exhibit random motion, and was first described by the biologist Robert Brown in 1827 while observing a pollen immersed in water through his microscope [35]. At that time, nobody could explain the origin of this phenomenon, and it was the physicist Albert Einstein who could explain more than 80 years later the random walk like motion of pollen through continuous interaction with the surrounding water molecules [36]. It is an excellent example of how the surrounding environment can induce randomness (in this particular case originating from physical properties of the underlying thermodynamic temperature) in a system. In a two dimensional, two states cellular automaton analogy of the described Brownian motion system one of the cells in the automaton's von Neumann neighborhood (also called 4-neighborhood) would be randomly chosen to change its state based on a simple (non-random) rule set. The random choosing of a neighboring cell simulates the random influence of the external environment. For comparison see picture 16 (a)-(c). Most left picture (a) is a camera-traced real system particle trajectory captured by special video imaging technology (see [37] for reference). Middle picture (b) shows a cellular automaton approach. Right picture (c) shows the extremely simplified cellular automaton analogy described above. As you can see, the real physical system (a) and the cellular automaton approach (b) are near-identical. Even the simplest cellular automaton case (c) shows patterns very similar to a real physical system.

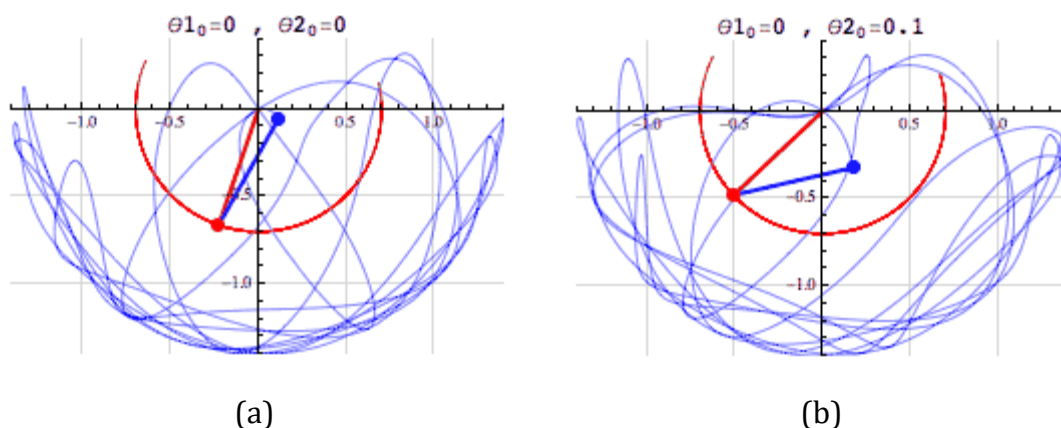


Picture 16. (a) - Real Brownian motion of an of 3T6 mouse fibro-blast cells endosome containing fluorescent Dil-LDL capture by a feature point tracking technology described in [37]. (b) and (c) show patterns generated by a cellular automaton approach [38].

2.1.2 Randomness induced by initial conditions

A second mechanism responsible for random behavior of systems is the randomness coming from initial system conditions. This topic is heavily studied by chaos theory and in principle applies to systems, that although being deterministic by nature are very sensitive to small variations in their starting conditions. Even an infinitesimally small variation in the systems initial configuration might result in a dramatical difference in its later state. A very famous metaphor mentioned in correspondence with chaos theory is the so called “butterfly effect” introduced by Edward Lorenz during his study of weather prediction models [39]. The metaphor mentions, that theoretically just a small butterfly flapping its wings might create tiny changes in the atmosphere, that could cascade and result into a tornado on the other side of the world. A simpler everyday example of how tiny changes in initial conditions of a system can affect the behavior and resulting state of a system can be found in dice games. Consider a well-known dice game called “craps”. In this game, players (called “shooters”) usually roll two dices in a way, that the throw is powerful enough to hit the farther back wall of the playing table. Theoretically, if a player would throw the dices two times with exactly the same initial position, strength, hand rotation, hand height and with all other throw parameters being exactly the same, the dices should show exactly the same result. Practically this not even close to possible, as no human being is able to control the throw in such a

precise manner and there will always be a slight difference in initial throw conditions. These tiny changes in the initial conditions can result in completely different outcomes of the throws in a complex way and such throws are considered uniformly random. There are many other physical systems showing this kind of initially introduced randomness, among them some of the most prominent being fluid flow, stock market, road traffic, double rod pendulum or the famous three body problem. A cellular automaton analogy of randomness induced by initial conditions is for example a one-dimensional cellular automaton with a neighborhood equal to the neighborhood described in picture 2 in chapter 1.1. The initial state of the automaton is generated randomly, with each cell having a certain probability to have state 0 (black cell). That means the initial conditions are completely random. After that, for each step of the automaton the cells are updated by an elementary rule - to change a cell to have black color only if its right cell has also a black color. The right cell is always set to have white color. In such a way, all black cells are shifted one cell to the left in each step. This update is completely deterministic and one can easily know the automaton state after arbitrary many steps. The black cells distribution though remains random as in the initial automaton state and is a result of the initial randomness propagating step after step through the automaton evolution.

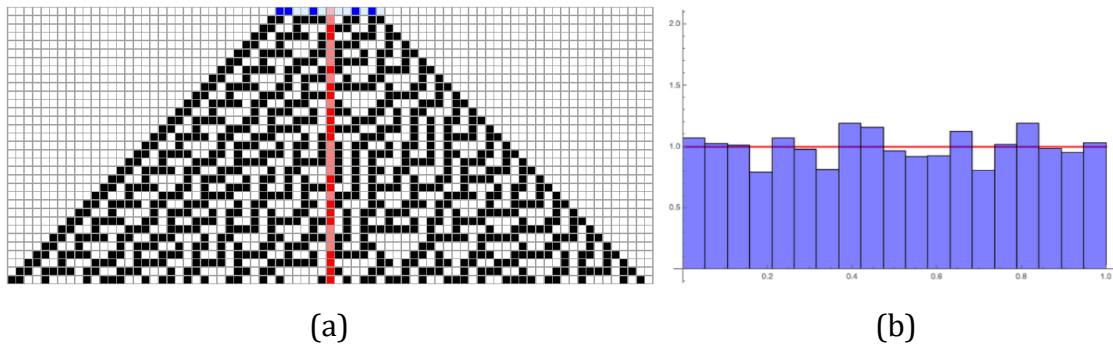


Picture 17. Example of randomness induced by initial conditions in a double rod pendulum system. The randomness is based on extreme sensitivity of a system to its initial conditions. Picture (a) and (b) show two separate double rod pendulum systems, where one system differs from the other only by an extremely small displacement of the second rod (displacement of only 0.1 rad). Even though the

initial conditions are nearly the same and both systems follow the same physical rules, each rod system generates a completely different trajectory.

2.1.3 Randomness intrinsically generated by a system

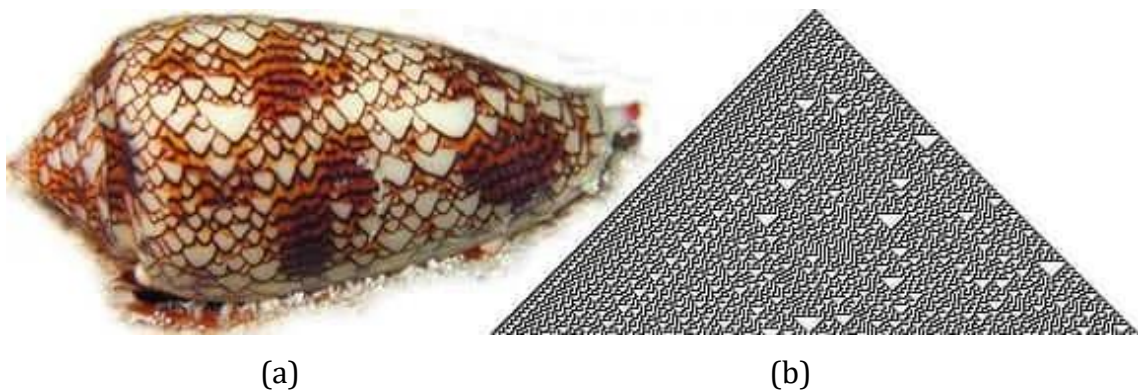
In the two previous chapters, two sources of randomness were discussed. Both had something in common. They described sources of randomness that essentially came from the outside of the system. Although in such a case a system based on its external random input (either continuous input or set up in its initial conditions) can show random behavior, it never can generate randomness by itself. This chapter will show that there are physical and artificial systems, that can generate randomness intrinsically, without utilizing external environment as a source for randomness. It will be shown that such a system does not necessarily need to be extremely complex and have sophisticated rules. In fact, a system might be (counterintuitively) extremely simple, working only with elementary rules, yet it still can generate randomness. A good example is the cellular automaton based on rule 30 described in [3] and show in pictures 10 and 11 in chapter 1.1. Even though the overall picture shows some regularities (for example stripe-like patterns to the left of the picture), if one considers only the middle cell of the automaton for each step (an array of cells going from top to bottom as seen schematically in picture 18 – a) and checks the color distribution in this array of cells (highlighted in red), the overall pattern is distributed uniformly random as seen in picture 18 (b) [40], [41]. In fact, the algorithm is utilized as a random number generator in the famous Wolfram Mathematica software [3].



Picture 18. Uniform random numbers generated by the rule 30 cellular automaton described in [3]. Left picture (a) shows a schematic representation of how the automaton intrinsically generates a uniformly random cell distribution (red cell array). Blue cells act as the seed for the generator and different seeds will yield different uniformly distributed cell sequences [40]. Right picture (b) compares the distribution generated by the rule 30 cellular automaton (blue bars) with the continuous uniform distribution (red line) [41].

As discussed in [3], the intrinsic generation of randomness might be the major source of randomness seen in natural system. This does not mean that external environment sources or initial configuration sources of randomness do not contribute to randomness in nature. But whenever there is a large amount of randomness generated in a natural system in a short time, intrinsic source of randomness is most likely the origin. As mentioned in the previous chapters, randomization of initial conditions can lead to a certain level of randomness in a system, but practically there is a limit to the amount of chaos (in the stochastic sense) that this source can contribute. During the systems evolution no additional randomness is added, and therefore it maintains certain limits imposed initially. Also, a system can be continuously affected by surrounding environmental noise. The issue with this source of randomness however is, that it can take a lot of time to reach a certain level of randomness, as the system does not contribute any portion of randomness internally. Therefore, the simplest way how to get a larger level of randomness fast is the intrinsic generation of randomness, especially with increasing system complexity, as the systems complexity has a dampening effect on the environmental induced randomness, but has an amplification effect on intrinsic randomness generation due to its inherent emergent behavior ability which in certain sense is a function of the systems complexity. And indeed, nature

contains many systems on all scale levels, which show intrinsic randomness generation, and among them there are even systems directly resembling cellular automaton behavior (see picture 19 as an example). Examples range from atomic scale physics, where the uncertainty principle guaranties an intrinsic source of randomness [42], through single cell living organisms - where intrinsic noise in biochemical processes in bacteria can deliver an evolutionary advantage [43], up to self-generated variability in decision making in higher organisms [44].



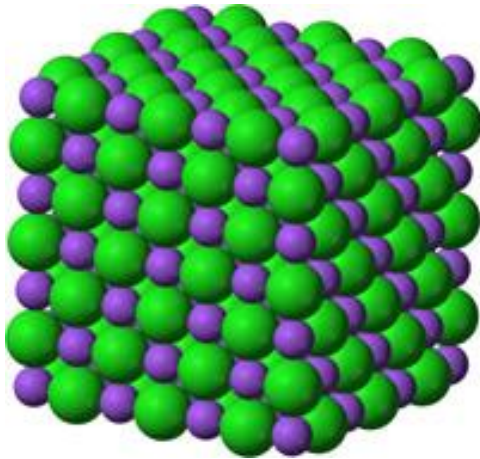
Picture 19. Comparison between the rule 30 cellular automaton output (b) and a shell of a sea snail of the species *Conus textile* [45]. The remarkable similarity is no coincidence. The snail grows (like a one-dimensional cellular automaton) one layer (line) of cells at a time. The cell color depends on interaction between neighboring pigment cells (similar to an automaton rule where a color of the cell is defined by its neighborhood state). It is an impressive example of how general principles yield - independently of the way how they are implemented (may it be artificially through a computer algorithm or naturally through a biological mechanisms) - similar patterns, further highlighting the deep correspondence between cellular automata and natural systems. Note, that the random like snail texture draws its randomness intrinsically through complex interaction between the snail's tissue elements.

As a final conclusion of this chapter, it needs to be noted, that both physical systems and cellular automata are perfectly capable of exhibiting random behavior. Furthermore, it is clear that both utilize the very same three mechanisms to do so. This shows that there is a deep correspondence between cellular automata and nature, which suggests that cellular automata resemble physical

reality on a far deeper level than it would be primarily expected. They do not just visually look alike, they share the very same fundamental principles (at least from randomness and random behavior perspective – but it will be shown later that in many other aspects), that make the systems behave like they do.

2.2 Continuity and discreteness in nature and cellular automata

Another fundamental concept in modeling physical reality is its apparent continuity. Many natural systems seem to exhibit behavior that is in many respects smooth and continuous (although many others exhibit discrete behavior as will be discussed later). So why should an artificial system like a cellular automaton, which features discrete elements (cells), be able to model a natural system with continuous behavior? The central point here is, that natural systems themselves can look on a microscopical level quite discrete (matter consists of discrete elements – atoms and molecules), but when looking on a large enough sample, the behavior can look smooth and continuous. An example is water. On microscopical level it's made up of molecules, but observed from a larger distance, it seems like a continuous fluid. Considering this example, it is completely plausible that also an artificial system (cellular automaton), which is discrete on a microscopic level, could exhibit continuous behavior when observed on a large enough scale or from a far enough distance. A fundamental question is, why systems consisting of discrete elements can have continuous behavior. And as described in [3], the key element seems to be randomness. Without randomness, a systems macroscopic structure in many aspects resembles its microscopic arrangement, like for example in case of crystals. In a single crystal, atoms are arranged near perfectly periodically and this order is reflected in the crystals macroscopic structure as seen in picture 20.



(a)

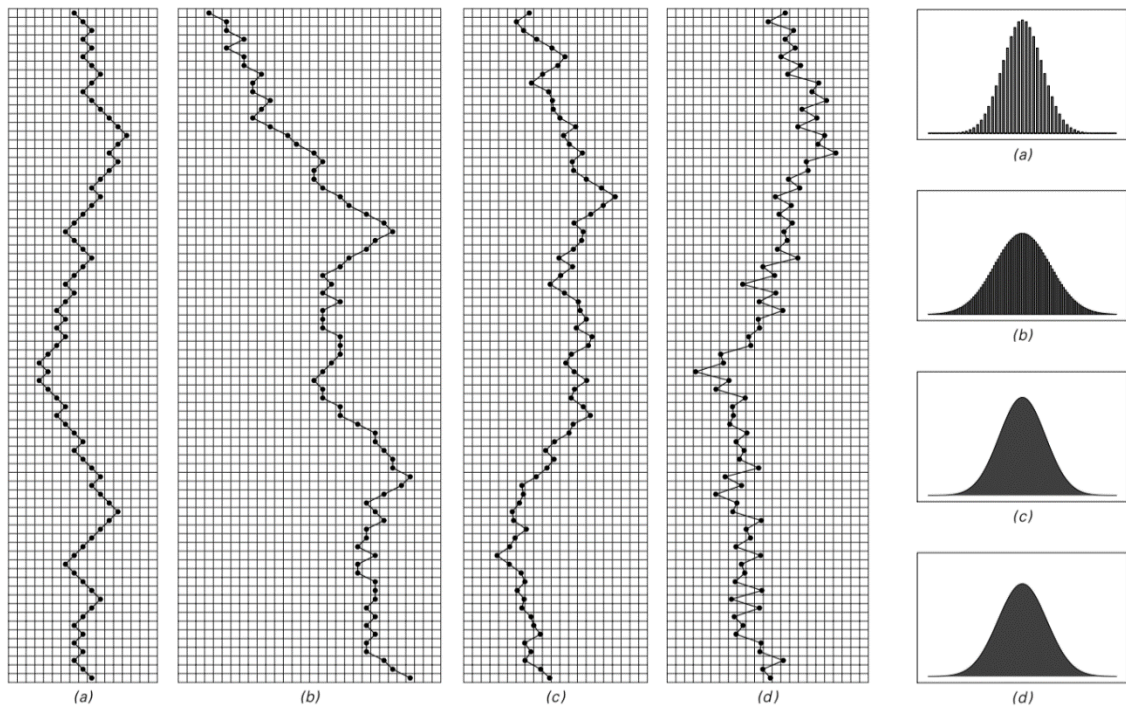


(b)

Picture 20. Microscopic and macroscopic structure of a halite (NaCl) crystal. The perfectly periodical cubic arrangement of atoms (a) [46], is reflected in the macroscopic structure of the crystal (b) [47].

But once randomness is present in a system, it tends to average out these microscopic arrangements, being able to smoothen out any traces of discreteness, so the final result might look continuous. This seems to apply independently of the systems underlying rules and independent of the system being an artificial cellular automaton, or a real physical system. To demonstrate this concept, imagine four one-dimensional cellular automation particle systems, where a particle exhibits a random walk-like motion (see picture 21 for reference). Each step, the particle can move randomly to the left or to the right. How exactly (how many steps to the left or to the right) this random movement is done depends on internal automaton rules (each of these four automatons have a different though still random movement rule). Independently of what automaton is observed, when considering just one discrete particle, it will exhibit its random-walk motion and end in a certain discrete position. But if one does not look at the individual particle positions (microscopic view), but rather takes into consideration the overall particle distribution after many independent runs of the automaton (macroscopic view), it can be immediately noticed that the resulting distribution is continuous and smooth. The randomness seems to completely wash away the microscopic details of the automaton and that despite the difference in each automatons rule set. In this particular random walk case (but in general this applies for many similar systems and for a wide range of individual microscopic structures and

underlying system rules), the resulting distribution will always be the so-called Gaussian distribution as suggested by the Central Limit theorem [3]. Similar systems can also be found in the physical world. An excellent example is the famous Galton board [48], which is vertical board consisting of rows of pegs and equally sized bins (and illustration can be found on picture 22). A large number of small beads are dropped from the above and bounce either left or right as they hit the pegs. Finally, dependent on the random path the beads have chosen, they land in one of the collecting bins at the bottom of the board. The number of beads in each bin (the height of the accumulated beads in each bin) approximates the gaussian distribution. Finally, it needs to be said that the resulting distribution does not necessarily need to be a Gaussian distribution. Dependent on the internal automaton or physical system structure, the smooth behavior and the resembled distribution might be any possible distribution. In natural systems the most famous distributions include the Poisson distribution, log-normal distributions, exponential and gamma distributions, uniform distributions, power laws, binominal distribution and even some discrete distributions [49]. All these smooth macroscopic patterns however are a result of the underlying interactions of many hidden small-scale discrete structures, and on top of that it does not even need to be a natural system at all as was demonstrated in [3].



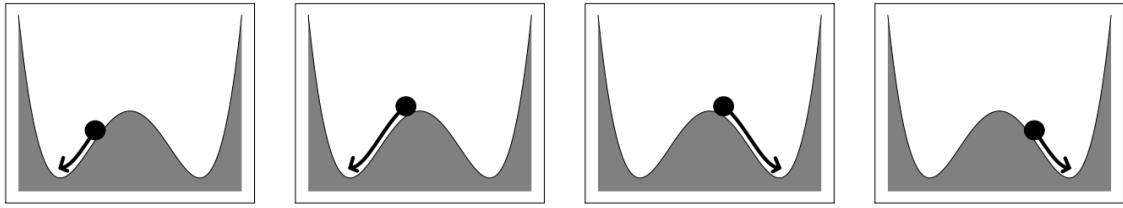
Picture 21. Four random walk one dimensional cellular automata. Each automaton has a different underlying rule for each step. In case (a), a particle can move one position to the left or to the right (chosen by random). In case (b), it can move either 0 or 1 or 2 to the left or to the right (chosen randomly). In case (c), it can move either 0 or 1 step to the left or to the right, and in case (d) it alternates by moving to the left or to the right. As can be seen, independently of the rules, the resembled distribution will always be a Gaussian distribution [3].



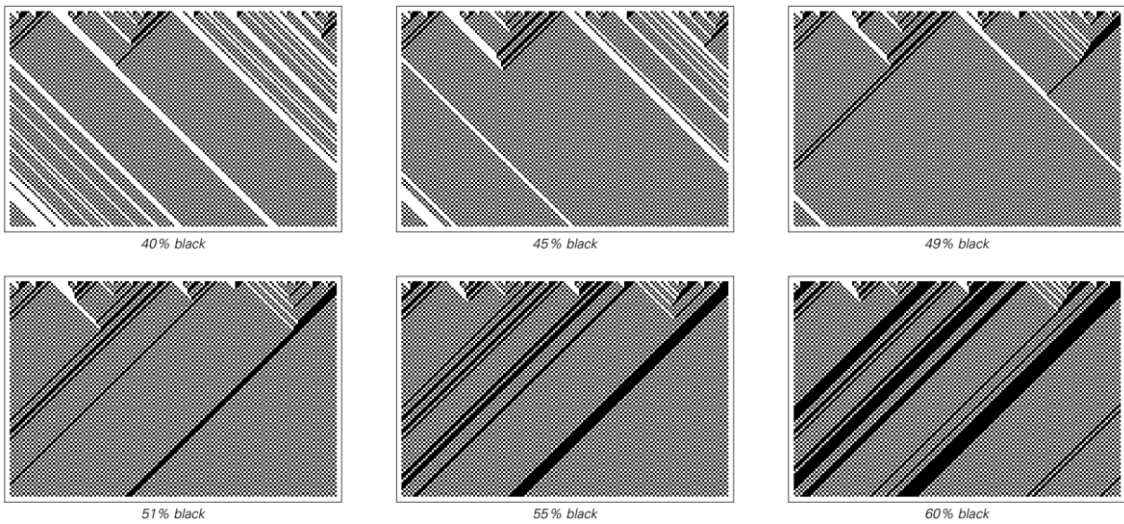
Picture 22. Example of a Galton board. The accumulated beads in the bins approximate the bell curve demonstrating the central limit theorem. [48]

But what about discreteness in nature and cellular automata? Alternative to the above-mentioned continuity coming from discrete structure, one needs also to consider that there are many systems in nature showing discrete behavior. A natural question arises in this context. If there is a possibility for a discrete system to show continuous behavior, is it also possible for a continuous system to show discrete behavior? And in deed that seems to be the case [3]. Many natural systems (even systems showing otherwise complex behavior) show at some level discrete behavior. A classic example is boiling water. When some water is taken, and its temperature is slowly but continuously increased (let's say starting from 10°C). First of all, not much happens. The water just gets hotter and hotter. But when the temperature of 100°C is reached, suddenly a sharp discrete transition occurs, and

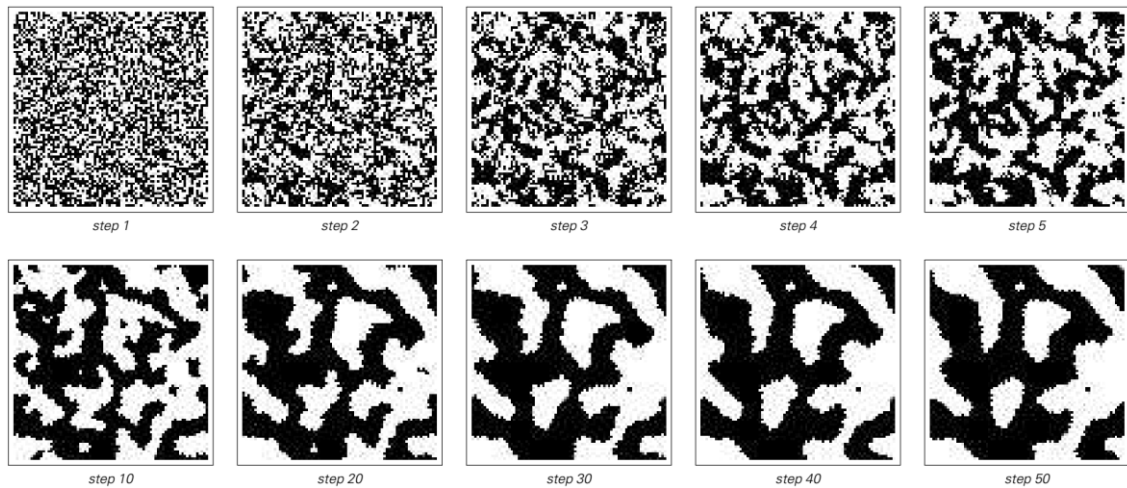
all the water is transformed into steam. Many other systems with otherwise continuous changes exhibit this sort of discrete transition behaviour. Some systems (traditionally gradient based systems) can lead to formation of discrete patterns (an example is a zebra or a tiger hide, where continuous interaction of individual pigment cells can lead to very discrete, sharp colour transition looking patterns). Yet another example of a simple physical system exhibiting sharp state transition (based on continuous change in initial conditions) is a ball on a wavy surface (see picture 23). When a ball starts to the left of the central hump, it will always roll towards the left-hand minimum, however if the initial starting position is changed continuously and the ball passes the top of the hump, suddenly the ball does not roll to the left-hand minimum anymore, but rolls to the right-hand minimum instead. A discrete transition in the systems behaviour occurs. Even though the mathematical equation which describes this system is very smooth and continuous, the behavior itself is essentially discrete [3]. Cellular automata can also exhibit such sharp transition behavior, even the variation of their initial condition is smooth and continuous. As an example, see picture 24. Until a certain threshold in black cell density is reached (very similar to the hump and ball example previously mentioned) the automaton produces only white stripes. However, once the density passes the 50% black cell threshold, only black stripes survive. As can be seen this cellular automaton is able to exhibit the sharp discrete transition behavior seen so often in natural systems. The automaton shown in picture 24 (based on rule 184 as described in [3]) is not some special case. Many other cellular automata of diverse properties are able to exhibit such sharp discrete behavior. A particularly interesting example can be seen on picture 25. The two-dimensional automaton used to generate this picture is able to produce (within several automaton steps only) patterns with continuous (but sharply separated) boundaries. Similar patterns are often found in nature in animal fur pigmentation.



Picture 23. A system of a ball and wavy surface. When the initial ball position is anywhere to the left of the central hump, it will always roll to the left. But once the initial ball position is anywhere to the right of the central hump, it will always roll to the right. Even if the change in initial ball position is continuous and smooth, eventually a sharp and discrete transition occurs [3].



Picture 24. A one-dimensional cellular automaton based on rule 184. The automaton shows discrete change of behavior based on continuous change of initial automaton conditions. After the number of black cells in the initial configuration reaches more than 50% off all cells, the automaton makes a sharp transition and show different behavior [3].



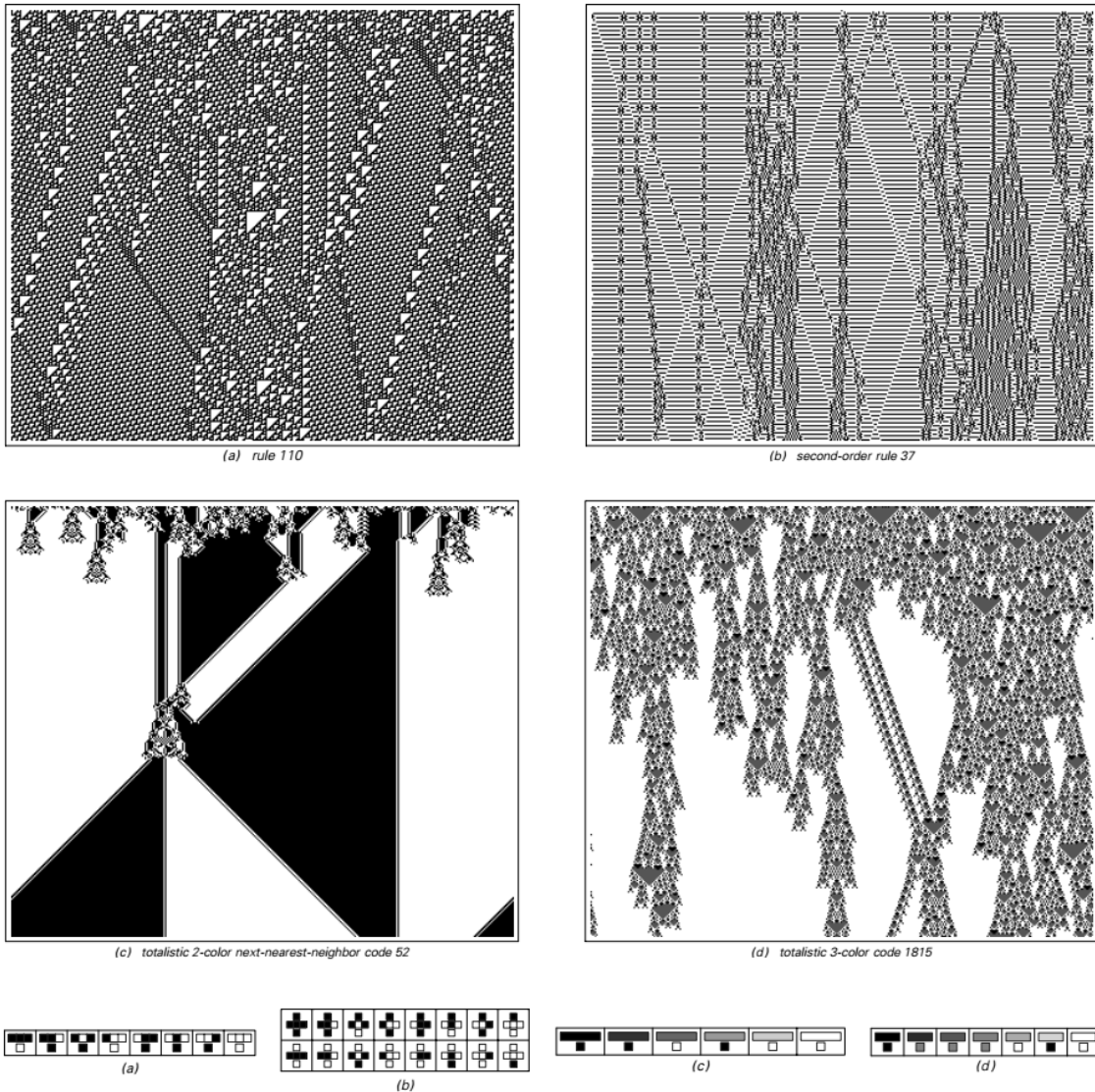
Picture 25. A two-dimensional cellular automaton which starts from a random initial condition. The rule set states that a cell in the next generation will have a white color, if there are less than 4 black cells in its neighborhood (diagonal cells included) otherwise it will have a black color. After only a small number of steps, continuous sharp borders between black and white picture parts arise. Although the border shape is smooth, the transition from one side of the border to the other is sharp [3].

As was discussed above, there is a remarkable correspondence between real physical systems and cellular automata also when it comes to the discreteness and/or continuity of the systems behavior point of view. It again shows how deeply cellular automata can resemble a real system, further strengthening the assumption that there is a deeper natural law acting on both cellular automaton as well as on a real system in nature, which is the real reason why they look so much alike, rather than just coincidentally look similar on a mere visual level. Therefore, the cellular automaton approach to modeling physical reality has a great potential, as both the modeled system as well as the artificial model in fact share common fundament.

2.3 Computational equivalence of natural and artificial systems

As was already discussed in chapters 1.2 and 1.3 but ultimately mentioned in [6] and [3], there are certain cellular automata (or Turing machines in general)

capable of universal computation. As a matter of fact, these automata or these Turing machines are not only able to compute and solve a certain specific problem described by their initial programming or configuration. They can be used to simulate and compute literally any other cellular automaton or Turing machine. This special property of automata is often referred to as computational universality. What's really interesting is, that such a universal automaton does not necessarily need to be extremely complex in configuration or rule set. In fact, some of the most basic automatons (like for example the game of life automaton with only a two-dimensional universe, two possible cell states, and with three basic rules) are already capable of universal computation, as was demonstrated in [14], [15], [16]. There are even one-dimensional cellular automata that are computationally universal, like for example the rule 110 cellular automaton described in [3]. It seems that universality is not some think uncommon in cellular automata, and especially class 4 automata are often regarded as universal. Four examples of class 4 automata can be found on picture 26.

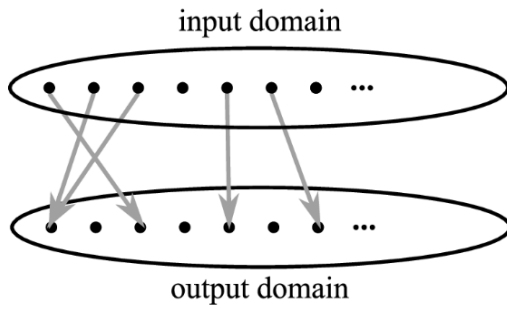


Picture 26. Examples of different class 4 cellular automata described in [3]. The top left automaton is the already discussed rule 110 which universality was confirmed. The remaining three shown automata are suspected to be universal, but were not yet confirmed universal. An assumption is made that all class 4 cellular automata, which are capable of forming a rich enough set of localized structures (like for example triangle patterns in rule 110) will support universality [3].

When considering how simply computational universality can arise in cellular automata, one wonders if such computational universality can also arise in natural systems. And indeed, it can be shown that it does. Schematically seen is a computational problem (as seen in picture 27 - a) basically a mapping of a certain input domain to a corresponding output domain. This is a very general think. It is not necessary to do any concrete assumptions about the origin or properties of the

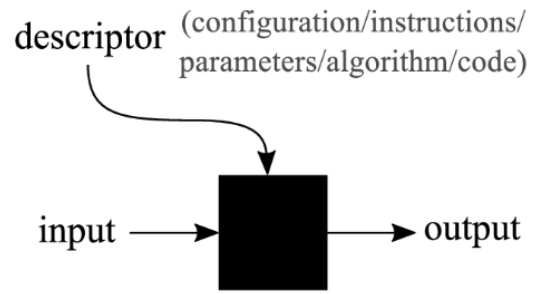
domains itself (like their nature, physical implementation etc). The input domain might very well be a multidimensional array of virtual cells (as in case of a cellular automaton) or an electrical signal. It can even be a quantum system (as demonstrated in quantum computing experiments [50]) or a set of molecules or chain of proteins as often seen in living organisms. Thus, even natural systems are able to solve computational problems. But to be able to assess computational universality in natural systems (in the same context as in artificial systems), one needs to prove that such a natural system is able to solve not just one, but many computational problems. A certain descriptor (as seen in picture 27 – b), needs to be present to specify which problem is determined to be solved. And indeed, there are systems in nature which show presence of such descriptors (or instruction sets). The most common example is a core biological process called protein biosynthesis which happens in living cells. During this process a certain input domain (proteinogenic amino acids) is transformed to an output domain (polypeptide chain) according a descriptor known as DNA, while following a certain grammatic while doing so. The genetic code (in other words the rule set to keep the analogy with cellular automata) is highly similar in all living systems and can be easily captured in a simple table of 64 entries [51] (again note the similarity to cellular automata and the rule look up table described in chapter 1.1). The molecular implementation of this process is extremely complex, and will not be discussed in detail, however note the remarkable similarity of this biological system to a general computer system which utilizes source code (set of instructions) interpreted by a compiler. It was shown, that DNA (or RNA) based universal computation is plausible [52], and that DNA/RNA based computational systems which exist in living cells, are Turing-equivalent and can compute any computable function.

Computation Problem



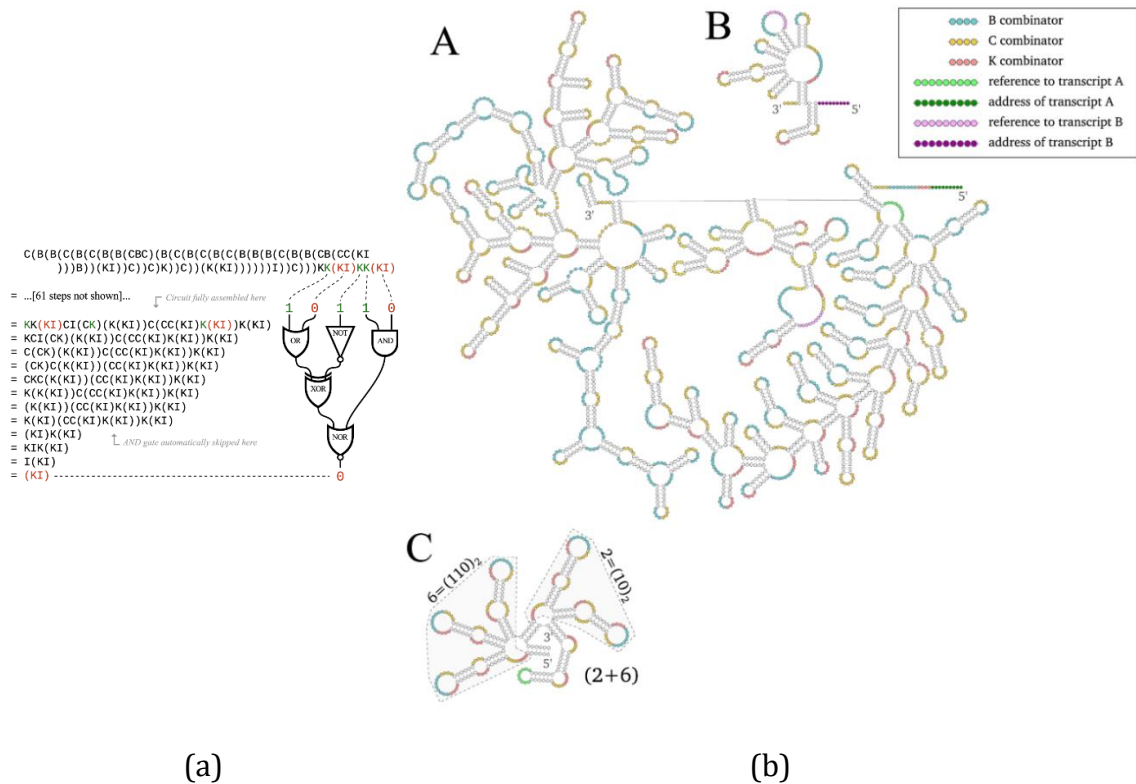
(a)

Computation System



(b)

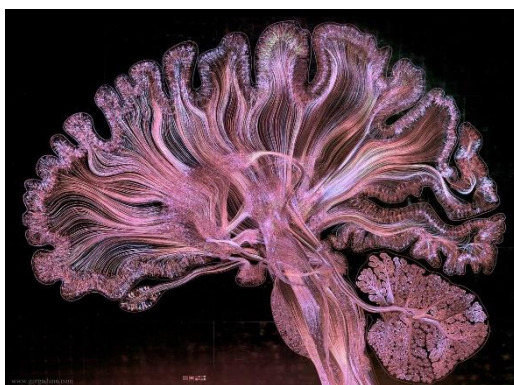
Picture 27. Schematic representation of a computation problem and a general computation system which can address such a problem. Note the black box of the computational system in picture b. The black box may contain any possible mechanism which translates the input domain to its output domain controlled by the descriptor [52].



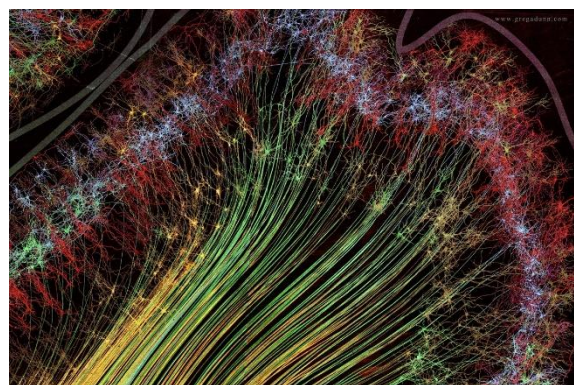
Picture 28. An example of a combinatorial logic circuit (a) utilizing combinators B, C, and K. Picture (b) shows an RNA based implementation of simple addition. The RNA program itself (c) represents an addition operation of 2+6. Transcript operations and references necessary for program execution, together with combinator definition are represented in A and B [52].

Another example of a natural system capable of universal computation is the human brain. Being one of the most complex systems in nature, even after decades of intensive research, the human brain was so far not fully understood. It contains billions of brain cells and more than 100 trillion connections through which the individual cells interact in a highly unilinear fashion accompanied by super-complex chemical interactions as well. Through this interaction of multiple physical and functional elements, complex mental states emerge. The emergent behaviour (being one key aspect of all complex systems) is thought to be key for further understanding of the human brain [53]. As can be seen both real physical systems and cellular automata are capable of universal computation. This is yet another common feature shared by both the artificial as well as the real-world physical system, which goes far beyond a simple visual correlation and again highlights how deeply cellular automata correspond to real systems in nature.

It is intriguing, how vastly both systems correspond. They share similarities on the origin of their random behaviour, similarities in experienced complexity and emergent behaviour, they resemble continuity and discreteness in their behaviour in the very same way, and they even share the same capability of universal computation. Therefore, if one describes a certain feature of a system utilizing an artificially implemented cellular automaton model, the knowledge or insight gained can be easily utilized when making assumption on how a real physical system works, just because they behave on similar fundamental principles.



(a)



(b)

Picture 29. Artistic representations of neural pathways in parts of a human brain. The structures are extremely complex [54].

3. Potential of cellular automata in didactics of physics

In physics, traditionally, a mathematical approach to research has been established, and indeed it always had a great success. This inevitably led to a general assumption, that serious physics research must always be founded on solid mathematical rigor, and possibly be backed up with a lot of complex equations. But even armed with solid mathematics, there are still very basic physical phenomena, which could not yet be explained. As an example, take fluid dynamics, and especially the phenomenon of turbulence. The state-of-the art mathematical description is realized through the famous Navier–Stokes equations [55], which is a set of non-linear partial differential equations which describe the flow of viscous fluids. Until now, it is not known, whether these equations have always a solution in three dimensions. In fact, it is one of the unsolved mathematical mysteries and one of the 7 so called millennium problems [56], [57]. Therefore, when modelling fluid dynamics (which has major importance in everyday engineering) a computer aided approach is always preferred, and an empirical measurement for both model validation as well as model initial input parameters is conducted [58]. There are many other physical phenomena, where a mathematical approach still could not provide a proper description, and theoretically, there might even be systems where a complete and consistent description will never be possible because of the very nature of the axiomatic system of mathematics [33].

Our educational system and approach to didactics of physics follows the trend of utilizing mathematical description of physical systems, and indeed our course books about physics are full of simple mathematical descriptions and models of the basic physical phenomena taught to today's students. This of course fulfills its purpose and is in many aspects excellent to teach physics, but some of today's students (especially the ones not interested in mathematics or the ones with poor mathematical understanding) have trouble to follow this approach, and as a result physics is sometimes regarded as a difficult and I dare to say "unpopular" subject, even for first grade and second grade students. But even for students familiar with mathematics who like the subject, today's physics course books offer only simple

models of very basic phenomena, which are easily captured with mathematical tools available for the everyday student, and are often stripped of any “extras”, just to make it enough elementary to be captured with a simple enough mathematical equation. Individual topics and example systems are picked up on purpose to meet the requirement for mathematical simplicity, and as a result a lot of interesting physics and physical systems are easily missed, because they just simply do not fit into the box defined by the mathematical constraints. Other topics are stripped of the very essence, that makes the system behave as it does, just to ensure application of mathematics is possible. Again, take fluid dynamics and turbulent flow as an example. In order to make the description possible (even for not elementary school students), the model is simplified, flow fields are considered absolutely symmetric, flow is modeled around a cylinder with uniform free stream flow by superimposing a flow field of an ideal vortex, the description is done in two dimensions and viscosity is not taken into consideration (no boundary layer), even though this in fact is the real source of turbulence and the experienced dynamics of the system [59]. It is far more interesting to model flow around real-life objects like fish or bird like shapes, or around airplanes or city buildings (instead of modeling flow around an abstract cylinder). More complex, real-life phenomena in nature and technology tend to be omitted in education, as their behavior and dynamics is so complex, that their rigorous description borders on several disciplines. Each of these disciplines tend to describe only part of the system with tools inherent to the respective subject, and fail in providing a general description of the system and introduce its beauty to students. Take for example the complex system of a superorganism called the ant colony. This topic is briefly touched in biology where a short description of ant morphology, reproduction, communication or nest construction is discussed - simply topics that can be easily captured by biological lessons because of their simplicity, and the didactical tools used by biology (more relying on description than abstract theories or mathematical description), but other aspects of the superorganism, like how it organizes, or where the extreme complexity of the system’s dynamics comes from (which is the real source of why are ants from evolution perspective so successful) is completely omitted. Here, physics could provide some description options and some valuable insight even for secondary school class if it would have the right

tools to do it (mathematical rigor is not the right tool here). It would promote synergy between individual school subjects, as the real-life phenomena are not restricted to some specific subject only. Further continuing with the ant example, there is a lot of potential for a physics lesson to describe the dynamics, chemistry lesson to describe the pheromones and concentration mechanisms, mathematics to describe the graph theory or the relation to computer science and computer search algorithms. Such a system would be a gold mine for education, if there was a way how to describe it in a simple enough way to catch the student's interest. Another example are traffic systems, for example freeway traffic. This subject is not included in our physics coursebooks at all, because although the experienced dynamics is interesting (take for example the famous congestion forming out of nowhere), the combination of complex mathematics and socio-dynamical interactions make it impossible to be described easily for a secondary school student. There are a lot of other interesting examples, and real-life systems exhibiting a lot of interesting behavior which could be introduced to students, were there a way how to do the description easy enough and without heavily relying on mathematical description. And exactly here it is where cellular automata could bring a completely new kind of description possibility. As discussed in previous chapters, the ability of a cellular automaton to exhibit even the most complex behavior, just by following very simple rules is an ideal foundation for this new kind of description. Such a cellular automaton, and especially its underlying rules could be explained in a very easy way to the student, and then the student could investigate the complex dynamics which is generated by such a system. The student can try to modify the rules and experience the influence of such a rule change of the system. In this way, a student could experiment and study systems, which current traditional mathematical approach to didactics of physics would never make possible. Some of these systems and the corresponding cellular automata will be presented in this thesis. It needs to be point out as well, that some of the cited literature suggests [3], that a description of physical (social, philosophical, computer and many other) systems is feasible (and even advantageous) by utilizing cellular automata and that it in fact represents a completely new kind of science which touches almost every scientific research area, without the necessity to heavily rely on complex mathematical rigor, and that

the fact that the systems can be represented by simple programs is not a coincidence but rather that here is a deep correspondence between simple programs and systems observed in nature [3]. Some of the literature even suggests, that the whole universe and every think in it is an output of a giant cellular automaton [23], [21]. The aim of this thesis is not to investigate whether this might be true or not, but if there is a solid scientific interest in explaining the universe with cellular automaton approach, there certainly is a solid possibility to utilize this approach also in traditional didactics, much like mathematics is utilized today for example in didactics of physics. Let us now explore some of the biological, physical and social systems, which might very easy by simulated by a cellular automaton approach.

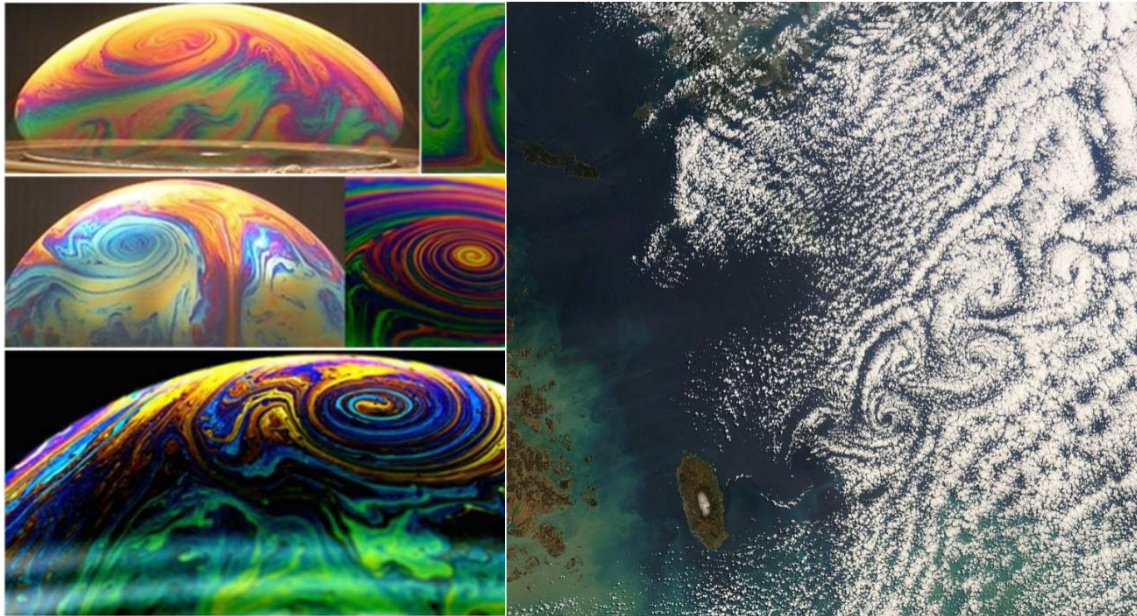
3.1 Cellular automaton approach to model fluid flow

As a first example of how a cellular automaton could be utilized in didactics of physics is a cellular automaton modeling fluid flow. Fluid flow was chosen as an example especially because it is so difficult to address with the standard mathematical approach to didactics of physics, and is therefore a good example how to address the topic by different means, and possibly bring the topic closer to a secondary grade student. First of all, a short introduction to fluid flow will be given to describe the topic from general point of view, after that, a cellular automaton approach of the flow description will be shown.

3.1.1 Introduction to fluid flow

In physics, fluid flow or fluid dynamics is studied as part of continuum mechanics. It basically describes the flow of fluids, liquids and gasses. Due to the complexity of the topics, there are several independent sub disciplines focusing on individual states of matter and their flow (for example aerodynamics is focused to study the motion of gasses, hydrodynamics focuses on the motion of liquids). Fluid dynamics in general has many practical applications, ranging from weather forecast, aircraft or car motion simulation (aerodynamical force calculations for fuel consumption optimization), animal locomotion study, urban planning and bridge building

(simulation of airflow around these objects is crucial for their stability in various environmental conditions), pipeline flow simulation (transport of petroleum or water), blood flow in medicine, up to nuclear fission weapon explosion dynamics modeling (the explosion dynamics is responsible for holding the fission material long enough together to assure enough energy is released) and gas motion study in stars or interstellar space (for example nebulae formation or convective zone dynamics in stars) [60]. In general, there are two types of flow patterns – laminar flow and turbulent flow. Laminar flow is characteristic with its streamlined flow where the fluid glides along distinct regular layers without mixing fluids from individual layers. Laminar flow is fairly simple to model and describe with simple mathematics. Turbulent flow starts to form when in some parts of the fluid the kinetic energies overcome the overall damping effect of the fluid's viscosity. It is characterized by the formation of vortices (turbulent flow patterns of various size), which interact with one another in a very complex way displaying chaotic dynamics. Turbulent flow in general is very difficult to model with mathematics and therefore, in general, science and engineering relies on computational fluid dynamics (CFD) [61]. Due to the microscopic nature of fluids (fluids on microscopic level consist of a large number of molecules), it is possible to model fluid flow with cellular automata [3].



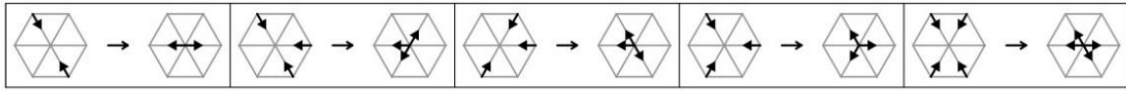
(a)

(b)

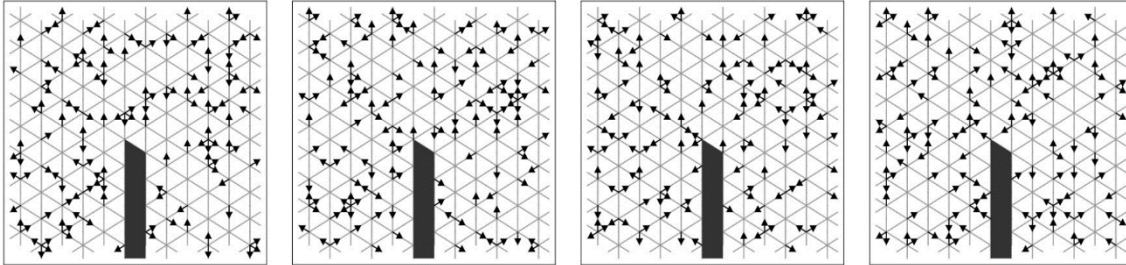
Picture 30. Picture left shows an example of vortices on a soap bubble. The patterns are extremely complex [62]. The right picture shows a vortex formation known as Karman vortex street. The street formed in Earth's atmosphere as a result on air flow around an island [63].

3.1.2 Fluid flow simulation cellular automaton

Fluids consist on microscopic level of discrete particles. These particles collide with each other, which is the origin of the experienced dynamics. A simple idealization of this concept can be given by a cellular automaton consisting of a fixed grid (the automaton universe) and a collection of discrete particles. The particles are allowed to move along the grid. If a particle meets another particle both particles adopt a new heading according a set of simple collision rules (described in picture 31). If a particle hits a foreign object (special part of the grid) it is reflected and travels in the opposite direction [3]. Four consecutive algorithm steps can be seen in picture 32.

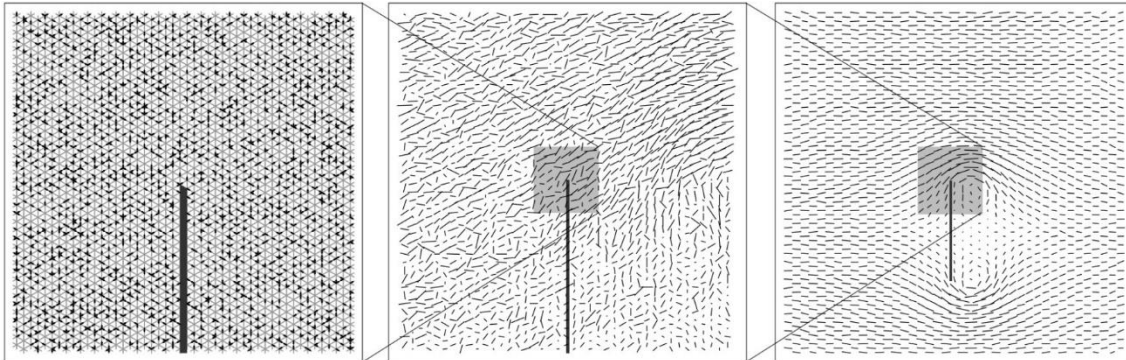


Picture 31. Particle collision rules applicable for the fluid flow simulation cellular automaton [3].



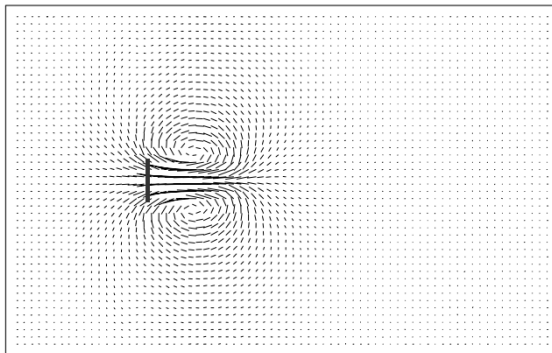
Picture 32. Four consecutive automaton steps. The particles collide according to the rules described on picture 31. When a particle meets a foreign object (in black), it gets bounced back [3].

When observed on microscopic scale, the automaton does not show any surprising patterns. However once zoomed out, the system shows a very interesting dynamics and remarkable fluid flow patterns, which are similar to patterns observed in nature. Pictures 33 and 34 shows how complex, vortex-like patterns start to emerge when the system is observed from a larger scale perspective.

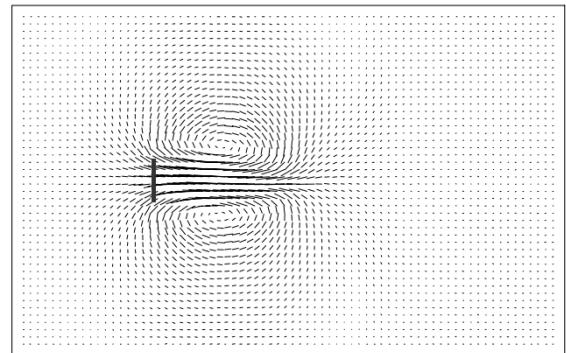


Picture 33. Remarkable flow patterns start to show up when the system is observed from a larger perspective. The picture most left shows the basic grid with the individual particles. Consecutive pictures show a zoomed-out view, which is obtained by averaging the particle headings. A steady and uniform stream of particles is inserted to the automaton (on a left side) to simulate a real fluid

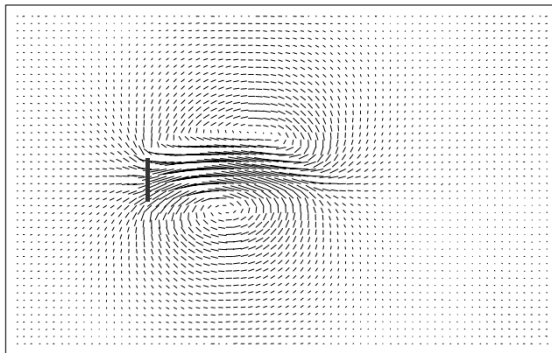
stream. In this example, the incoming particle velocity is 30% of maximum velocity defined for the automaton. [3]



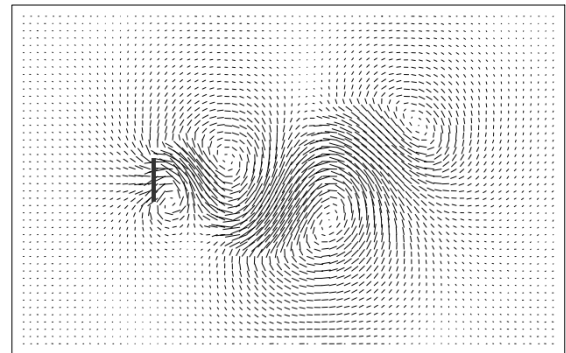
step 10000



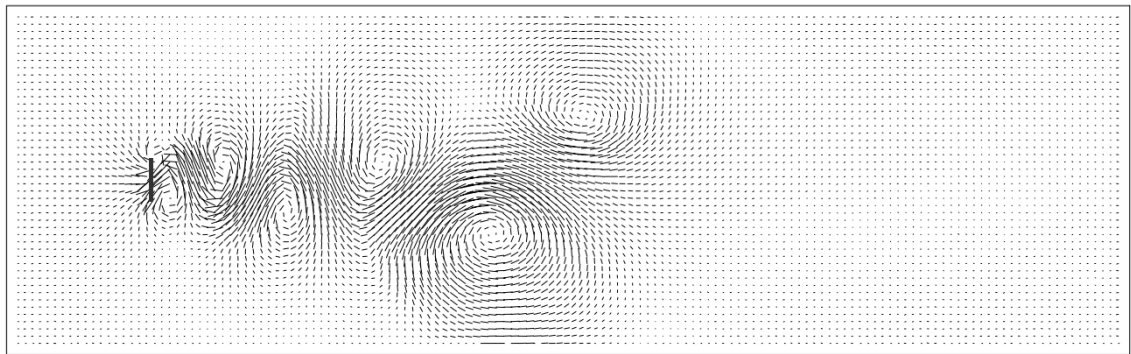
step 20000



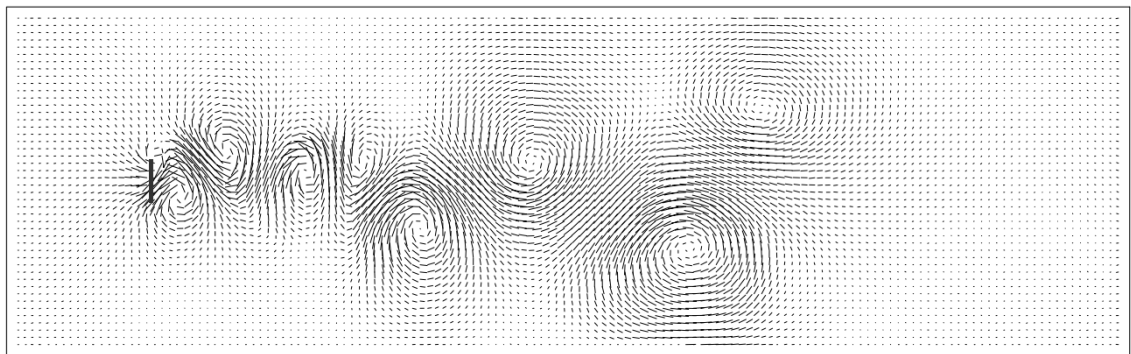
step 30000



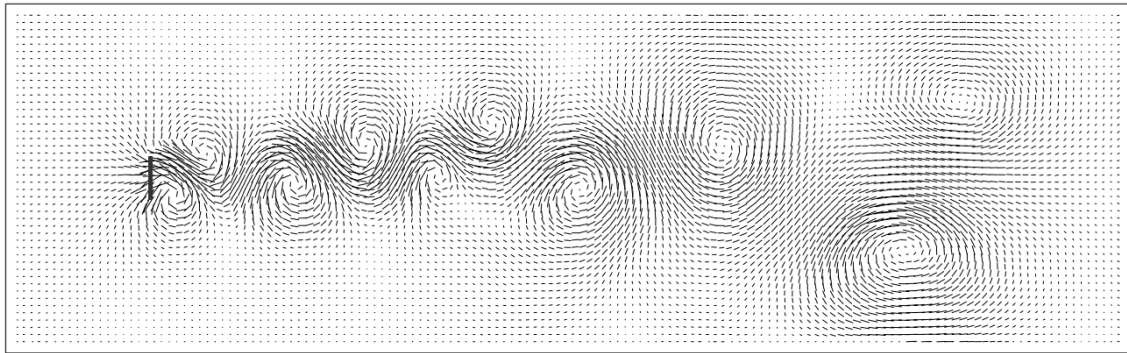
step 40000



step 50000



step 60000



step 70000

Picture 34. Further evolution of the cellular automaton for another 70000 steps. The average speed of incoming particles is about 40% of maximum speed. The example consists of about 30 million cells and each individual velocity vector is calculated as an average of 20x20 cells. [3]

Even the cellular automaton rules are very simple, again the dynamics it exhibits is extremely complex, much like in a real-world vortex exhibiting system (compare with picture 30). The remarkable similarity to a real system is not only based on a visual perception of the dynamics. When the physical quantities of the system (like viscosity or Reynold's number) are calculated (this can be done based on particle numbers and flow speed), and based on these quantities a comparison to a real experiment is done, it can be seen that the agreement with the experimental result is very good. This is remarkable concerning the simple underlying rules of the automaton [2]. In fact, the automaton and its rules are so simple, that they can be easily explained to a secondary school (or even a primary school) student with plain word, and literally no mathematical description is necessary to explain the phenomenon of turbulence and turbulent flow to a student.

4. Pilot didactical purpose cellular automaton models

In this chapter, three pilot cellular automaton models will be explored to explain the potential of cellular automaton description approach in didactics of physics. Because of practical reasons, these models were implemented in Microsoft Excel.

4.1 Microsoft Excel as a cellular automaton programming interface

As discussed in the previous chapters concerning cellular automata, the key elements of every cellular automaton are a regular uniform grid of cells from which each can have a specific state (represented for example by a discrete number, or a color), and which is governed by a set of rules describing how a cell should change based on its own state and the state of other cells. To model such a system is fairly easy. For example, in Conway's "Game of Life", a piece of graph paper (grid of cells) and a pencil (to change the cell states) is sufficient in order to explore the whole game and all the possibilities it provides. There is, however, a variety of other tools. For scientific research, Matlab [64] is used regularly as the state-of-the-art tool for modeling and simulation. Unfortunately, for the purpose of didactics and simple modeling, such advanced software is simply too complex and expensive to be bought by a standard elementary or secondary school, and therefore Matlab remains a domain of technical universities or large corporates, which have their own research and development and can afford the related costs. And even if a university student has the opportunity to utilize Matlab during his study, the exploration of the tool is rather limited (it is usually used only for a few highly specialized courses), and after leaving university, the student most probably never gets to utilize Matlab ever again (if he does not continue his career as a researcher, which is rather rare). There is a tool however, which is fairly common both for secondary school, as well as universities and further in most of the companies (no matter the size), which can be used for simulation and modeling.

The mentioned tool is Microsoft Excel [65]. Although it is usually used in a completely different context (Excel is largely regarded as a spreadsheet software, rather than a tool for simulation or modeling). In the consecutive chapters a robust framework for utilizing Microsoft Excel as a simulation and modeling tool will be presented, primarily to implement simple cellular-automaton-based models of real physical systems. The potential of these models in education, and in foremost in didactics of physics, will be further discussed. The main and fundamental advantage of Excel hereby is, that it is present on most of the computers in schools and business environments and is usually already present in the installation package utilized to set-up the computers in these environments. Excel, as its inherent feature, contains “cells”, and an integrated development environment, based on the programming language Visual Basic 6 [66], which can programmatically access these “cells” (the cells are regarded as objects and Visual Basic utilizes standard object-oriented approach much like Matlab to access these objects). This means Excel contains all necessary tools for implementing a cellular automaton - a grid of cells (needed to construct the cellular automaton universe), an environment for designing governing rules of any possible cellular automaton, and an environment to run the resulting automaton. These features, together with its near to omni-presence in today’s school and university environments make it a perfect tool to be used in application of cellular automata in didactics of physics (and possibly in didactics of various other school subjects). It will be shown, that Excel can be utilized in much more ways than just for standard spreadsheet calculation, and that it has a vast potential in didactics of physics. In the consecutive chapters, three cellular automaton models will be shown, each representing an interesting physical system. The systems were chosen on purpose to be sort of “border systems”, which are on the edge of physics and other school subjects (in this case biology and traffic research) and which would be very difficult to describe by utilizing standard mathematical description approach common in today’s didactics of physics. It will be shown, that by utilizing the concept of describing a system by a cellular automaton with a set of simple rules, even such complicated “border systems” can be effectively described and brought to the attention of students, and that even very complex system dynamics can be a result of very simple underlying rules, which can be comprehended even by

elementary school students, and that literally no understanding of mathematics is necessary to study such a system from an educational perspective.

4.2 Ant simulator

The first example of a cellular automaton modelling a physical system is the so called “ant simulator”. The simulator will show some of the basic concepts of how ants search for food to keep their bodies alive. However, before moving to a detailed description of the automaton itself, let’s first explore the world of ants.

4.2.1 Introduction to ants

Ants are one of the most successful groups of insects in the animal kingdom. They dominate their respective environments as predators, scavengers and indirectly also as herbivores [67]. One can argue, that much of the success can be related to the fact, that ants are eusocial insects – they have the highest level of social organization in animal society, featuring cooperative brood care, existence of castes (specialized behavioral groups performing only a certain specialized task – for example workers perform food production and brood care, soldiers perform defense tasks, egg-layer assure offspring), common food procurement and distribution and overlapping generations [68]. Ants form colonies that range in size from only a dozen individuals, up to highly organized super-societies containing tens of millions of individuals which form diverse specialized groups. Ant colonies are sometimes described as superorganisms, because individuals collectively work together to support the colony and operate as a unified entity. Ants as a species are extremely successful. They have colonized almost every landmass on Earth, excluding only Antarctica [69], [70]. They are estimated to form 15-25% of the terrestrial animal biomass. In fact, if compared to the number of humans on earth, there is more than a million ants for each human being on earth [71]. Ants show a variety of interesting behavioral patterns. They range from nomadic “hunters”, “gatherers” and “cattle breeders” up to species cultivating fungi as a food source [69]. Some species carry on slavery by kidnapping the ants of

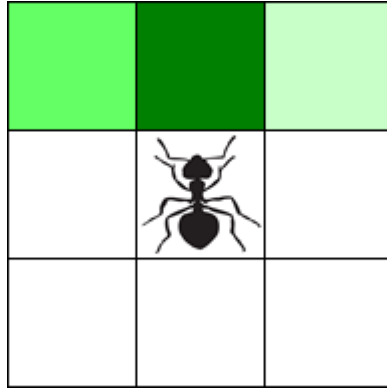
other species to work for them, other show social parasitism - by allowing females to migrate into colonies of a different species and let them raise their descendants [72]. Due to the division of labor and communication between individuals, ants are able to solve complex problems. Task like transportation of food, overcoming obstacles, building anthills are performed almost optimal [73]. Principles of their behavior have withstood the proof of one hundred million years.

One of the key aspects of why ants are so much successful, is the way how they share information, especially information about food source location. This communication is extremely sophisticated. It does not merely show other nest mates the direction to food, but it rather organizes the whole system (ant colony) in a very interesting way, allowing the system to self-regulate its food search activity. It is able to promote food locations with higher profitability, while keeping memory of previously profitable locations. Investigation showed, that ant communication is mainly based on chemical marking. Ants put pheromone trails (there are many different types of pheromones secreted from different ant body parts), which can provide either positive feedback or negative feedback to the ant colony to organize its foraging activity. When a successful forage ant finds a food source, and returns to the nest, it lays down a pheromone trail. Other ants, attracted by the pheromone trail, finally also find the food source and put down a pheromone trail during their way back to the nest. In such a way, the pheromone trail marking the path to the food source gets reinforced steadily while more and more ants find the food source and put more and more pheromone trails providing positive feedback. On the other hand, when the food source is depleted (or is too far away), the pheromone trail does not get reinforced fast enough and eventually evaporates, providing negative feedback [73]. Even though the individual ants possess only minimal intelligence, the system as a whole is able to organize itself in a very complex way solving many difficult problems (for example find the shortest path between two points - in context of ants between food source and nest) not unlikely a cellular automaton, which in mathematics (especially graph or network theory) is a well known problem difficult to solve, and while it can be solved in linear time, the related algorithms are quite sophisticated [74] (in comparison to what a second grade student has in its mathematical portfolio for comprehension). One way how to make this intriguing topic available even for second grade school

students is to describe the system not mathematically, but by a cellular automaton with some simple rule set. A student could study this rule set and the resulting systems dynamics. By making changes to the rules, the student could study the influence of each rule on the dynamics and with this experimenting and hands on approach even such a complex system could be available for study in a secondary grade school environment. To following example implemented in Microsoft Excel will show the basic principles.

4.2.2 Ant simulation cellular automaton

The universe of the ant simulation cellular automation consists of a two-dimensional grid of cells. Each cell can have one state of a possible set of different states. The states are no longer so simple like it was for elementary cellular automata – just black and white color, but they are still simple enough to be described in plain sentences. A cell can contain a pheromone trail (a discrete number describing the pheromone scent intensity), or food (again a discrete value describing the richness of the food source), or an ant, or a superposition of the mentioned states (a cell state can contain an ant, food, pheromone – all this at the same automaton step). Important is, that even the automaton states are complicated objects, a cell still can have only one specific discrete state from a finite discrete cell state set. The neighborhood is defined to be only directly adjacent cells both vertically, horizontally and diagonally, with the direct neighborhood being the 3 cells directly in front of the ant cell.



Picture 35. Example are from the ant simulator cellular automaton universe. A cell can contain and ant, food or pheromone or a superposition of all these states. The direct neighborhood of the ant is highlighted in green color (darker green means higher pheromone value).

At time ($t = 0$), a state is assigned to each cell in the universe based on initial configuration of the ant simulator (the number of ants, food source location and other variables). The whole cellular automaton is governed by simple rules, which can be described in two sentences:

- 1) An ant searching for food will always make a step towards the neighbor cell with the highest pheromone value, if there is none it will choose a neighbor cell at random.

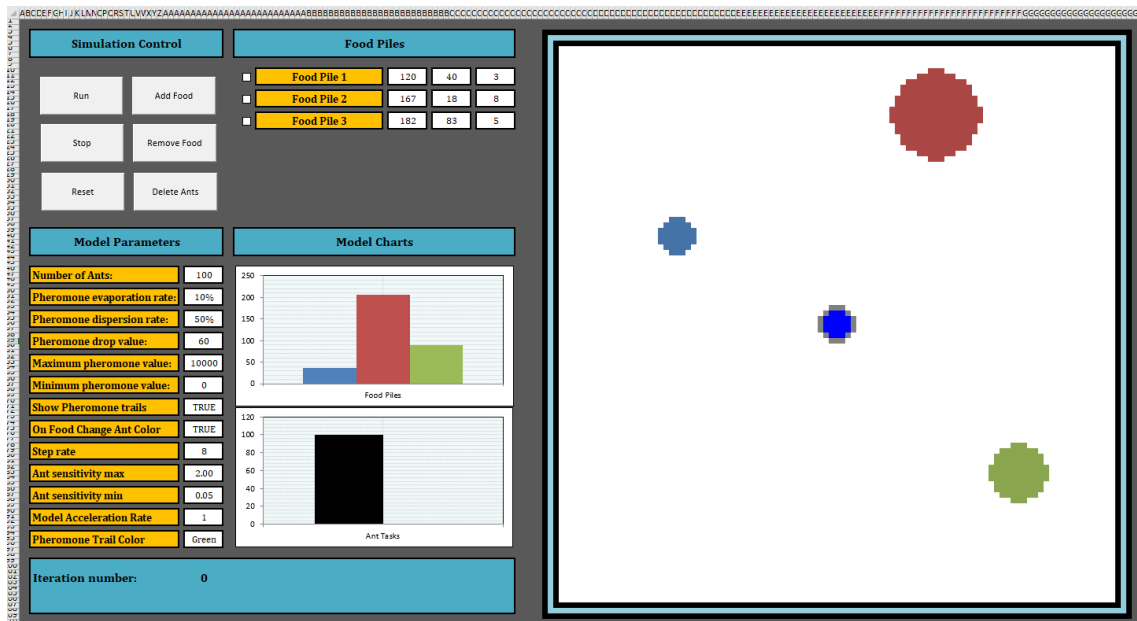
- 2) An ant which already found food will return to the nest by the shortest possible way and drop pheromone trails each step.

For better visualization of the rule set, the rules are described as actions done by each ant as listed in table 1. Each action is done in a top-down consecutive order as listed in the table. Please note that each ant action is in fact a whole set of rules which apply to the ant cell and neighbor cells, and which define how the cell states should change in the next automaton step based on their current values.

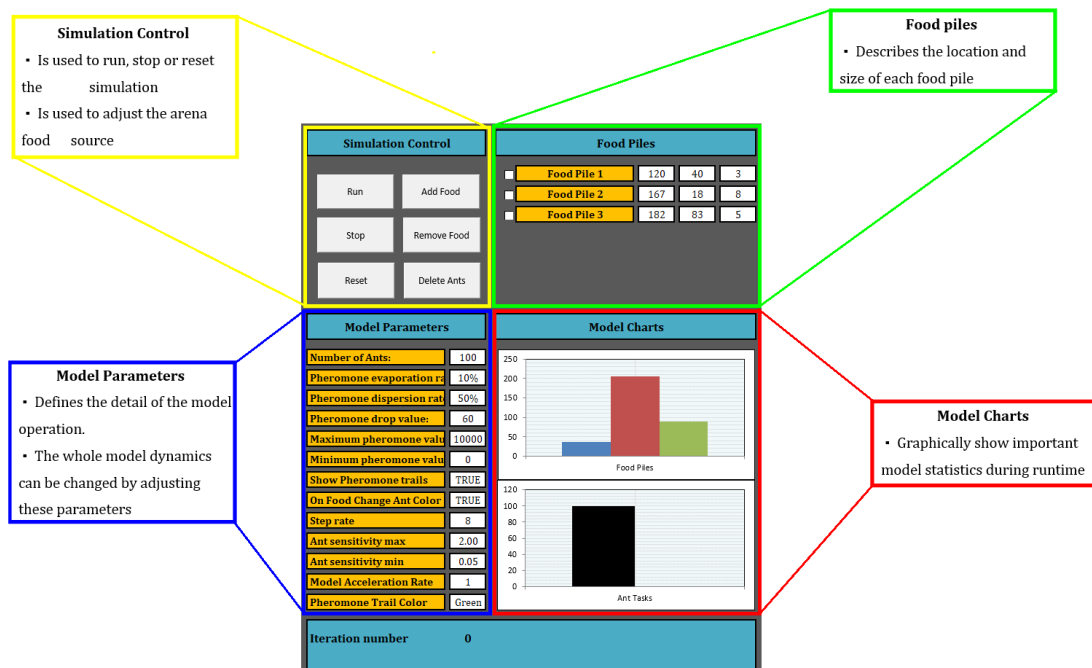
Table 1. Summary of cellular automaton rules, for simplification described as individual ant actions rather than a look up table.

Ants searching for food	Ants returning with food
Scent for pheromone (3 neighboring cells)	Drop a pheromone
Do a step towards the cell with the largest pheromone value.	Do a step towards the nest
If no pheromone, pick one of the 3 neighboring cells at random	
If food is found, return with food	

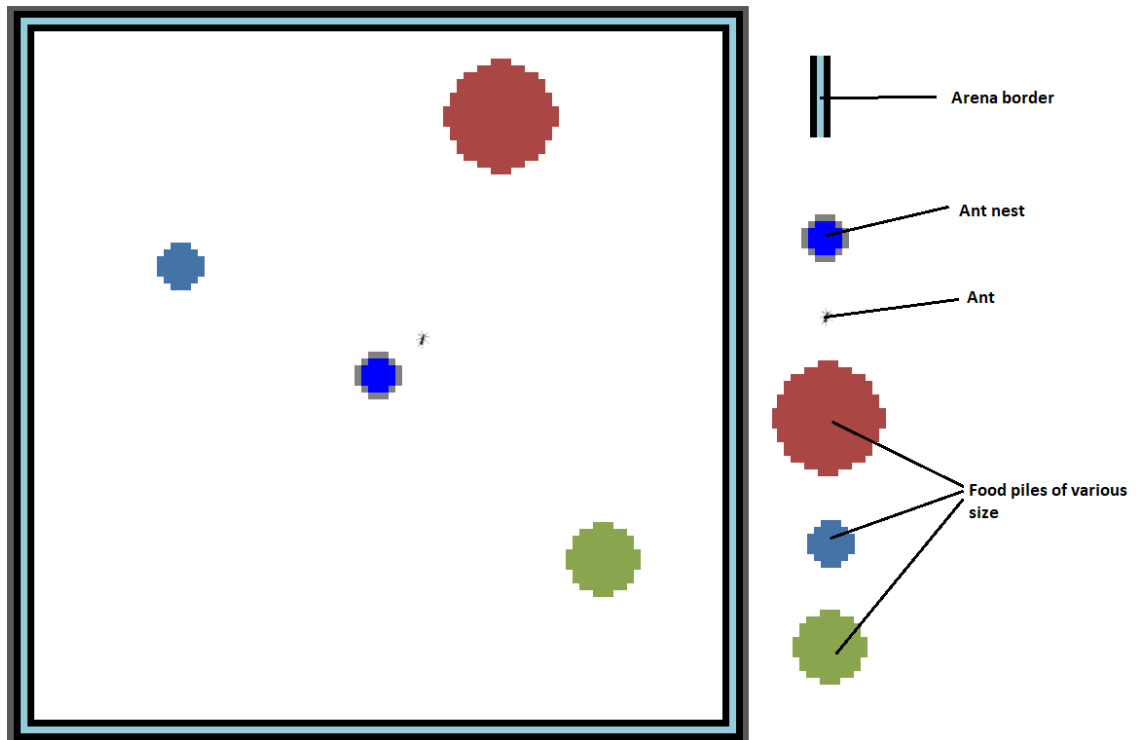
The simulation itself is carried out in an excel sheet. The excel sheet is divided into 2 separate parts. First, the so called “arena” (see picture 36 right), is the place where the cellular automaton runs. All steps are executed here. Second part is the GUI part (graphical user interface part – see picture 36 left). In this part, the student can modify individual model parameters, place food sources and control the simulation. A short description of the individual GUI parts can be reviewed at picture 37, and a short description of the arena and its elements is present on picture 38.



Picture 36. The ant simulator excel sheet is divided logically into two separate parts. Left, the GUI is intended to adjust the simulation parameters and for general simulation control. Right, the “arena” is where the cellular automaton simulation actually runs.



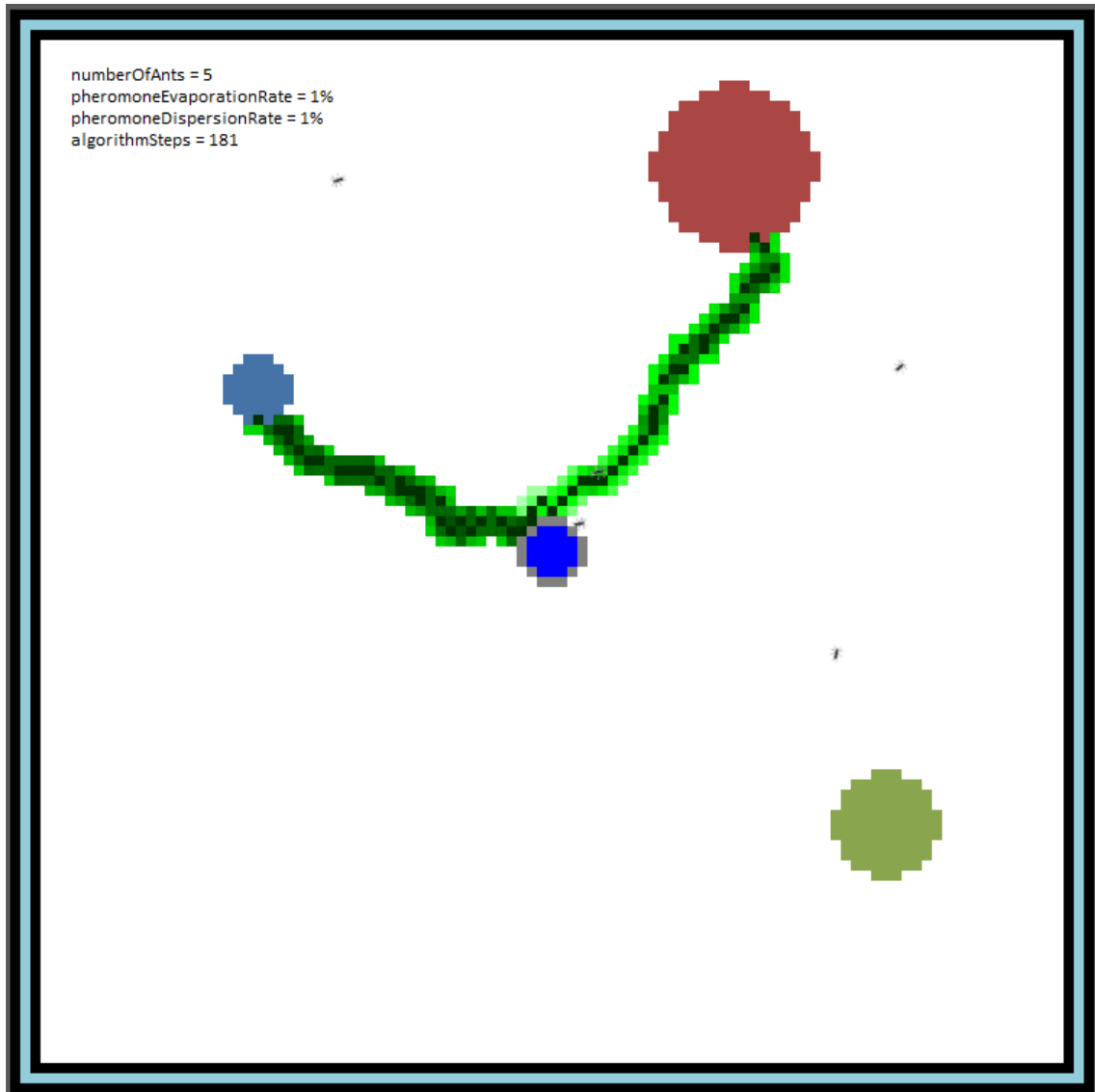
Picture 37. Short description of the individual GUI control units. A more detailed description together with a program manual will be provided in a separated document.



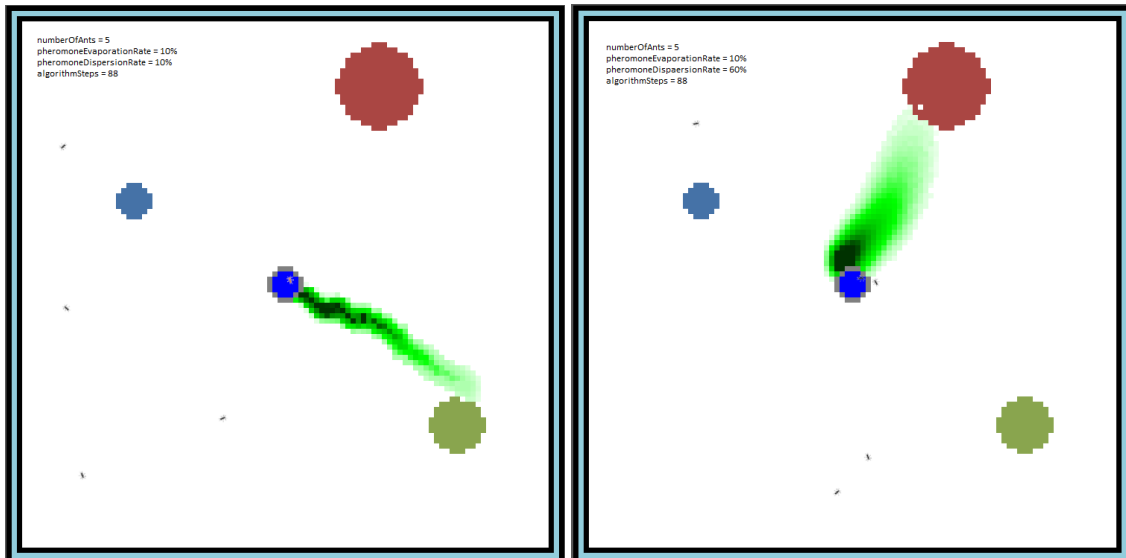
Picture 38. The ant simulator arena where the cellular automaton runs. Some of the arena elements are described individually on the right side of the picture.

4.2.3 Examples of interesting ant simulator dynamics patterns

Even though the underlying rules of the cellular automaton are fairly simple, the exerted complexity of the systems dynamics is not. Dependent on the automaton's initial configuration, several very interesting patterns emerge. Some of these patterns will be show here as an example, and the reasons why such a pattern emerged will be discussed. Finally, several questions will be asked, as an example what questions could be asked to a student investigating the system.



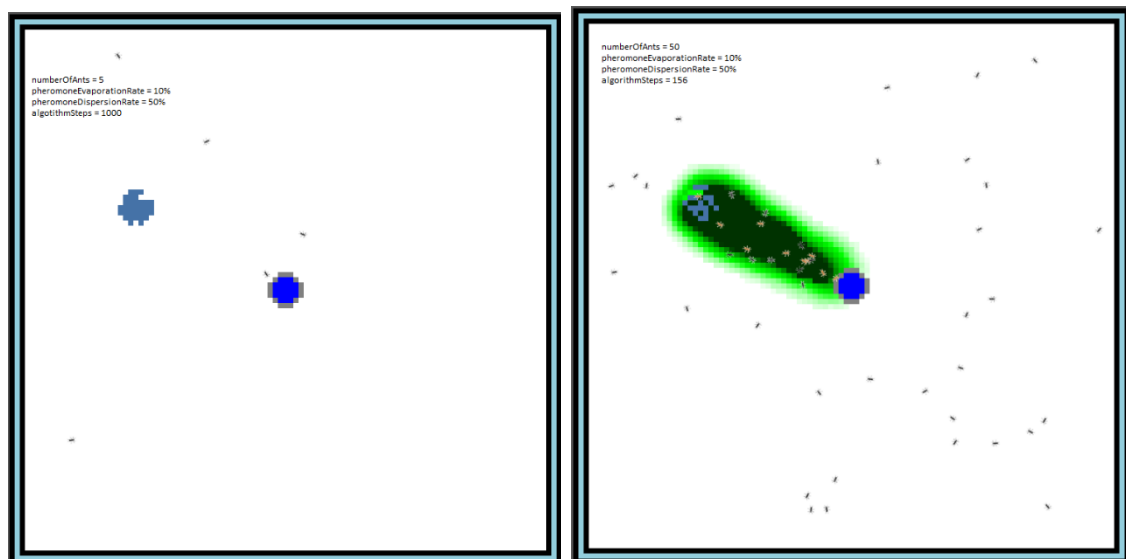
Picture 39. Example of pheromone trail formation. Darker green represents a higher pheromone concentration. The pheromone evaporation rate was set to be extremely low. Left trail is older than the right trail and exhibits more pheromone concentration at the outer parts of the trail, due to the fact that pheromone dispersion was working for a longer time.



(a)

(b)

Picture 40. Example of pheromone trail formation. While both trails show a uniform evaporation rate (set to 10%) resulting in higher concentration of pheromone near the ant producing the trail, the trail in the right picture is broader due to a higher pheromone dispersion rate (set to 60%).

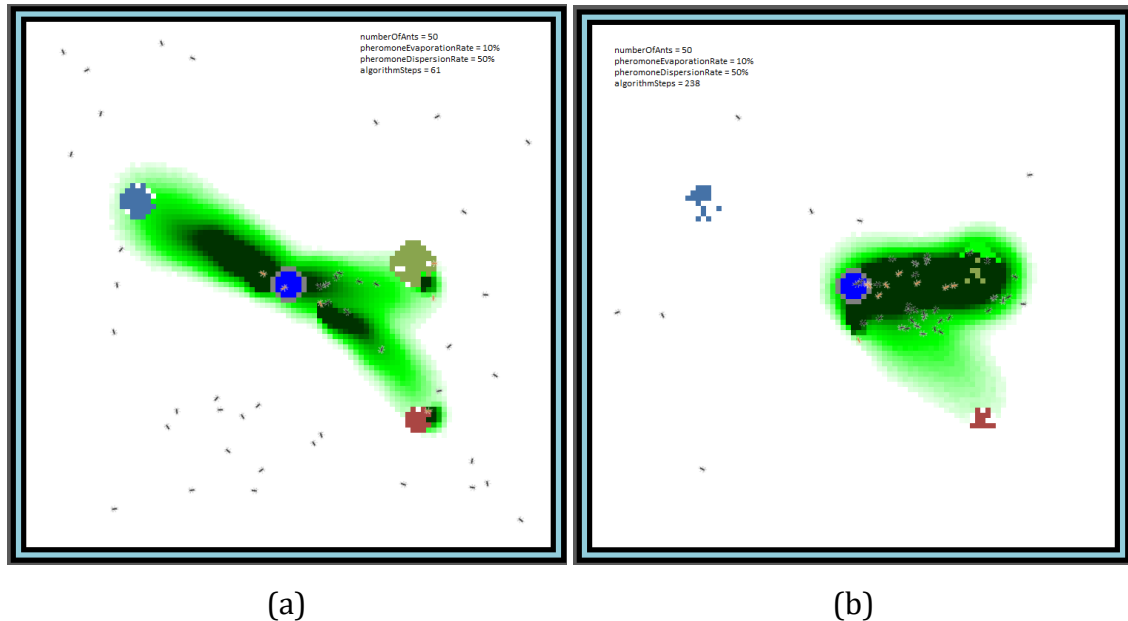


(a)

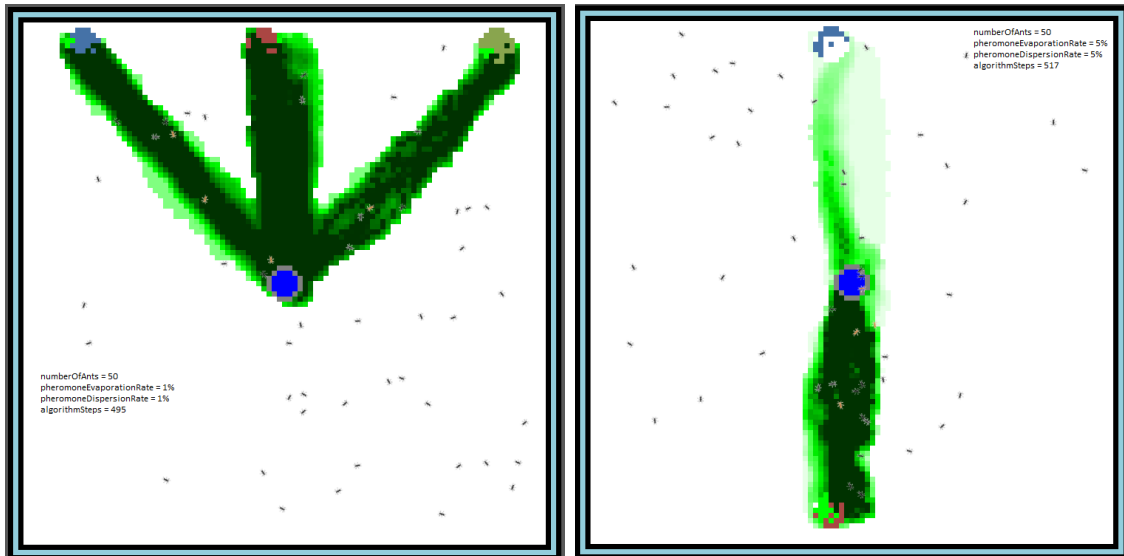
(b)

Picture 41. Example of pheromone trail formation. While for the left picture, a stable path from nest to food source could not be established (not enough positive feedback enforced by strong enough pheromone trail - because of limited number of ants), the right picture shows a stable path between food source and ant nest. In the right picture, the number of ants was increased to have a strong enough

positive feedback to form a stable path. Whether the feedback is strong enough to maintain a stable path between food source and nest depends on the environmental conditions (pheromone evaporation and dispersion rates) and on the number of ants that produce pheromone.



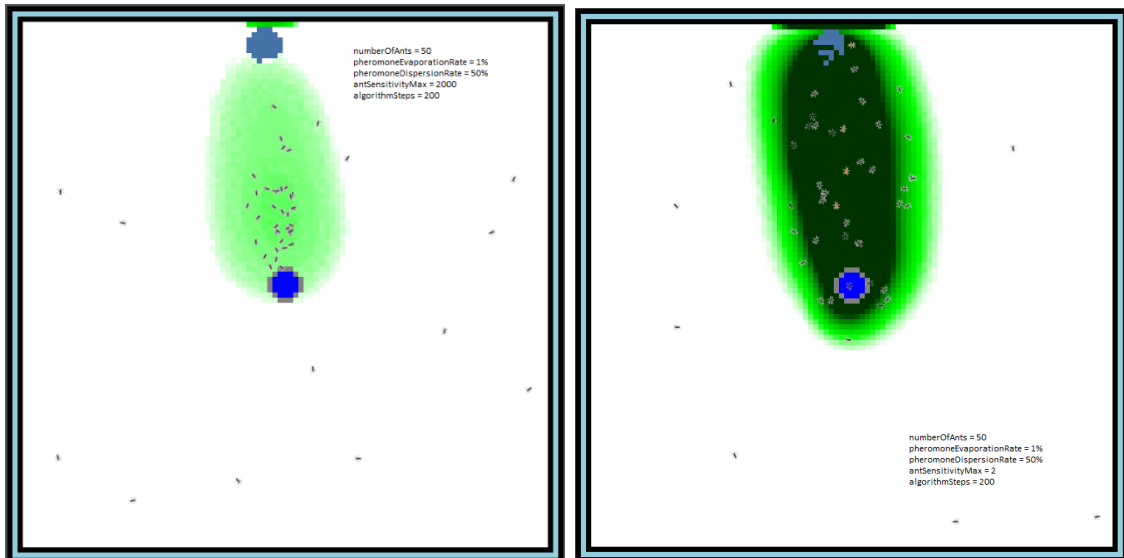
Picture 42. Example of pheromone trail formation with multiple food sources available. After an initial phase of gathering, where all three food sources were selected (left picture, after 61 algorithm steps), one main path was established between the closest and largest food source (right picture after 238 algorithm steps). Eventually, one of the paths (solutions) was reinforced so much, that it dominated the other paths (solutions). This is an example how ants can put focus on the most promising food source first, gaining the best ratio between spend energy and amount of gathered food, which results in an evolutionary advantage.



(a)

(b)

Picture 43. Example of pheromone trail formation in dependence on the surrounding environmental conditions (pheromone evaporation rate and pheromone dispersion rate). As can be seen, that if there is no “natural selection” force acting on the pheromone trails (the trails never evaporate, nor disperse) stable paths are always formed no matter the food source location or the number of food sources (picture left). However, if there is a selection force acting on the pheromone trails (negative reinforcement of the trails is possible), semi-stable paths start to emerge and disappear in dependence on food location and distance. In the picture right, after some time, one of the paths was reinforced enough to stabilize. The other one nearly evaporated.



(a)

(b)

Picture 44. Example of pheromone trail formation in dependence on the maximum sensitivity of an ant towards pheromone concentration (if pheromone value is above the antSensitivityMax threshold, the pheromone value is considered to be zero). Interesting to see is, that if the ant sensitivity is unlimited (responding to any pheromone concentration) as shown in the left picture, a stable path between food source and ant nest will not be established. In contrary, if there is a maximum limit on sensitivity towards pheromone, a stable path between food source and ant nest is established immediately. This is because if there is no threshold on the sensitivity towards pheromone, the ants always follow the highest pheromone gradient. But this gradient points towards the ant (which is returning to the nest, moving effectively from the food source rather than towards it). As a result, ants follow other ants to the nest, not towards food. If, however, there is a defined threshold on the maximum sensitivity towards pheromone, some of the ants are able to follow lower pheromone concentration on the edges of the trail, and in some cases finally reach the food source.

Interesting questions to ask the student:

- 1) What is the reason for forming of a positive feedback loop resulting in promotion of one of the food source selection solutions?
- 2) What is the reason for forming a negative feedback loop resulting in demotion of some of the food source selection solutions?

- 3) What does trail evaporation mean? How is it done?
- 4) What does trail dispersion mean? How is it done?
- 5) Why is always the closest food source selected?
- 6) What is the effect of the existence of a maximum pheromone sensitivity threshold?
- 7) What happens if an ant trail never evaporates? How does it affect the systems dynamics?
- 8) What is the potential of this ant behavior in robotics and swarm intelligence? List some application possibilities

As can be seen, even such simple rules can generate a system of remarkable complexity, which in many aspects reflects the dynamics of an ant society. Because the environment of the simulation is Microsoft Excel, it can be immediately made available on most of the computers available in school environments. As a complementary didactical material, it can be utilized in didactics of physics and biology. It is important to be said, that the implementation of the algorithm itself is fairly easy, as the algorithm itself is not complicated. There is a potential of this approach to be utilized in didactics of computer science or programming, as it demonstrates very simple principles of object-oriented approach to programming and such an algorithm could be easily implemented by a talented second grade school student. There is also a vast potential in didactics of cybernetics and robotics, as the utilized algorithm principles in many ways correspond to artificial intelligence and bio-robotic modelling [75]. As can be seen, by utilizing cellular automaton approach for description of a physical system, many interesting systems can be explored, which otherwise would be unavailable for didactical purposes. This promotes interdisciplinary approach to education, which is an undisputable advantage.

4.3 Flocking simulator

A second example of a cellular automaton modelling a physical system is the so called "flocking simulator". The simulator will show some of the basic concepts of

how flocking behavior in bird flocks emerges and what rules can lead to such and interesting dynamics. But first of all, a short theoretical description of the topic will be presented.

4.3.1 Introduction to flocking and swarm formation

A flock or a swarm is usually a cluster of objects (in most cases biological objects of similar size like insects, birds or fish) which exhibit collective behavior (much like ants in the previous example), and is extensively studied in many fields of science, especially in physics, biology, network theory, information theory and computer science [76]. Flocks and swarms are one of the most sophisticated achievements in collective behavior in animal kingdom and are inspiration for both science as well as engineering. The complex behavior is thought to be a result of simple local interactions between individual members, and is again an example how simple underlying rules can form a very interesting and complex dynamics. All swarming systems share some common features like the lack of a central controlling element (a leader), only local perception of the environment, and a fast adaptation possibility to a sudden change in the environment or surrounding. Due to a high degree of emergent behavior (behavior which is not present in the individual agents, but which emerges as a result of interaction of these agents) presence, a swarm can solve complex problems essential for swarm individuals survival – like for example predator avoidance, locomotion energy saving, food gathering or nesting [76]. From a broader perspective, swarm systems are studied in physics as systems which are not in a thermal equilibrium (so called active matter physics and active matter system) [77], [78], however the utilized mathematics is far beyond the target of a second grade student. Therefore, we will utilize the cellular automaton description approach for simulating a simple flocking system to bring this system to the student's attention without relying on mathematics.

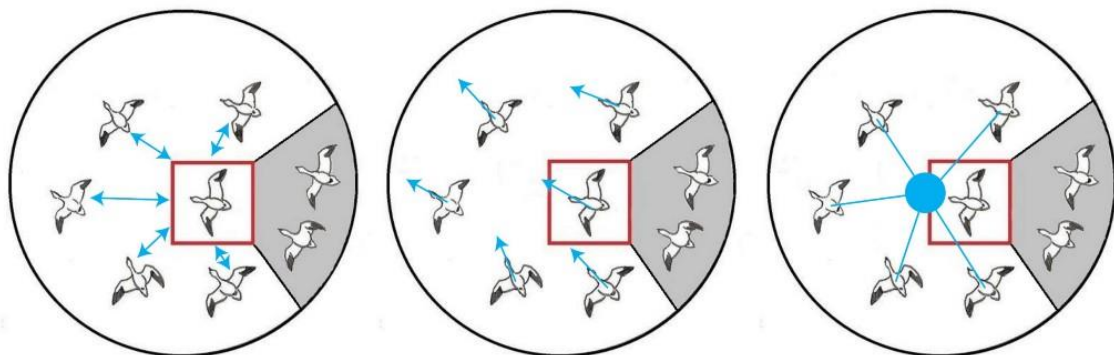
4.3.2 Flocking simulation cellular automaton

Similar to the ant simulator, the universe of the flocking simulation cellular automation consists also of a two-dimensional grid of cells. Each cell can have one

state of a possible set of different states, where a cell state is a discrete number giving information about bird presence, its speed, and its heading. The neighborhood is a configurable parameter, and is usually composed of all cells in a certain radius around a cell. At time ($t = 0$), a state is assigned to each cell in the universe based on the initial configuration of the flocking simulator (let n be the total number of birds, then n cells from the universe are picked by random and a bird with a random orientation is assigned as the cell's state, all the others cells are left blank). The whole cellular automaton is governed by simple rules, which can be described in three sentences:

- 1) If a bird is too close (what is too close is defined by a configurable parameter of the simulator), turn away (change orientation to face in a different direction). This is called separation.
- 2) If a bird is not too close, adjust its orientation to face in an average direction of all birds in its neighborhood (flock) and towards the position average of all birds in its neighborhood. This step is called alignment and cohesion.
- 3) Advance the bird by a certain step (speed is a configurable parameter of the simulator). This is called motion.

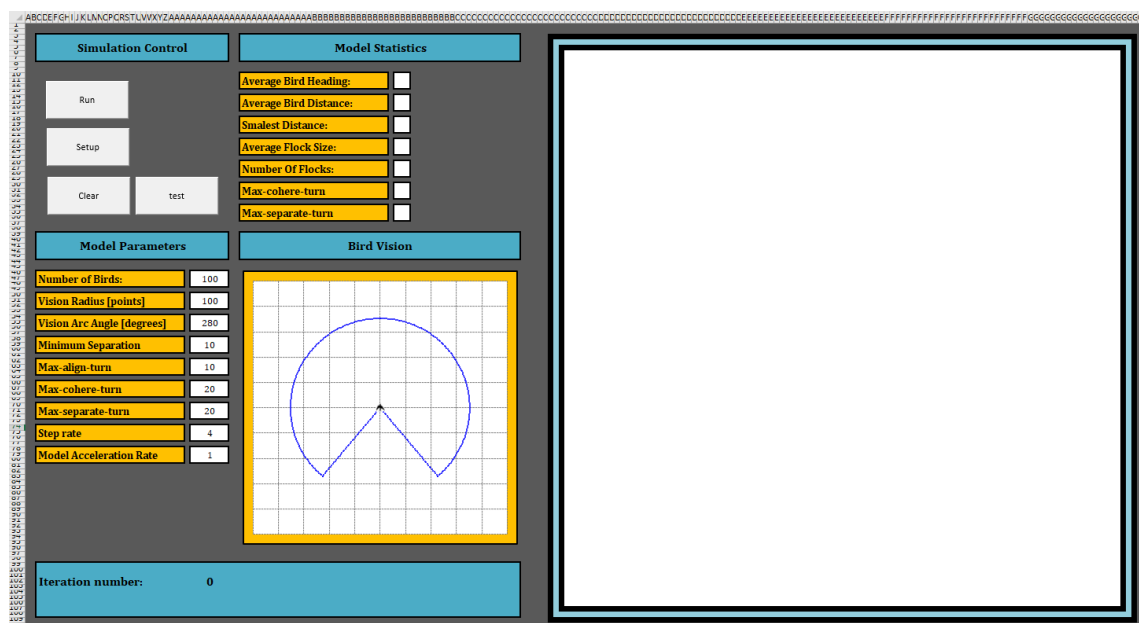
For better visualization of the rules, please see picture 28.



Picture 45. Visualization of the flocking simulator rules. Picture to the most left shows separation behavior, and is the upmost important biological imperative

(collision avoidance is essential for survival and is therefore evaluated first). The middle picture shows alignment behavior - align towards the average direction of surrounding flock members. The right picture shows cohesion behavior – align towards the average position of the surrounding flock members. Alignment and cohesion are the second important biological imperative (staying close together with other flock members assures lesser attack surface and protection) [79].

Also similar to the ant simulator, the simulation itself is carried out in an excel sheet. The excel sheet is divided into 2 separate parts. First, the so called “arena” (see picture 46 right), is the place where the cellular automaton runs. It is in many aspects the same as in the ant simulator with the only difference being the arenas topology, where the ant arena is simply a rectangular “box” with rigid borders and an ant will bounce of these borders, whereas the flocking simulator topology is a torus, and the left and right (or top and bottom respectively) border are wrapped. That means if a bird moves beyond the edge of the border, it appears directly at the opposite border edge of the arena. Second part is the GUI part (see picture 46 left). In this part, the student can modify individual model parameters like number of birds, the visual perception of birds, separation distance and so on to control the simulation.

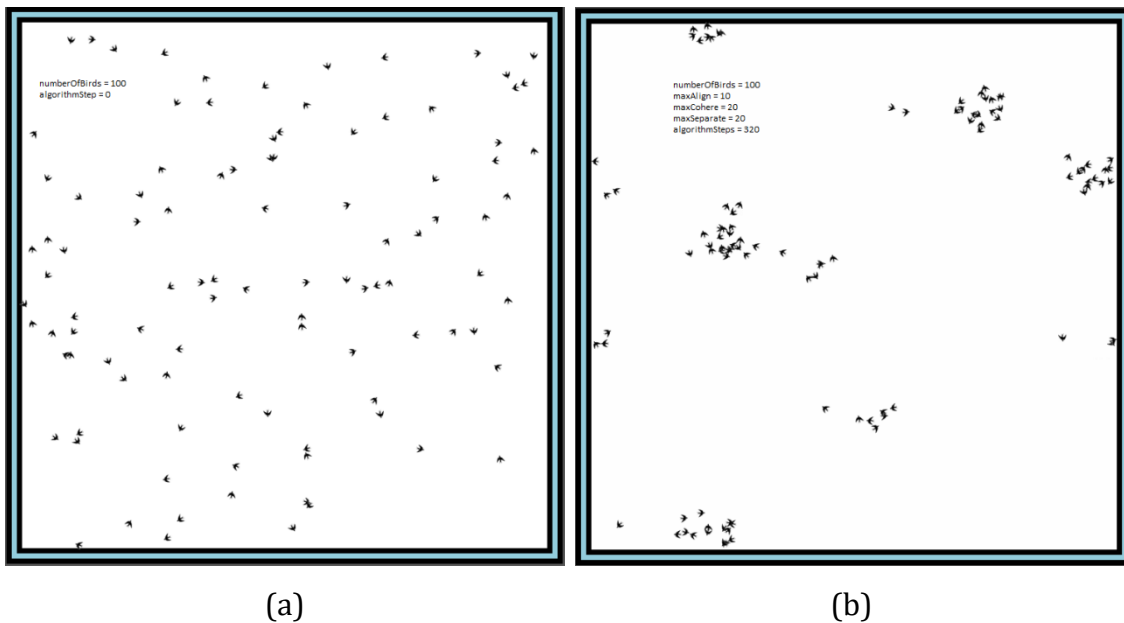


Picture 46. The flocking simulator excel sheet is divided logically into two separate parts. Left, the GUI is intended to adjust the simulation parameters (like number of

birds, or bird vision) and for general simulation control. Right, the “arena” is where the cellular automaton simulation is carried out.

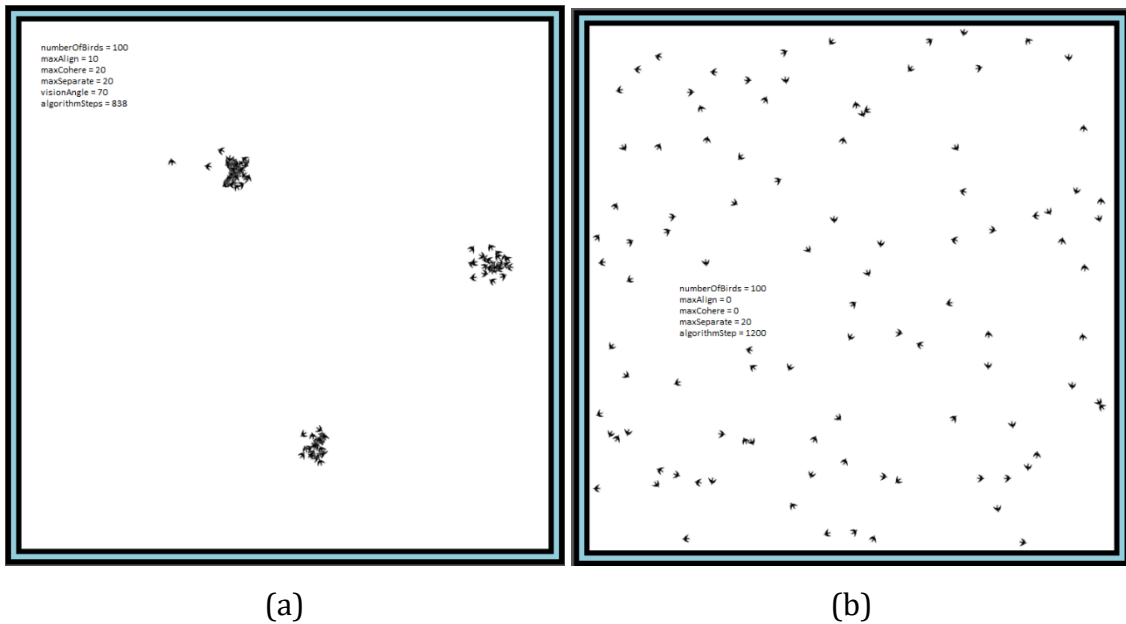
4.3.3 Examples of interesting flocking simulator dynamics patterns

Consistent with other cellular automata, the dynamics observed as a result of the flocking simulator is quite complex, even though the underlying rules are quite simple. Dependent on the automaton’s initial configuration, several very interesting patterns emerge. Let us now discuss some of these patterns in detail, and explore what lead to the observed behavior. Finally, similar to the ant simulator example, and consistent with all the other examples delivered, several questions will be asked, as example questions for students investigating the system.



Picture 47. The picture to the left shows the cellular automaton at time ($t = 0$). As can be seen, bird position and bird alignments are distributed randomly. The picture to the right shows further evolution of the automaton. As can be seen, after only a few steps, the automaton starts to form compact bird clusters, each with a dozen bird individuals. A cluster, once formed, stays reasonably compact. The individual birds perform a circling motion around the center of the cluster, and the central spot itself exhibits a random walk like motion in relation to the ever-

changing bird position distribution. The resulting dynamics is very similar to what can be seen in real flocking systems.



Picture 48. The picture to the left shows, what happens if the bird vision is restricted from its original 360° to only 70° . The flock formation still works, but the clusters are more compact compared to the example with unrestricted vision. This is a result of a change in rule 1. Because the vision is now restricted, far less birds are considered neighbors (flock members) and the collision avoidance behavior towards them is not executed. As a result, the cluster is more compact. The picture to the right shows how the dynamics is affected if rule 2 would be omitted (no alignment and cohesion behavior). As can be seen, the automaton does not form compact aggregates anymore. Although in some cases (when the birds come too close to another bird) a collision avoidance maneuver is executed and as a result the bird heading is slightly changed, the overall dynamics shows bird motion following straight paths.



(a)

(b)

Picture 49. The picture to the left shows, how a restriction of the cohesion behavior affects the overall dynamics. As can be seen, after only a few steps, the bird headings get synchronized for all birds in the cellular automaton. As a result, all birds uniformly fly in the same direction forming a very regular pattern. The picture to the right shows how the magnitude of rule 1 and rule 2 parameters affect the flocking dynamics. As can be seen, under a certain combination of alignment, cohesion and separation, a different flock shape is formed. The flock is no longer a cluster, but while still showing compact behavior, it is stretched in one direction. Under this setting (especially at the distant edges of the flock) birds can spontaneously leave the flock (the forces imposed by rule 1 and 2 are not strong enough to prevent the bird leaving the flock).

Interesting questions to ask the student:

- 1) What behavioral elements need to be present in order to flock?
- 2) Under which minimal vision angle flocking starts to work?
- 3) With limited vision, much more dense bird aggregates form, even the separation distance parameter didn't change. Can you explain why?
- 4) Why do birds in nature form flocks? What is the evolutionary advantage?
- 5) What is the maximum separation distance in order flocking to work?
- 6) What if there is no bird alignment? Will flock still form? Why?

- 7) What happens if alignment, cohesion and separation happen at the same rate? Why?
- 8) Can you name other flocking systems in nature?

4.4 Freeway traffic simulator

The third example of a cellular automaton modelling a physical system is the so called “freeway traffic simulator”. The simulator will show some of the basic concepts of how congestions or traffic jams formations can occur in freeway traffic, even there is no blocking object (like works on road or traffic accident) or speed restriction imposed. The automaton is based on the so-called Nagel–Schreckenberg model, and is an example on how human psychology can have an impact on traffic microstructure, and traffic jam formation. First, some of the theoretical aspects of the Nagel-Schreckenberg model, and traffic in general will be explored.

4.4.1 Introduction to traffic flow modelling

Traffic on freeways is a highly complex phenomenon. Traffic agents, driven by their need to reach their travel targets, form a complicated transport network which is a subject of scientific interest ever since automotive traveling and transportation started to be affordable for the major population. Although the individual agents may (and do) significantly differ in their properties (each human being is an individual, and traffic participants are no exception), they all share the same roads and freeways. By operating on the same resource, the agents interact with one another and form a specific microscopic and macroscopic structure. During the last twenty years, a variety of models describing traffic and traffic flow were developed. While some of the models focus on the time-space evolution of traffic flow quantities like traffic density or velocity, and review the system from a large scale perspective and collective vehicular flow point of view (macroscopic view of traffic flow) [80], [81], [82] other models focus predominantly on the dynamics of individual traffic agents, and how they influence or are influenced by other agents (microscopic view on traffic flow) [83], [84], [85]. Between these two

worlds, there is a variety of hybrid model approaches which utilize in some ratio both the macroscopic and the microscopic perspective [86], [87], [88]. Due to the wide range of application, mathematical modelling of traffic flow remains a big challenge even for scientific research, and is therefore not suitable for didactics of physics in a second-grade school environment with the standard mathematical approach to didactics of physics. However, researchers in [85] showed, that a simple cellular automaton model can be utilized to simulate and explain some of the basic aspects of traffic flow, especially how traffic jams can form without any apparent reason. Such an automaton might be utilized for didactical purpose.

4.4.2 Nagel-Schreckenberg model cellular automaton

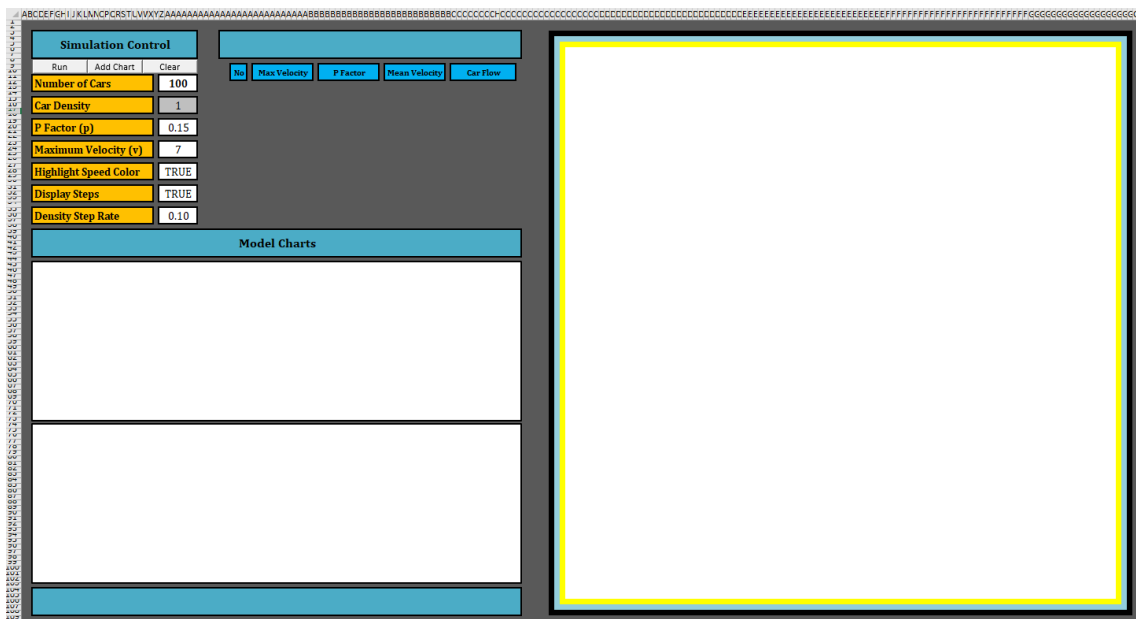
The Nagel-Schreckenberg cellular automaton is much simpler than the previous two examples. The universe of this automation consists only of a one-dimensional line of cells (representing a road), which ends are wrapped (the ends are connected so the whole line forms a circle, much like a giant roundabout). Each cell can have one state of a possible set of different states. It is either empty, or contains a car with an assigned single discrete velocity value. At time ($t = 0$), a state is assigned to each cell by placing a fixed number (configurable parameter of the model) of cars with random initial velocities (between 0 and the maximum velocity). For the cellular automaton the following simple rules apply:

- 1) For all cars, which didn't reach maximum velocity (a configurable model parameter), the velocity is increased by one. This step is called acceleration.
- 2) Each car checks the distance (in cells) to the next car in front of it. If this distance is lower than the actual velocity value of the car, the velocity is adjusted to be equal to the number of empty cells in front of the car (this is done in order to avoid collision). The step is called slowing down.

- 3) For each car with a non-zero velocity, the velocity is reduced by one unit with a certain probability p (for example if $p=0.1$, then in 10% of the cases the velocity is reduced by one unit. This step is called randomization

- 4) At least, all cars move forward by number of cells defined by their velocity. For example, if the velocity is 4, the car moves forward by 4 cells. This step is called car motion.

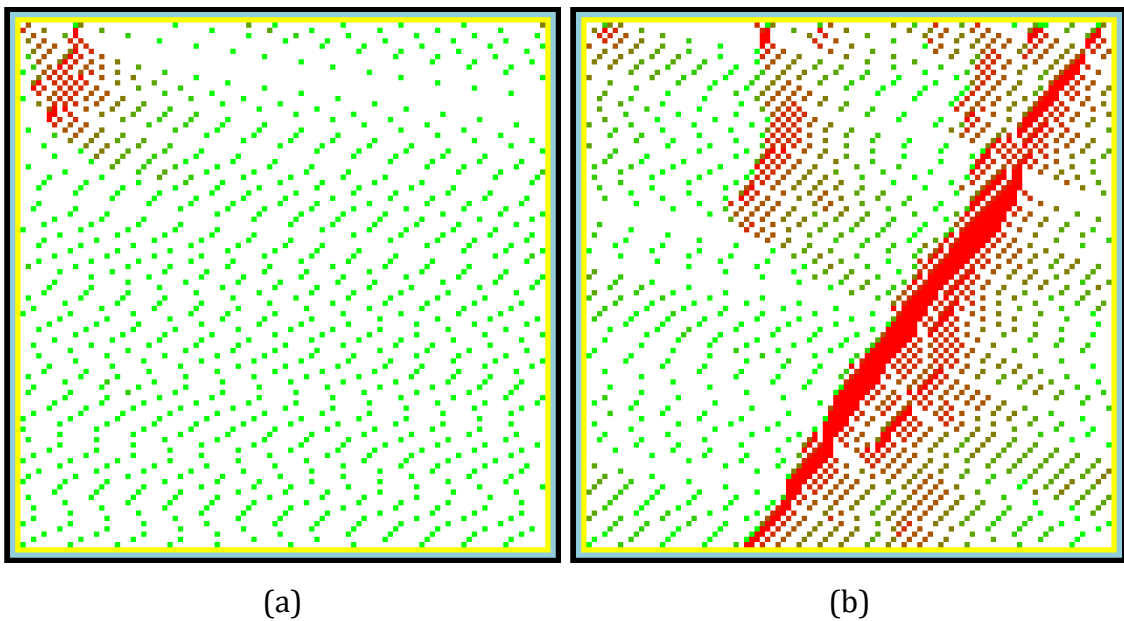
The simulation is carried out in an excel sheet. Again, the excel sheet is divided into 2 separate parts. The GUI part and the arena part (please see picture 50), where the GUI part serves for simulation control and the simulation itself is carried out in the arena part.



Picture 50. The freeway traffic simulator is divided logically into two separate parts (left the simulation control and right the arena where the simulation takes place). The GUI part contains far more charts than the previous two examples. The charts display basic traffic macroscopic quantities – traffic density, traffic intensity and mean velocity and capture the relation between these quantities.

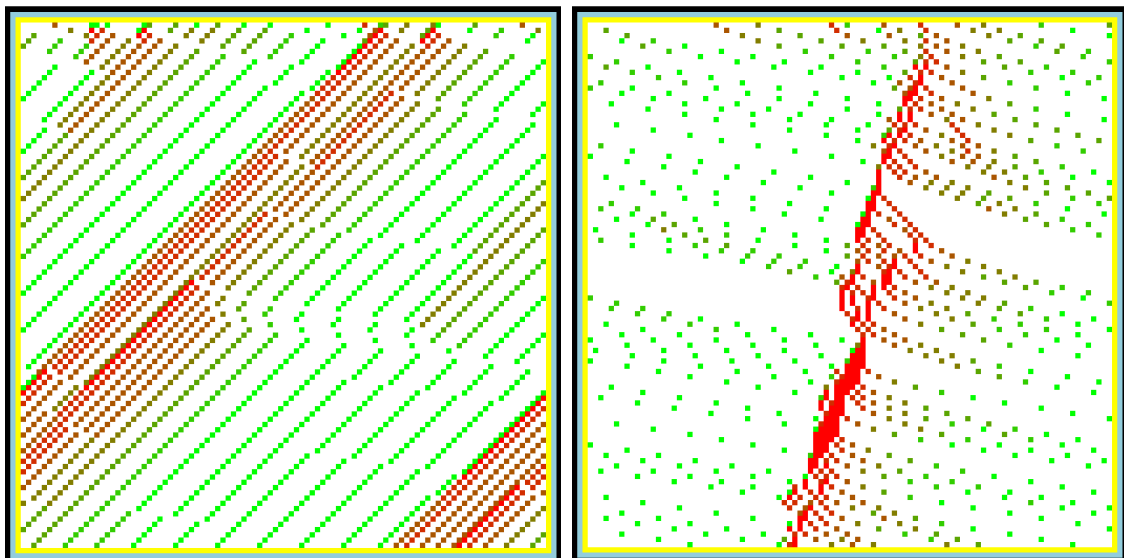
4.4.3 Examples of interesting freeway traffic simulator dynamics patterns

It is not surprising, that the dynamics of traffic flow is heavily dependent on traffic density, and in context of the Nagel-Schreckenberg model, also heavily on the step 3 probability (please see the cellular automaton rules – step 3 in the previous chapter). In fact, the stochastic parameter p is fundamental. Without it, the model is reduced to a deterministic cellular automaton, where the cars move in a set pattern and do not model the behavior of a real human driver anymore. The stochastic parameter p is what allows for spontaneous traffic jam formation in this model [89]. The following examples (summarized in pictures 51-54) show, how the dynamics can change with increasing traffic density (number of cars) and how it is dependent on the noise parameter p .



Picture 51. The picture left shows the evolution of the automaton with 10 cars and $p = 0.15$. Car speed is highlighted by color, where brighter shades of green correspond to higher car speed and shades of red correspond to low speed (eventually zero speed for dark red). As can be seen, even though there was a randomly introduced congestion (upper left part of the picture), it quickly dissolved and never formed again. The car density is simply too low to spontaneously form traffic jams. The picture right shows the same simulation, however the number of cars was doubled (now featuring 20 cars). As can be seen, although the noise parameter didn't change ($p = 0.15$), a traffic jam formed (thick

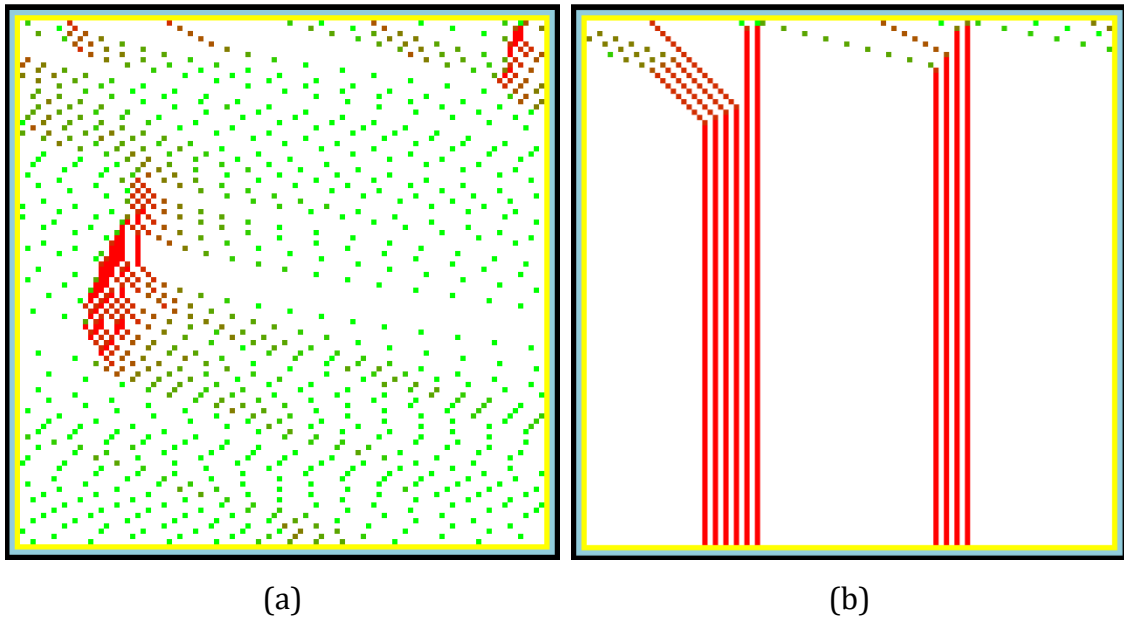
red line). With increasing algorithm steps, the traffic jam seems to be moving to the left. The same dynamics can be experienced in real freeway traffic, where sometimes a traffic jam forms out of nowhere (such a jam is also called a ghost jam) and the resulting disturbance in the car distribution starts to travel backwards in form of a wave (sometime also called a traffic wave).



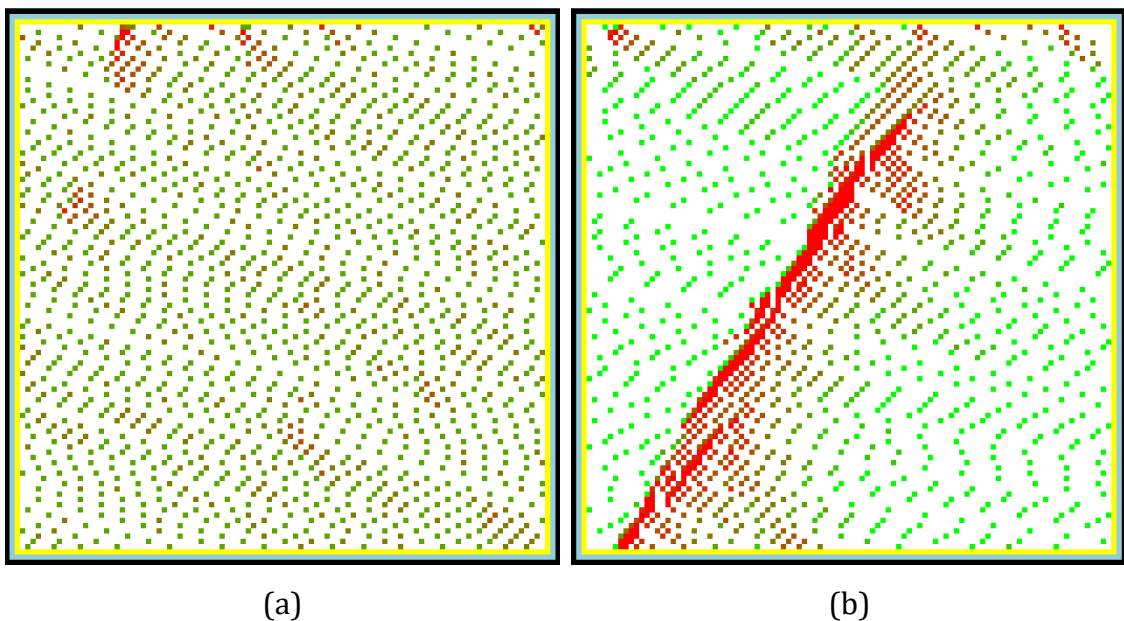
(a)

(b)

Picture 52. Influence of the stochastic parameter p on the model behavior. The picture left shows evolution of an automaton with 20 cars, but an extremely low noise parameter ($p = 0.01$). As can be seen, the automaton is reduced to a deterministic model and no traffic jam formed (compare to picture 34 right), where for the same number of cars a traffic jam formed immediately with a noise parameter $p = 0.15$. The picture right shows evolution of an automaton with only 10 cars, but with a high noise parameter ($p = 0.40$). It can be seen, that even with a small number of cars, a traffic jam can form if the noise parameter is high enough (compare to picture 51 left where for the same number of cars but with a lower noise parameter a traffic jam didn't form).

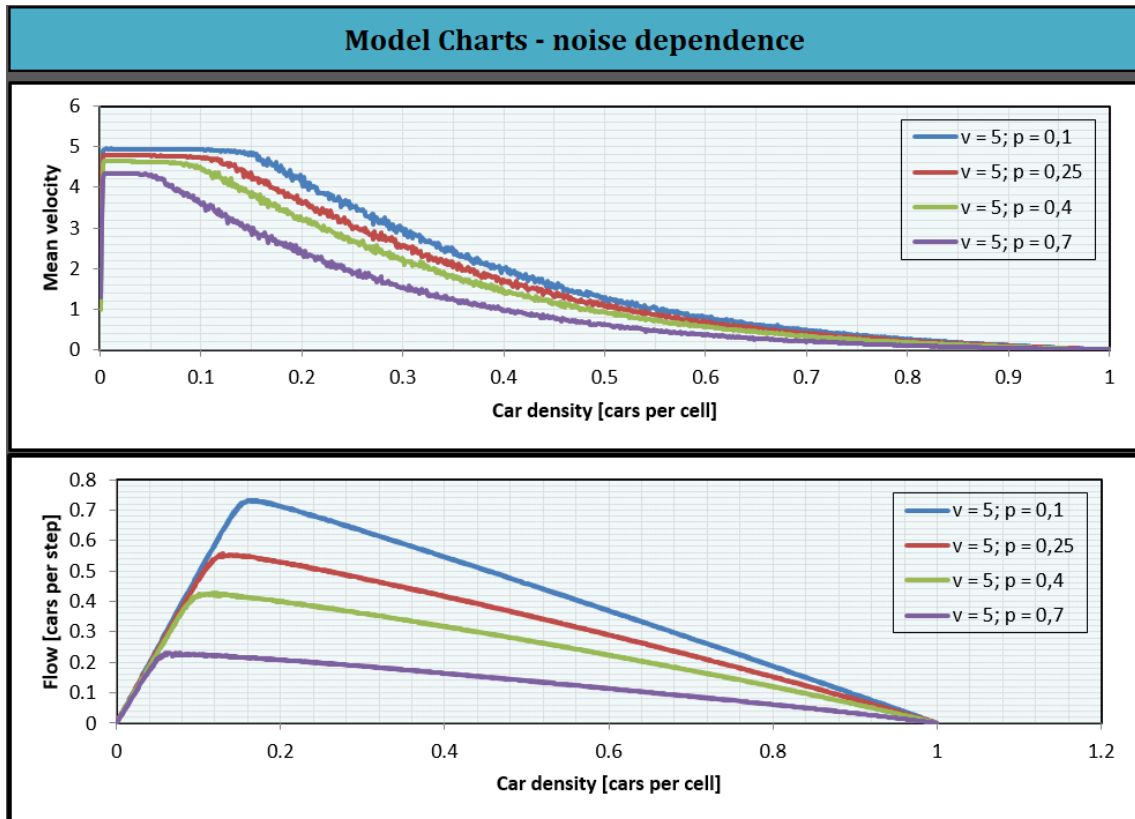


Picture 53. Similar to real road traffic, a traffic jam can form spontaneously, and can also spontaneously dissolve (see picture left; number of cars = 10, $p = 0.4$). Picture to the right shows what happens if the noise parameter is equal to 1. The resulting model is reduced to a deterministic cellular automaton and does not reflect real road traffic anymore.

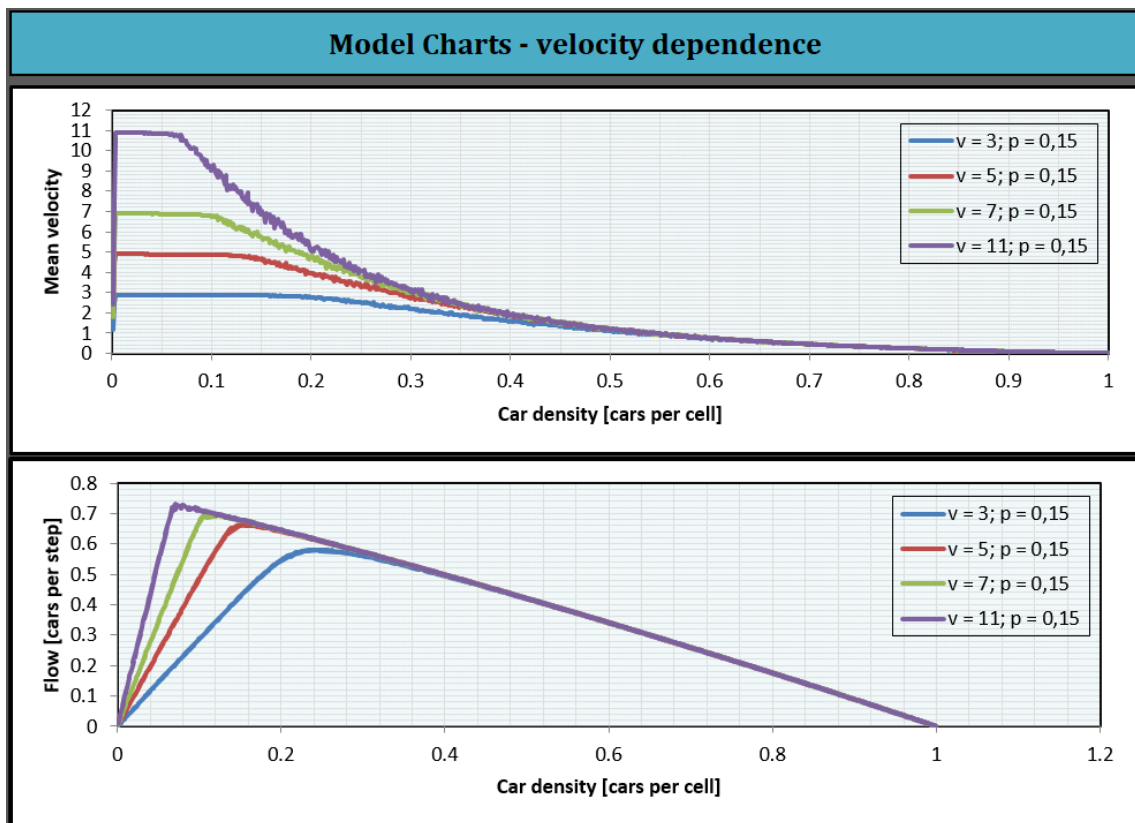


Picture 54. The influence of maximum velocity on the model dynamics. Although both pictures (left and right) share the same number of cars and noise factor (number of cars = 15, $p = 0.2$). In the picture left (maximum velocity = 4) traffic jams do not form. In the picture right (maximum velocity = 7) a traffic jams forms almost immediately. It is widely known, that maximum velocity can have a big

impact on traffic jam formation. In fact, in many countries inclusive Czech Republic, freeway traffic is usually monitored and simulation of future system development are carried out. Based on simulation results, maximum speed is adjusted to prevent spontaneous traffic jam formation and optimizing car through put rate (traffic intensity). This allows for better road (limited resource) utilization.



Picture 55. Upper figure shows a mean velocity vs density plot for several different noise parameters p . As can be seen, with increasing noise, there is a lower mean velocity for the traffic flow, and traffic starts to condense (sudden break down in mean velocity) at lower densities. The condensation is a sign of congested traffic. The lower picture shows the fundamental diagram (special diagram utilized in traffic research showing a plot of traffic intensity vs traffic density) for several different noise parameters p . This diagram shows a sudden break down in traffic intensity highlighting that from a certain density, the traffic intensity stops to grow and starts decrease almost linearly. As can be seen with increasing noise, this breakdown point is shifted to lower densities, and affect the maximum traffic intensity.



Picture 56. Upper figure shows a mean velocity vs density plot for several different maximum velocity parameter values. As can be seen, the higher the velocity limit is, the sooner (sooner means at lower densities) the transition to congested flow happens. The lower picture shows the fundamental diagram for several different maximum velocity parameter values. As can be seen, with increasing maximum velocity limit, the flow intensity gradient is also increasing, but the transition to congested flow is sharper and happens at lower densities.

Interesting questions to ask the student:

- 1) How does the noise parameter p affect traffic jam formation?
- 2) What does the noise parameter p represent in real road traffic?
- 3) What model setting allow for best resource (road) utilization (maximum traffic intensity)?
- 4) What is a fundamental diagram?
- 5) Why do traffic jams appear out of nowhere?
- 6) How does vehicle speed affect traffic jam formation?

- 7) Why does a traffic jam seem to move backwards against traffic flow?
- 8) Is it possible for a traffic jam once spontaneously formed to also spontaneously dissolve? Can you adjust the model settings to show an example?

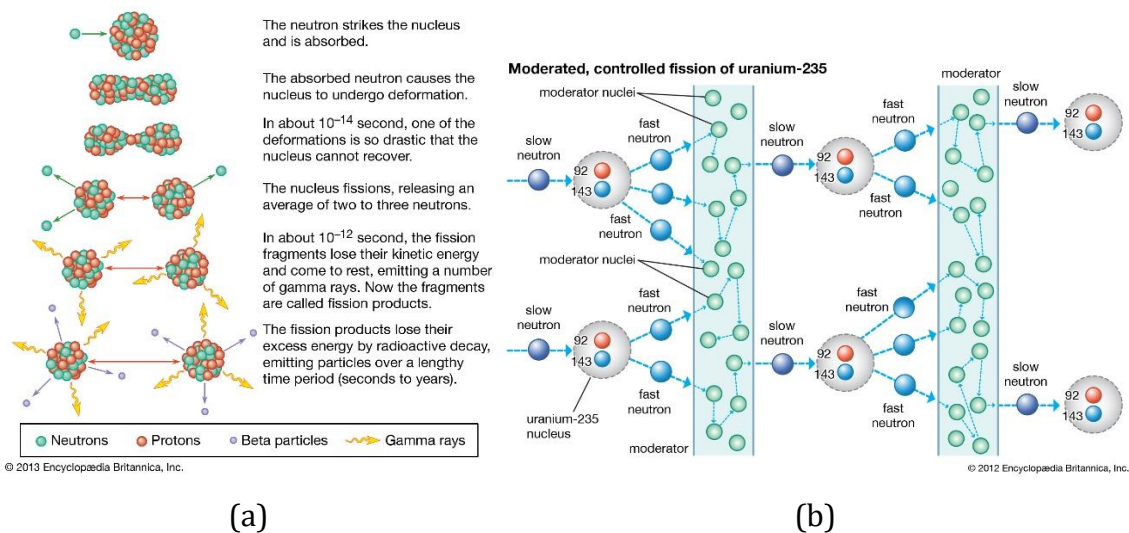
4.5 Further simulator ideas and potential in didactics of other school subjects

Due to the vast range of application of cellular automata (as demonstrated in chapter 1), and due to their extensive ability to model all different kinds of systems in nature (as asserted in chapter 2), cellular automata certainly show great potential also in didactics of other school subjects. Some promising models with great didactical potential (which in their nature are easily implementable by a cellular automaton) will be shown. As discussed in the previous chapters nearly any natural phenomenon can be modeled by a cellular automaton, but because the target group are mainly first grade or second grade students, models with interesting dynamics or models which yield complex or aesthetic patterns were chosen, simply to attract and provoke curiosity in students.

4.5.1 Nuclear reaction simulation

In physics and in chemistry a process called nuclear reaction is well known and is studied in physics or in chemistry class throughout the world. In a very simplified schematical description, the process involves two nuclei (or a nucleus and a subatomic particle) which collide and produce new nuclei or new subatomic particles. One of the most prominent examples of a nuclear reaction is the nuclear controlled chain reaction of Uranium-235 in nuclear power plants or in nuclear weapons. The reaction starts, when a Uranium-235 atom absorbs a neutron, and as a result, fissions into two fragments releasing three new neutrons and a vast amount of energy. If further Uranium-235 atoms are present, they might collide with the newly generated neutrons and the fission process repeats, releasing even

more neutrons and more energy (see picture 57 – a). In power plants, this reaction is controlled by an additional mechanism, which absorbs (or slows down) some number (the number can be controlled) of the fast neutrons prohibiting their future collision with a Uranium-235 atom and a potential fission (see picture 57 – b). The process is schematically described on picture 57.



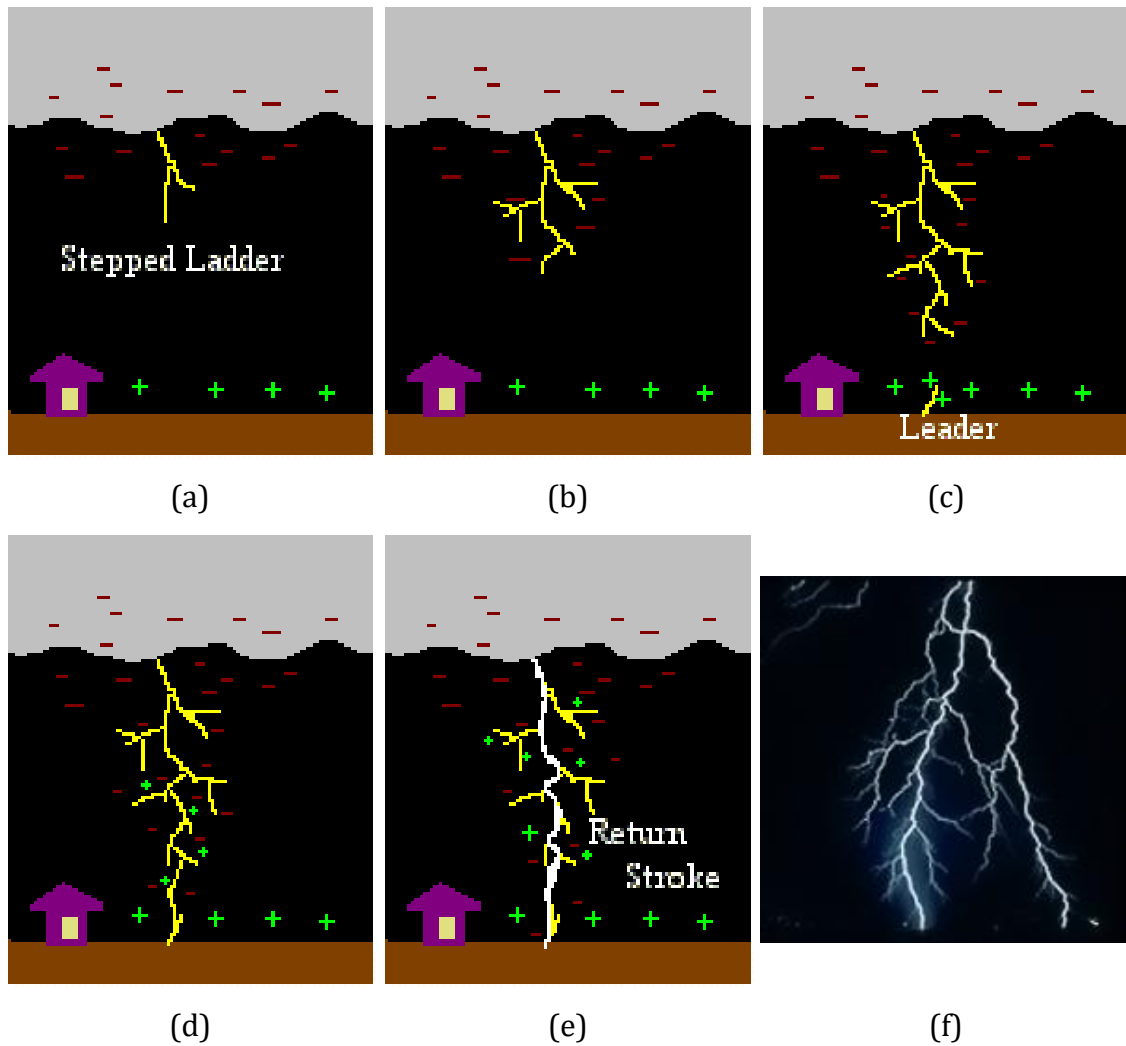
Picture 57. Schematic representation of a controlled nuclear fission of uranium-235 [90].

What one can immediately notice is how easy this process could be modeled by a two-dimensional cellular automaton. This automaton would consist of certain cells representing the Uranium-235 (with colors representing before/after collision states), other cells would represent neutrons (with cell states either “present” or “non present”) and yet other cells would represent the moderator (a neutron cell colliding with a moderator cell would switch to “non present”). A control GUI of this automaton would interface with the student and assure the model is configurable (the student could set the number of Uranium-235 cells, number of initial neutron cells, number of moderator cells, it could provide options for random initial cell distribution or allow for certain structures to be set) and a certain chart filed showing the cellular automaton current macroscopic state (how many Uranium-235 cells are still present, how many neutron cells are present, what is the amount of released energy or if the reaction is increasing or diminishing. It could even report if the reaction is out of control and if the reactor

will explode). Certainly, it would allow for an interactive environment, in which the student could learn a lot not only about nuclear reactions or nuclear power plants, but also about self-regulating systems.

4.5.2 Lightning strike simulator

A lightning strike is an electrical discharge between atmosphere and ground. It often occurs in nature as a repeated event during a storm and is visually very impressive. In a simplified understanding, the lightning strike starts in clouds by a polarization of positive and negative charges within the cloud. Usually, the positive charges accumulate at top of the cloud and the negative charges at bottom. As the static charge in the cloud builds up, it starts to ionize the surrounding air, making it more conductive. Electrons start to travel through the conducting air forming a *step ladder* (with a familiar zig-zag pattern which is thought to be attributed to dust particles present in the atmosphere). As the step ladder approaches the earths surface, positive charges from the earth start to migrate upwards towards the step ladder. The upwards migrating positive charges are often referred to as *streamers*. Once contact between the streamer and ladder is made, the positive charges on the earth surface fly very quickly towards the negative charges in the cloud. The flash of light seen is called lightning. A schematic representation of whole process can be seen on picture 58 a-e.



Picture 58. A schematic representation of how a lightning strike forms (a-e). On picture f (bottom right) a picture of a real lightning is shown. [91]

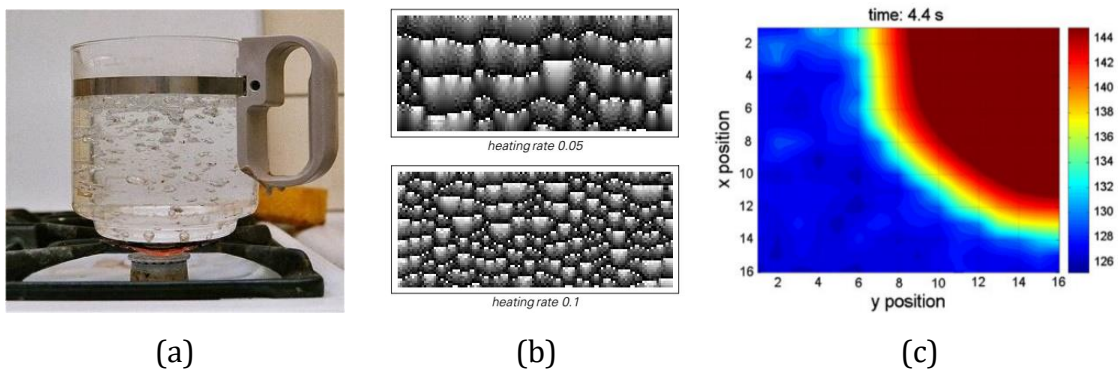
It needs to be mentioned, that the above-mentioned description is extremely simplified and in fact one needs to have deeper understanding of electrical physics and thermodynamics to have at least some understanding of the process. It needs to be pointed out as well, that even though this phenomenon is subject of scientific research for many decades, the process is not yet fully understood. Therefore, a cellular automaton model of this process could certainly support in teaching of this complicated matter. The cellular automaton again could contain a GUI and an arena where the actual automaton would run. Inside the arena, three separated areas (cloud, air and ground) would contain specific types of cells. The cloud cells (at the bottom region of the cloud) would be generated by random at initialization phase of the automaton (the exact number of charge cells would be a configurable

parameter) and would perform random motion inside the cloud. The air area would contain randomly distributed dust particles (the number and maybe also the distribution pattern could be a configurable parameter). The ground area would contain cells representing positive charges and could contain some peak-like positive charge displacements (representing houses or trees) which would be a subject of initial configuration and could be placed randomly in the ground area. During the actual run of the automaton, certain rules (gradient rules similar to the ant simulator related to positive and negative charges would represent the electric field, certain random walk rules including the dust cells would assure the top-down movement of negative charges from the cloud toward ground). Finally, when the random path like trajectories of the step ladders and the streamers connect a discharge would be released (basically just a graphical highlighting in white, blue or yellow of the drawn trajectories). Such a cellular automaton could help to provide a solid understand of the rules behind lightning strike formation just by focusing on charge movement rules instead of the complicated underlying forces behind the charges themselves. This would make the topic more accessible for first and second grade student.

4.5.3 Simulation of water boiling

Everybody who prepared tea or who cooks eggs for breakfast knows the phenomenon of water boiling and how fascinating it is. As a standard in today's first and second grade physics class, the water boiling phenomenon is simply explained as the related phase transition of water to steam which occurs in water when a certain boiling point heat threshold is reached. The physics behind the intriguing (seemingly random) bubble pattern formation and the specific noise which boiling water is producing is usually completely omitted. When water boils, a certain kind of inhibition process occurs (in some way similar to dendritic crystal growth), which is related to the energy consumed by the phase transition of water to steam. As the steam bubble forms, the necessary phase transition energy is drawn from the surrounding water heat, decreasing locally its temperature and inhibiting further boiling its direct vicinity [3]. This phenomenon can be very easily

simulated by a two-dimensional cellular automaton [92]. The principle is based on a slight disproportionality of the heat distribution among the cells (each cell state is defined by an integer number representing the temperature) which is randomly set up during initialization phase of the automation. After the water (cells in automaton) is heated (gradual step by step increase of the integer number of each cell which represents the temperature) and upon certain cells reach the phase transition temperature, energy from surrounding cells is drained (a process similar the diffusion step of the ant simulator but with an opposite gradient). If the cell temperature is represented by color, interesting bubble patterns will form, much like patterns in a glass of boiling water.

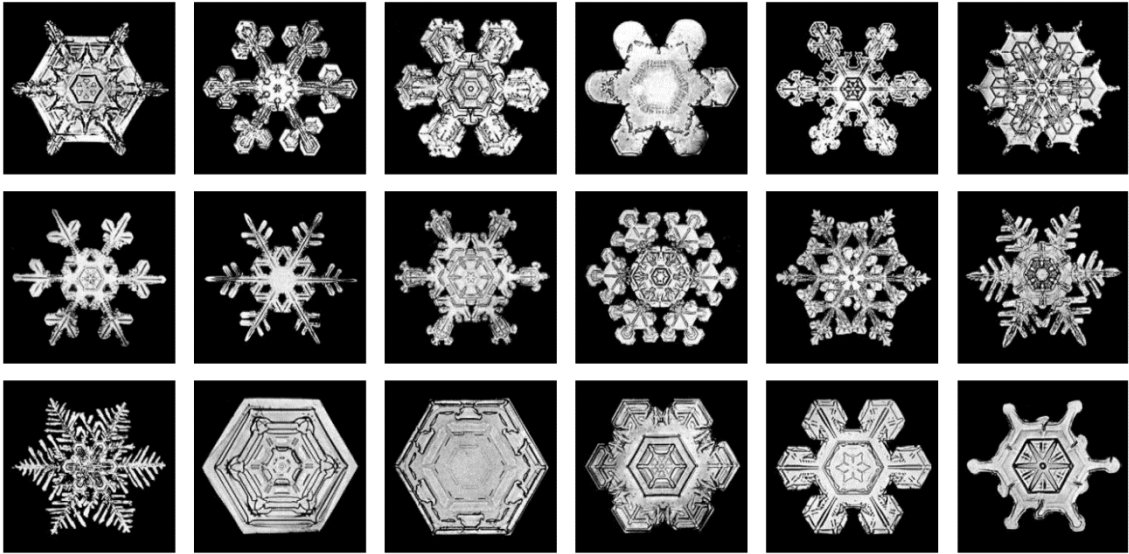


Picture 59. A real glass of boiling water (a) [93] a one-dimensional cellular automaton output pattern simulation boiling water (b) [3], and a two-dimensional cellular automaton showing heat transfer in a bubble (c) [92].

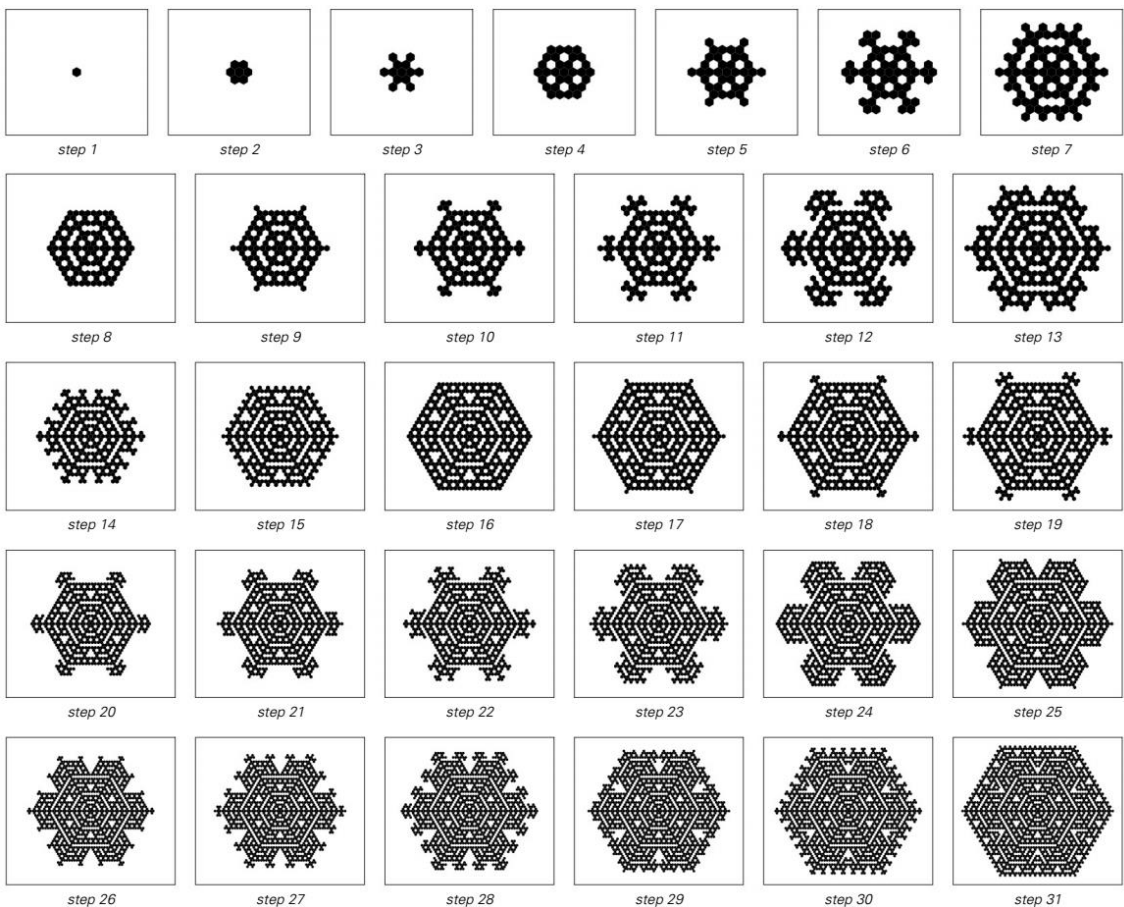
4.5.4 Crystallization of water and snowflake formation

It is well known, that water, upon freezing, can generate strikingly beautiful patterns. The physical mechanism behind snowflake formation is very similar to the boiling mechanism described above, but goes in the opposite direction. Once a certain part of the forming snowflake solidifies (freezes), certain amount of heat is released, preventing the water in its direct vicinity from further freezing. This simple rule, when reflected by a simple two-dimensional cellular automaton can generate patterns which remarkably resemble real snowflake patterns [3]. For

comparison see picture 60 (real snowflakes) and picture 61 (cellular automata generated patterns).



Picture 60. Example of different shapes of real snowflakes [3].

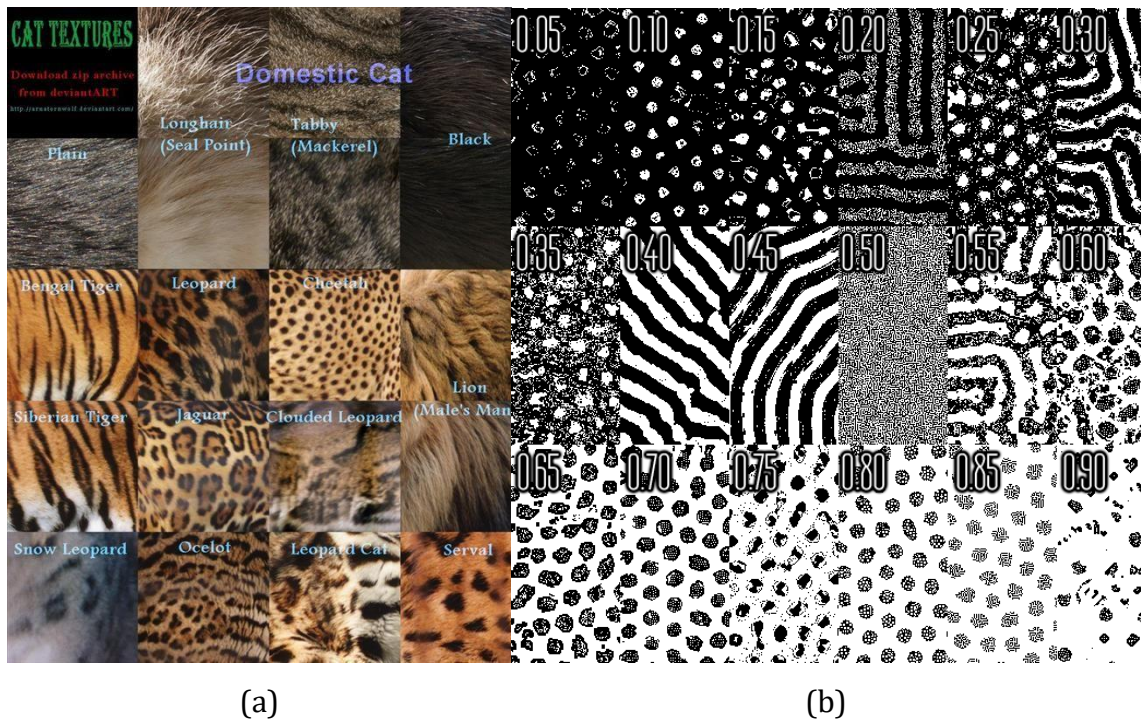


Picture 61. Evolution of a two-dimensional cellular automaton. The automaton rule states, that a cell shall be black in the next step only if exactly one of its neighbors

was black in the previous step. The patterns are remarkably similar to real snowflakes [3].

4.5.5 Fur pattern formation

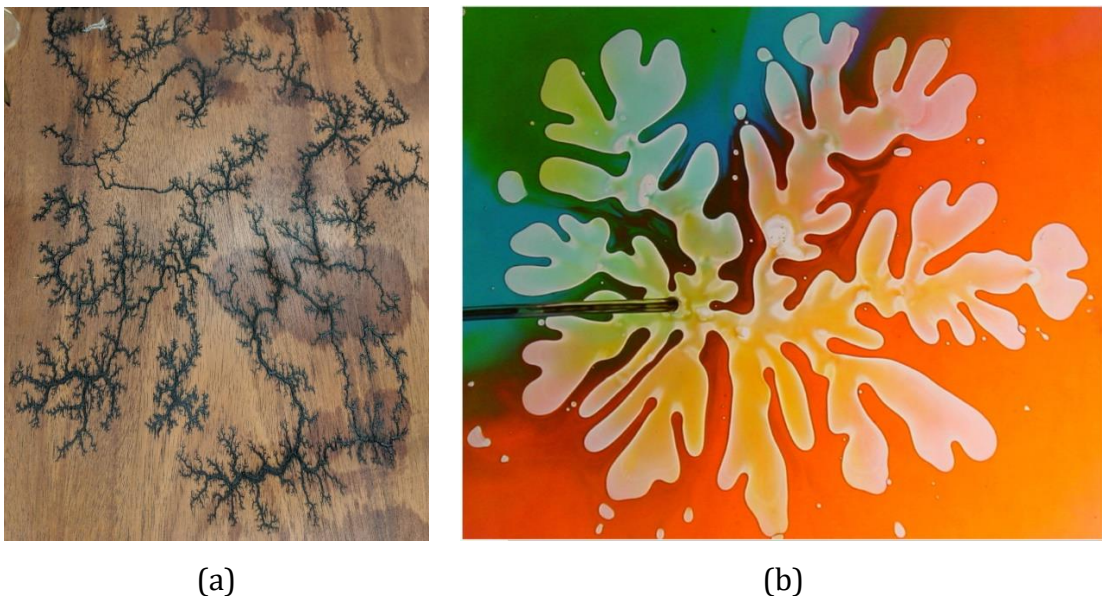
In animals interesting fur coat or skin patterns emerge. This pattern formation is thought to be a result of evolution, as animals with specific coat patterns gain a significant survival advantage. Some animals develop patterns which help them blend with their environment to avoid potential predators [94], other (often poisonous) animals show bright colored warning patterns to scare of an attacker [95]. The mechanism of the cellular automaton class resembling these kinds of patterns was discussed in chapter 2. Here, I would like to present a comparison between real fur patterns and cellular automaton outputs to further highlight how similar they can get – see picture 62.



Picture 62. Fur textures of real feline like animals (a) [96] vs patterns generated by a cellular automaton (b) [97].

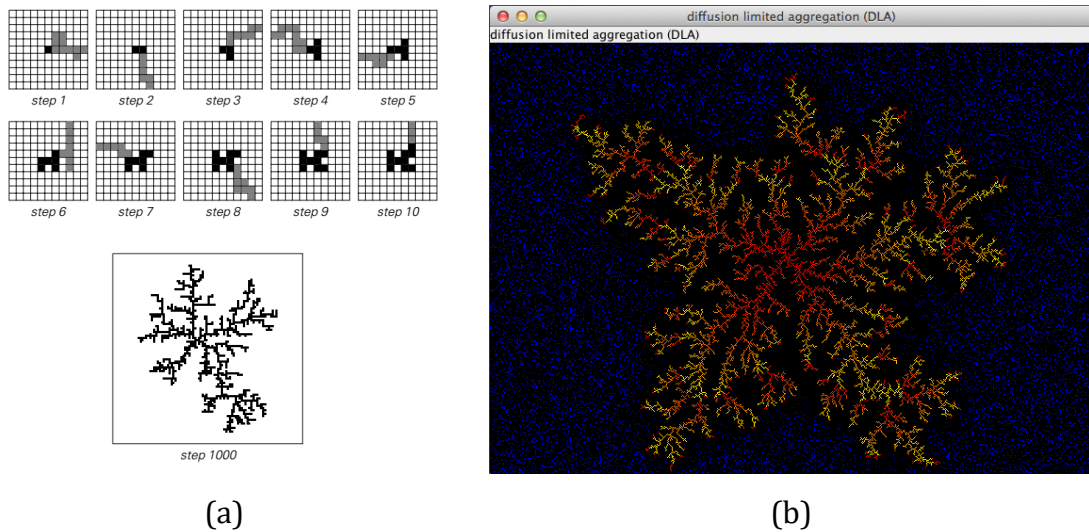
4.5.6 Diffusion-limited aggregation

Diffusion-limited aggregation is a process often described in chemistry and physics, which is related to processes where particles perform a random walk due to Brownian motion and then settle and form aggregates. They often occur in systems where diffusion works as the primary mechanism for particle transport [98], and can be observed in many systems including mineral deposit, dendritic growth of crystals, coral growth, but also in a system with a dielectric breakdown or the Hele-Shaw flow (flow between two parallel plates separated by a very small gap) which can sometimes be observed when injecting a large quantity of oil into water. The fractal like patterns generated by these systems are visually very intriguing and could therefore provoke interest in the topic in students. They are extremely hard to rigorously study and only a few non-trivial solutions are known [99], but are very easy to reproduce with a cellular automaton. The idea behind the cellular automaton is to add cells to a cluster based on a random walk picking of the added cell position. The random walk starts far away from the cluster, but once the random-walking cell reaches a cell adjacent to the cluster, it will keep its position. Only one cell at a time can perform this aggregation algorithm [3].



Picture 63. Left (a) a so-called Lichtenberg figure burned into wood. Such figures often appear within dielectric breakdown and is an example of a diffusion-limited

aggregation pattern [100]. Right (b) shows a viscous fingering picture often occurring in Hele-Shaw flow [99].



Picture 64. Picture left (a) shows a diffusion-limited aggregation model based on a simple cellular automaton described in [3]. Right picture shows a multi color example of the aggregation where the cell colors were chosen based on time of arrival of the random particle [101].

4.5.7 Cellular automata in didactics of computer science

An absolutely typical example is the application of cellular automata in didactics of computer science and informatics. Not only that computer science directly borders on physics (system modelling is a typical tool used in physics, and computer science provides one of the most common tools utilized in modelling of these systems – programming languages and computers), cellular automata themselves are also a typical field of study in computer science, due to their connection to artificial languages and automated computing. There is however a fundamental difference in the substance of the didactical aspect. While for physics (and also other similar subjects, like biology or chemistry as will be shown later in this chapter) the potential of cellular automata lies in their ability to describe a complex system with simple rules - which can be expressed in natural language, for computer science, the benefit is simply the fact, that they can be very easily implemented in any programming language. That makes them perfect as a sandbox environment

for demonstrating basic programming archetypes as are for example object-oriented programming, accessing classes and methods, working with arrays and indexes or parsing strings and basic MISRA application. To further demonstrate this concept, let us return to the ant simulator example described in chapter 4.2. Even though the ant simulator looks complex, it in fact is not. Very basic programming tools and very basic object-oriented approach was utilized in its implementation, and any second grade student interested in informatics and programming can implement a similar automaton. As an example, refer to picture 65, which shows two print screens of two ant simulator source code parts. Both source code examples show basic programming structures taught in programming classes.

<pre> For antIndex = 1 To n oColl_ants.Add New clsAnt oColl_ants.Item(antIndex).antShape = ActiveSheet.Shapes(antIndex) oColl_ants.Item(antIndex).antName = "Ant " & str(antIndex) oColl_ants.Item(antIndex).antStatus = "searchingForFood" oColl_ants.Item(antIndex).antShape.Rotation = rand(360) oColl_ants.Item(antIndex).antShape.Top = y oColl_ants.Item(antIndex).antShape.Left = x Next </pre>	<pre> Function BubbleSort(ByVal v_tempArray As Variant) As Variant Dim v_Temp As Variant Dim i As Integer Dim b_NoExchanges As Boolean Do b_NoExchanges = True For i = 0 To UBound(v_tempArray) - 1 If v_tempArray(i) > v_tempArray(i + 1) Then b_NoExchanges = False v_Temp = v_tempArray(i) v_tempArray(i) = v_tempArray(i + 1) v_tempArray(i + 1) = v_Temp End If Next i Loop While Not (b_NoExchanges) BubbleSort = v_tempArray End Function </pre>
(a)	(b)

Picture 65. Screen shots of source code parts of the ant simulator. Only very basic programming principles were utilized, making the source code easily accessible to any programming student. Picture left (a) shows an example of how ants are initialized at the beginning of the simulation. An array of instances of the clsAnt class is iteratively generated and configured by a for cycle. Picture right (b) shows a classic example of a sorting algorithm commonly known as bubble sort which is a standard example used in any programming class.

5. Cellular automata and the physics of traffic

As could be seen during the exploration of various cellular automata and their ability to model interesting phenomena in nature, the underlying rules of even a very complex system do not necessarily need to be complex as well. Remarkably simple rules can capture the essential mechanisms responsible for many phenomena seen in nature. Some of the phenomena (usually the very basic phenomena easily described by mathematics) are subject to school education, other are not yet fully understood and are subject to scientific research. The ability of cellular automata as a new kind of description tool to be applied both for known phenomena as well to unknown phenomena make it a very interesting tool to be utilized in didactics of physics. It does not only make it possible to investigate complex systems that border on several school subjects (like ants in physics, biology or computer science, or snow flake formation in chemistry and physics) but also promotes synergy between individual school subjects. It can be in the same way utilized to explore systems that are not yet “discovered” and that are currently subject to scientific research. Similar to the promotion of interdisciplinary thinking, this approach promotes synergy between science and education. It encourages and supports a student in trying to figure out, why an unknown, not yet understood system exhibits a certain behavior, and puts them temporarily in a role of a researcher. They are challenged to try out their reasoning and critical thinking, and explore their creative potential to come up with some think new. In this way, a student can not only learn to understand, but a student can learn how to think [102].

In this chapter, some of our recent research on physics of traffic will be presented where simple cellular automata were utilized to model the studied systems. In contrary to the previous chapters, this chapter will utilize a far more mathematical approach and a more rigorous language for describing the explored systems, following standard notion utilized in theoretical physics. And it will seem to the reader that the whole style in which this thesis is written has changed. The reader, until now exploring certain new concepts in didactics of physics, will be challenged with concepts and language utilized in theoretical physics rather than in didactics,

which at first can look confusing. The reader could argue that it does not correspond to the topic of this thesis at all, but there is a certain very important logic behind why the following chapter is part of this thesis. This whole thesis emphasizes a certain (highly theoretical) concept, namely that cellular automata represent a completely new and fundamentally different approach for description of physical systems, and that this approach has a certain potential in didactics of physics. It was argued, and backed up by multiple examples and numerous references, that cellular automata basically embody a new description language and represent therefore potentially a completely new vector of approach in didactics, bordering upon being a completely new paradigm in education. Therefore, it is so much important to prove, that when cellular automata are being referred to as a new “language”, they should be capable of delivering the cognitive access to literally any topic, no matter how complicated or abstract it may be. Therefore, in this last chapter a completely different topic is raised (physics of traffic), and although accompanied by advanced statistics and within the framework of random matrix theory, there is always a cellular automaton utilized in describing the topic. It is therefore always possible to understand any of the modeled systems and any of the assessed topics, just by understanding the governing rules of the corresponding cellular automaton. This should act as a proof of concept - a proof that cellular automata are powerful enough to explain even the most theoretical concepts about physics of traffic in a natural language, which is otherwise only explainable by the formal language of mathematics.

5.1 Quantitative analysis of probabilistic dependencies in a thermal balanced traffic gas

As briefly discussed in the previous chapter about traffic flow modeling, traffic in its essence is a highly complex phenomenon. The agents (traffic participants) exert influence on each other during their trips, and organize themselves in a very interesting way, which leads to emerging of complex micro structural patterns. A key aspect of the system is the interaction happening between the traffic participants, and a lot of thought has been given about the nature of these

interactions, especially about their range. While some of the research on traffic considers the interaction to happen only between the directly neighboring agents (short-ranged interactions) [85], [103], [104]. Other research suggests that there might be more agents interacting [105]. The interaction range is a measure of how many cars ahead of the driver's car still have influence on the driver's decision making, and this chapter will explore some of the tools which might be utilized to quantify (in a sense to assign a certain real number) this measure. The tools (mainly mathematical tools) are quite simple and can easily be a subject of technical university study for a bachelor degree. To create the substrate on which these tools can be tested a cellular automaton approach will be utilized. The reason for this is the ability of a cellular automaton to generate a complex enough system to reflect reasonably on real road traffic, while still maintaining a good enough ability to design the microstructure of the system just by carefully choosing the underlying automaton rules. The approach is not very different from the presented cellular automaton utilization approach in didactics of physics. First, a simple way how to generate complex behavior is selected (the cellular automaton), and then the dynamics of the system is studied by utilizing certain tools. The difference here is, that for the scientific perspective (or educational perspective at university level) the tools utilized to study the system might be quite advanced (rigorous, mathematical approach) while for first and secondary grade school a verbal description or a visual evaluation is quite sufficient to have a grasp on the core properties of a system.

5.1.1 Model description

The model utilized to study the interaction range and related applicable tools for its quantification is based on the modified Metropolis algorithm [106], [107], [108] (the algorithm is part of the Markov Chain Monte Carlo method family of algorithms). From physics point of view, the operation of the automaton can be understood as relaxation of a one-dimensional gas (one dimensional set of particles) towards its thermal equilibrium (the ensemble of particles exerts repulsive force on each other, until they reach some equilibrium state – much like a

classical gas exposed to a thermal bath). From traffic research point of view, the particles are considered traffic agents and the repulsive forces acting represent the collision avoidance behavior of a driver. It is well known, that once this gas (also called traffic gas) stabilizes in its equilibrium state, the resulting interparticle spacing statistics (i.e., the spacing distribution) is very similar to intervehicle spacing distribution seen in real road traffic. The automaton works as follows:

Imagine M point like particles located equidistantly on a circle with a mean distance equal to 1. The particles move on the circle, but are prohibited to change their order. An inverse temperature parameter β (also called *statistical resistivity*) specifies the systems entropy. A positive β (i.e., a positive value of entropy) represents the amount of chaos in the generalized stochastic sense, and when related to traffic gas models, it can be thought of as a parameter reflecting the mental pressure the driver is experiencing during his trip. An integer parameter N specifies the number of interacting agents. The particle positions are repeatedly updated according to following simple rules:

- 1) Calculate the potential energy of the particle ensemble using the following formula:

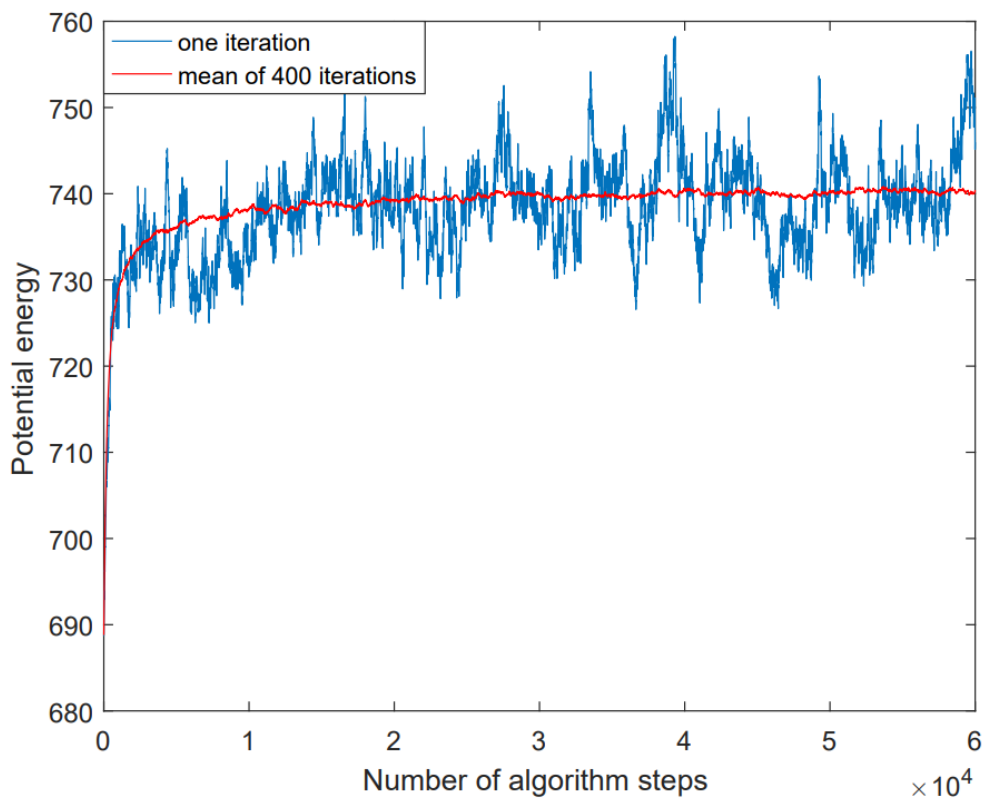
$$U_1 = - \sum_{k=1}^M \sum_{l=1}^N \ln(x_{k+l} - x_k) \quad (1)$$

where M represents the number of particles on the circle, N represents the number of interacting agents, and x is the particle position.

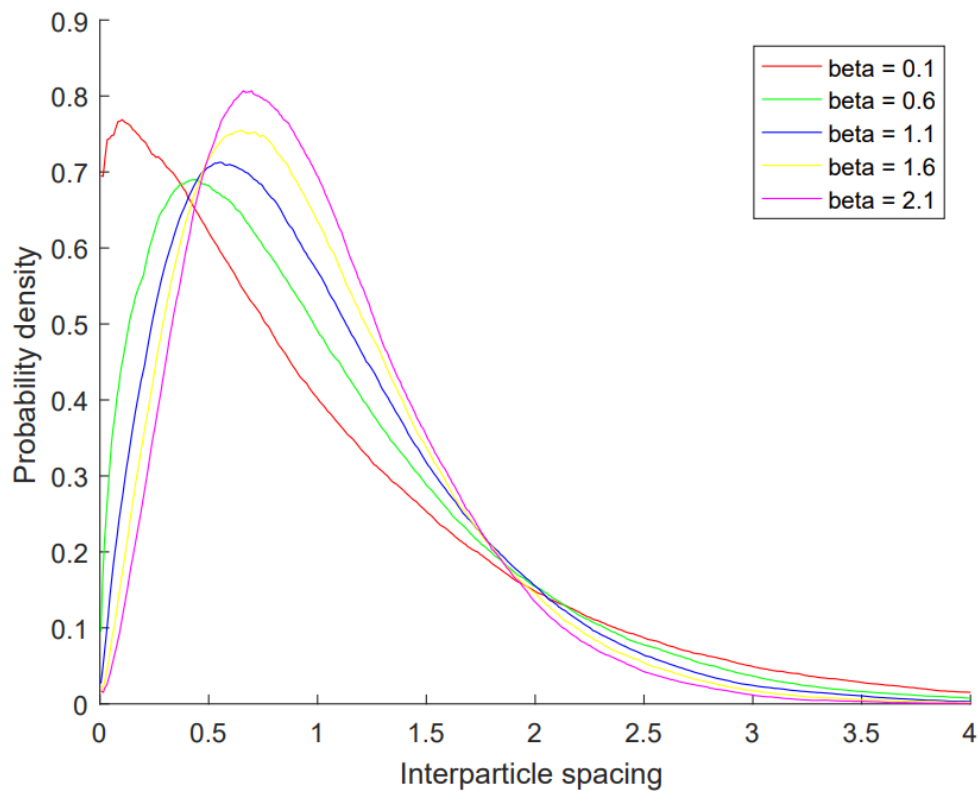
- 2) Pick a random particle-index $j \in \{1, 2, \dots, M\}$.
- 3) Draw a random number γ uniformly distributed in the interval $(0, 1)$.
- 4) Compute a new position for the particle $x'_j = x_j + \gamma$. Because the particles are prohibited to change their order, only values of γ that are less than x_{j+1} are accepted.
- 5) Calculate the potential energy U_2 using the same formula as for U_1

- 6) If $U_2 \leq U_1$, then the move is accepted, the particle changes its position, and the traffic gas takes its new configuration. However, if $U_2 \geq U_1$, then the move is accepted only with a probability of $e^{-\beta\Delta U}$, where β specifies the systems entropy, and $\Delta U = U_2 - U_1$.

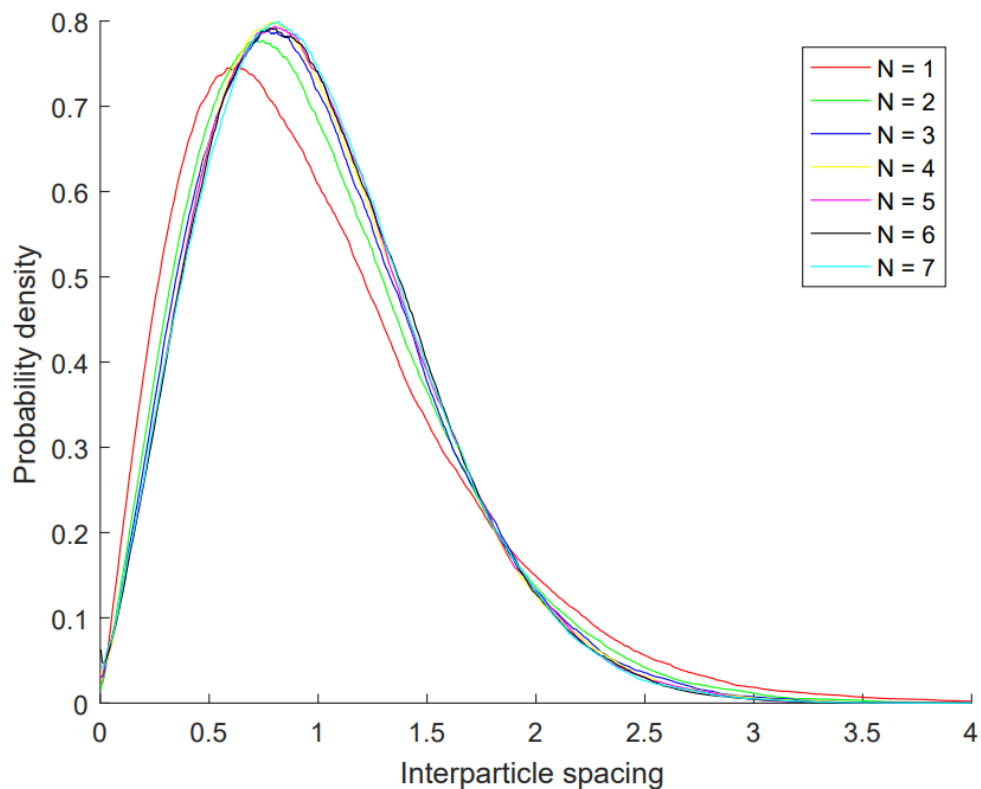
This system reaches its equilibrium state very quickly (typically within a few thousand iterations – see picture 66 for reference). The resulting inter-particle spacing distribution is used as a substrate to test the mathematical tools for interaction range quantification.



Picture 66. Relaxation of the particle system into associated thermal equilibrium. The data displayed is the result of 60 000 iterations of the above-mentioned algorithm for the temperature parameter $\beta = 1$, $N = 2$ and $M = 100$. The blue line represents the potential energy for one complete realization of the model. The red line represents the mean potential energy of 400 realizations of the algorithm. As can be seen, the particle system very swiftly reaches its equilibrium state (only about 8000 iterations are needed), and then fluctuates around a certain mean value of the potential energy.



Picture 67. Probability density functions for diverse temperature parameters β . $N = 1$ and $M = 100$. The shape of the density function describing the interparticle spacing distribution changes with increasing β . While for β approaching 0, the distribution describes a stochastically independent process, for increasing β (i.e., increasing mental strain of the driver), the distribution starts to be similar to spacing distributions seen in real traffic situations.



Picture 68. Probability density functions for various interaction ranges N . $\beta = 1$ and $M = 100$. The shape of the density function changes with increasing N , but after $N = 3$ there is no further significant change in the distributions shape. The interaction range N seems to have influence on the distribution shape only for a maximum of 3 interacting elements.

5.1.2 Mathematical tools for quantitative analysis of probabilistic dependencies

Measuring dependencies among data is a crucial part of statistical inference and is essential for understanding the nature of relations between elements of a system. This is especially valid for traffic systems. There are many dependence measures. The most prominent among them are the Pearson's correlation coefficient, distance correlation and mutual information [109], [110], [111], but there are also other measures like kernel measures of conditional dependence, mutual dependence, number variance or convolution perturbation [112], [113], [114], [115]. In the following sub-chapters, we will discuss the Pearson's correlation

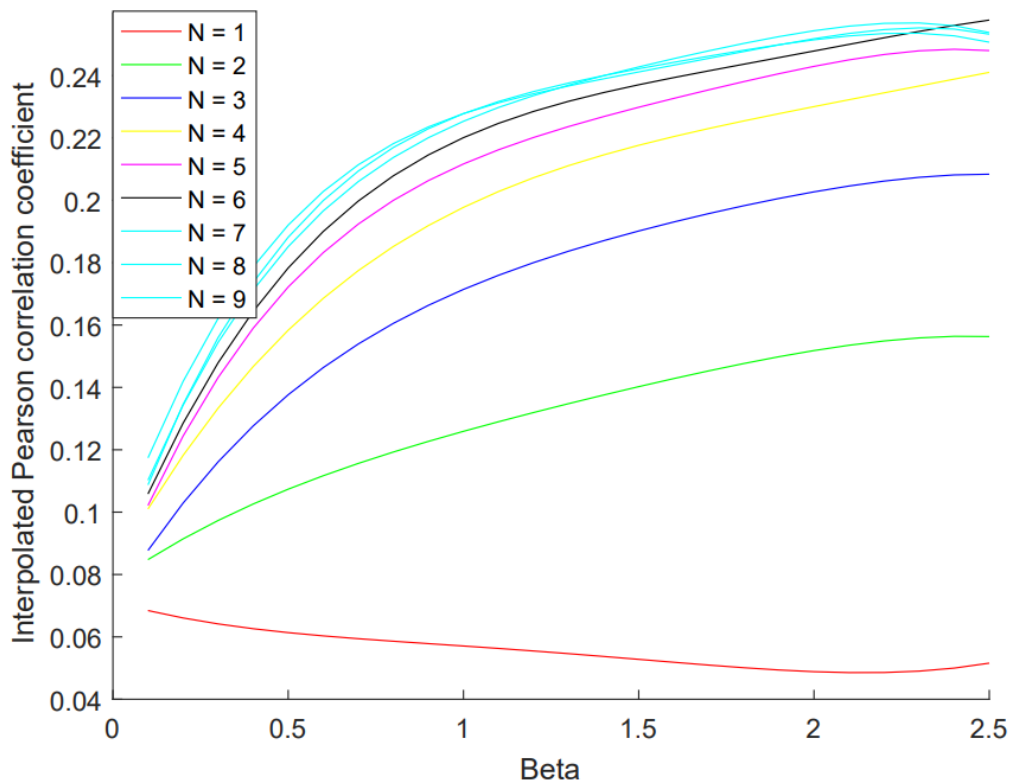
coefficient as one of the most used tools for dependence detection, the number variance – which comes originally from random matrix theory, and convolution perturbation – a relatively new approach for dependence measure. These mathematical tools will be applied on the data generated by the model described in the previous chapter, and the obtained results further discussed.

5.1.2.1 Pearson's correlation coefficient

Pearson's correlation coefficient is a measure of the linear correlation between two variables x and y . It has a value between +1 and -1, where 1 is a total positive linear correlation, 0 is no linear correlation, and -1 is a total negative linear correlation. It is defined as the covariance of the two variables divided by the product of their standard deviations:

$$\rho_{x,y} = \frac{Cov(x,y)}{\sqrt{Var(x)Var(y)}} \quad (2)$$

Pearson's correlation coefficient is symmetric: $Corr(x,y) = Corr(y,x)$. A key mathematical property of the coefficient is that it is invariant under changes of scale and location of the random variables. The disadvantage of the coefficient is that it captures only a linear dependence. A zero value of the coefficient does not mean that the two random variables are automatically independent. It only implies that they are linearly independent. Unfortunately, dependencies upon traffic data are thought to be highly nonlinear [115], [116]. Nevertheless, the Pearson's correlation coefficient is a valuable tool for a first glance assessment of the level of dependence in the data.



Picture 69. The figure shows the interpolated Pearson's correlation coefficients for diverse interaction ranges N . While for $N = 1$, there is only a limited correlation related to statistical noise of the sample, for $N > 1$ there is a clearly visible increase in correlation. The correlation coefficient continues to grow until $N = 6$ (black line). After $N = 6$ there is no further significant increase in correlation. The interaction range N seems to have major influence on the amount of correlation only for a maximum of 6 interacting elements. As can be seen, the correlation coefficient also increases with increasing β . Especially interesting is, that with increasing N (the number of interacting agents) the amount of correlation starts to significantly increase already for lower values of β . As β represents the mental strain experienced by the driver (which is usually highly dependent on the traffic density, as will be shown later), it is clearly visible that if the driver needs to react to multiple traffic participants (for example not only the car directly ahead of him, but also to other cars farer ahead), the amount of dependance (or amount of correlation) he introduces to the data by making adjustment of its speed and position increases very fast even in the lower traffic density region. This means, that if a driver faces a situation where he needs to react to multiple drivers, the amount of action he takes towards the traffic participants (adjusting position or

speed) increases dramatically with the stress he experiences. This is very similar to what can be seen in real traffic.

5.1.2.2 Number variance

Number variance was originally used to describe the eigenvalues in random matrix theory, i.e., for describing the spectral rigidity of energy levels in quantum chaotic systems. It also accurately describes the variance in particle position for a certain class of interacting gases (for example Dyson's Coulomb gas) [117], [118]. It can be used for the investigation of statistical variances in traffic data, and it can deliver information on the amount of dependence among a data set. We have used the number variance for the detection of previously introduced dependencies among the data generated by the above-mentioned model. The number variance is calculated as follows:

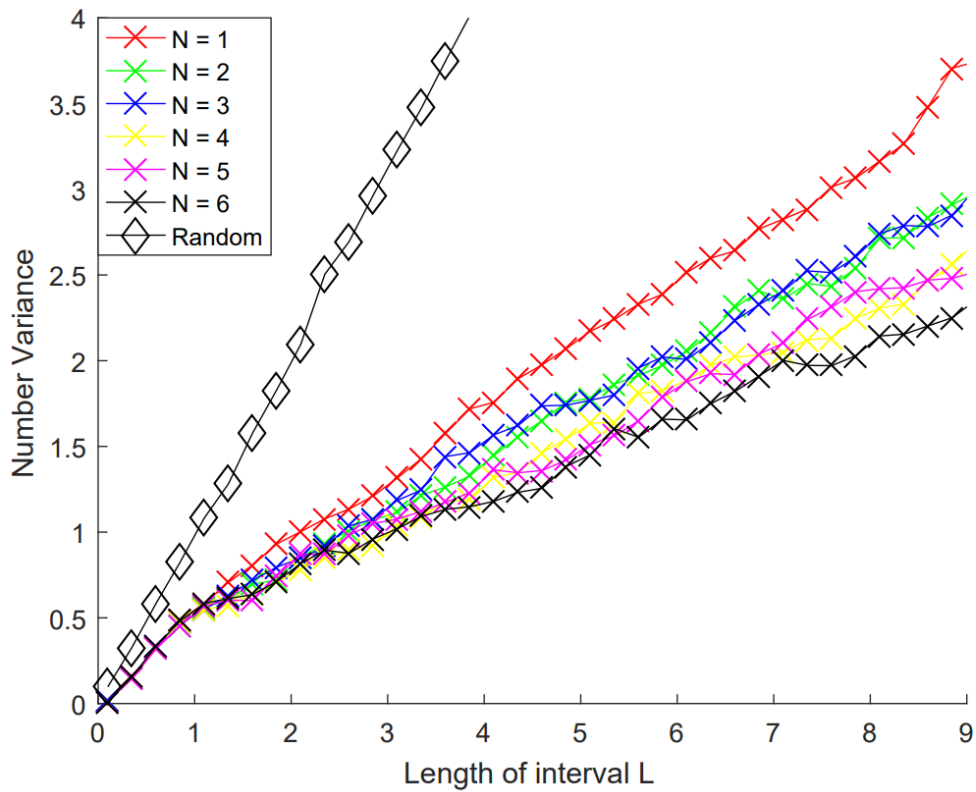
Imagine a set $\{r_i : i = 1..M\}$ of distances between point-like particles located on a circle. The mean distance over the complete set is equal to one. If we divide the interval $[0, M]$ into subintervals $[(k-1)L, kL]$, each of a length L and define $n_k(L)$ to be the number of particles in the k th subinterval, we know that the average value $\bar{n}(L)$ taken over all subintervals is equal to:

$$\bar{n}(L) = \frac{1}{M/L} \sum_{k=1}^{M/L} n_k(L) = L \quad (3)$$

The number variance $\Delta_n(L)$ is then defined as:

$$\Delta_n(L) = \frac{1}{M/L} \sum_{k=1}^{M/L} (n_k(L) - L)^2 \quad (4)$$

This quantity describes the variance in the number of particles contained in a fixed part of the circle, and measures fluctuations of this number. A significant advantage of this method is that it can capture also non-linear dependencies upon a dataset.



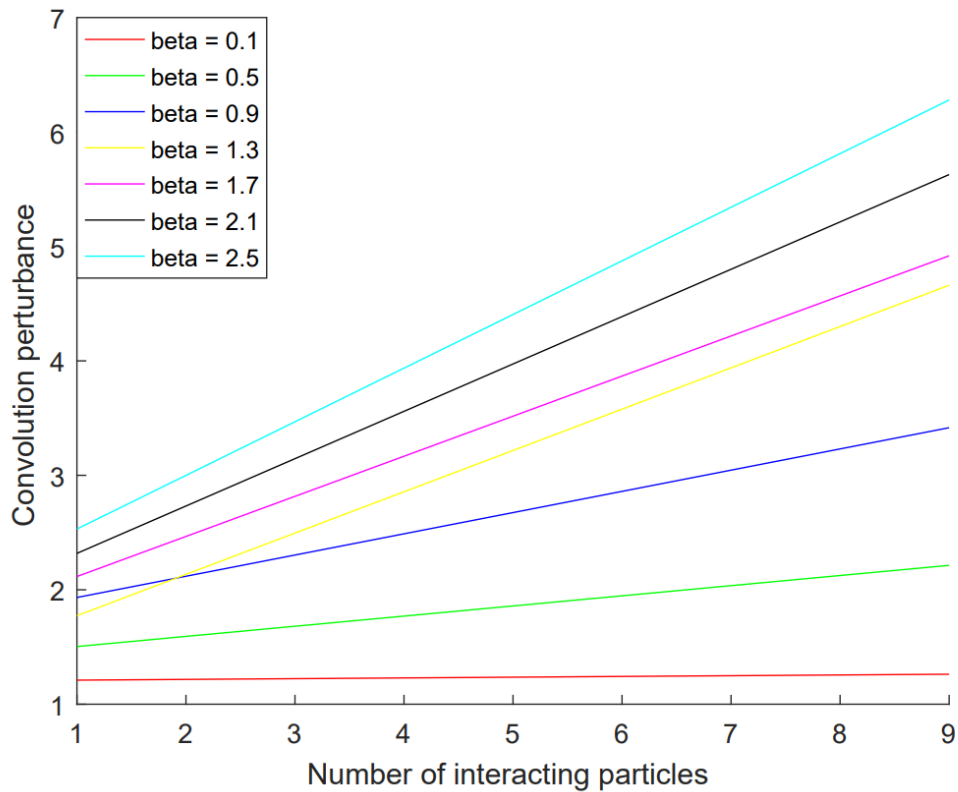
Picture 70. Plot of the number variance for diverse interaction ranges N , where $\beta = 1$ and $M = 100$. While the number variance of independent events (black line with diamonds) is a straight line with a slope (gradient) of 1, the slope of the lines representing the results for different interaction ranges N is shifted to lower numbers. Hereby lower gradients represent higher levels of dependence. The gradient of number variance (also called *statistical compressibility*) is an important indicator of the traffic regime it describes, and can help to deliver important inference on the corresponding traffic microstructure.

5.1.2.3 Convolution perturbation

It is well known from probability theory, that the probability density of the sum of two (or more) independent random variables is the convolution of their individual densities:

$$h(z) = (f * g)(z) = \int_{-\infty}^{\infty} f(z - t)g(t)dt \quad (5)$$

But what if the variables are not independent? Does this convolution property break down? We have investigated the data generated by our model and were looking if there are any differences between the convolution of the probability densities describing the inter-particle spacing, and the density of the sum of these inter-particle spacings. In a system, where only two particles interact, it can be reasonably expected, that successive inter-particle spacings are not correlated, and therefore the density resulting from the convolution should match the density of the sum of the spacings. If, however, there are more particles interacting, and there is a certain correlation between individual inter-particle spacings, the convolution should not be equal to the sum of the individual inter-particle spacing densities. We have interpreted the level of difference between these two densities, i.e., the sum of the absolute distance between each point of one density to the corresponding point of the other density, as a probabilistic dependence of the random variables describing the inter-particle spacing. We call this measure “convolution perturbation”.



Picture 71. Plot of the convolution perturbation for diverse values of β where $M = 100$. As can be seen, the amount of difference (the distance) between the convolved densities, and the density of the sum of the inter-article spacings does increase with the interaction range N , and also increases with the temperature parameter β . Such a behavior has been expected due to the nature of β and N , and as can be seen, the convolution perturbation was able to meet this expectation and give information about the dependence upon the dataset.

5.1.3 Potential in didactics of physics

The previous chapters have shown a simple way how to set-up a system potent enough to model automotive traffic (although no comparison to real road traffic data was delivered yet). Hereby the cellular automaton approach discussed in this thesis was selected, mainly because of the ability of cellular automata to generate very complex dynamics based on very simple rules. Traffic in its essence is also a system with a very complex dynamics, which is also based on very simple rules (simple actions like “accelerate”, “break” or “change direction” are enough to let

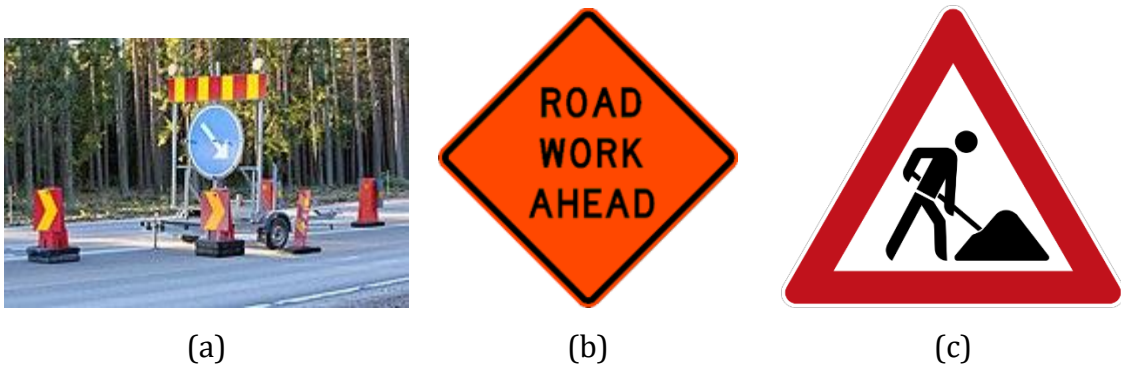
the complex microscopic and macroscopic structure seen in real road traffic to emerge). The rules of the above-mentioned model were carefully selected to introduce artificial correlation to the model's output, and a special attention was given to the rules to be easily configured (an integer N describes the number of interacting agents and a driver's mental strain factor β describes how likely the drive is to react to its environment and both of these parameters can be easily configured by the student itself, just by changing the initial configuration numbers of the model). In addition, several tools to detect the introduced correlation were given to the student to be applied on the output data (the tools match the requirement to be simple enough to be taught to bachelor degree students). Now, under the teacher's guidance, the student is able to investigate what happens to the system if the initial configuration is changed, and the student is encouraged to apply the received mathematical tools on a system that very closely matches real road traffic system. The benefit of this interdisciplinary approach (in this case the disciplines are physics and mathematics) is, that the student is immediately able to utilize the tools learned in one subject (mathematics) in the other subject (physics) and on top of that in physics of a very concrete every day experienced system (real road traffic). The student learns to understand how basic underlying rules of a system affect its dynamics while utilizing tool acquired in another subject to study the system from a mathematical perspective both at the same point in time.

Interesting is, that the same types of tools are utilized in current state-of-the-art scientific research related to traffic, and similar cellular automata are utilized to construct traffic models which are an essential part of such research. The remarkable ability of cellular automata to model the most complex phenomena just by applying several very simple rules can be utilized both in science as well as in didactics and shows how thin the border can be between school subjects and scientific research if the same tools are applied. It is a great example of the potential of cellular automata in didactics. The following chapters will show several other examples of scientific research on real road traffic, where, similar to the example above, cellular automata were used to model the studied system and mathematics to study the systems properties. This time however, these examples will contain also real road data, taken from real road measurements, which will be

compared to the cellular automaton output, and the similarities and differences between a real system and the cellular automaton system will be evaluated.

5.2 Traffic Flow Merging – Statistical and Numerical modeling of microstructure

This chapter will show a freeway traffic system, which especially people commuting by cars on freeways to major cities for work know all too well. The discussion is about construction works on freeways.



Picture 72. Road work ahead. A very typical situation experienced by drivers on a freeway in real road traffic.

What actually happens to traffic macroscopic and microscopic structure in the vicinity of a region where traffic streams are forced to merge? We have investigated the statistical distribution of the time headways, as well as their changes induced by a merging process, and verified through measurement, that the resulting statistics can be well described by the generalized inverse gaussian distribution, and on top of that, that the same distribution (but with different parameters) can be utilized also describe the headway distribution of classical free flow traffic). Furthermore, we can show, that the dynamics of the merging process can be easily described by a simple cellular automaton like model (a thermodynamic particle-like model, very similar to the model described in the previous chapter) with an implicit gap-acceptance rule controlling the merging process. It is yet another example, how a simple cellular automaton can describe even the most complex systems. It has also an important practical application.

Road works in general, and line reduction in particular have a crucial impact on traffic capacity. Compared to a free flow regime on a resource (road) without a bottle neck, the capacity of a bottle neck can be reduced up to 30% [119]. Furthermore, traffic flow withing the bottleneck itself is significantly unstable and traffic conditions may change suddenly in a very short time. It can easily happen without any obvious reason, that a free-flow regime suddenly changes to synchronized flow, or to a stop-and-go regime. A good model of this process would help to apply dynamic traffic control, and support prevention of complications resulting from such sudden changes like loss of road capacity. The detection of individual vehicular interactions is very difficult, as the information provided on individual cars by single point measurements is usually not sufficient. However it has been demonstrated in [104], [120], [121], that one can detect such interactions by means of a segmented analysis of vehicular headways/clearances and make assumption about the interactions by analyzing the statistical properties among these segments. It opens up an opportunity to comprehend the essence of vehicular merging (zipping). By analyzing real road data (particularly from construction works on Czech freeways) we can show, that before, during and after the merging process, the distribution describing the time clearances is a generalized inverse gaussian distribution. The consecutive chapters will also show how *stochastic resistivity* (a parameter reflecting on the mental strain of the driver) evolves during the merging process. Finally, we will show the implementation of a simple merging model which can reasonably reflect on the vehicular microstructure withing the zipping area, and compare the model outputs with the data measured on a real-road. From practical point of view, the results of the model can be used for example for optimized traffic dynamics control of real road zipping.

5.2.1 Classical approach to traffic merging

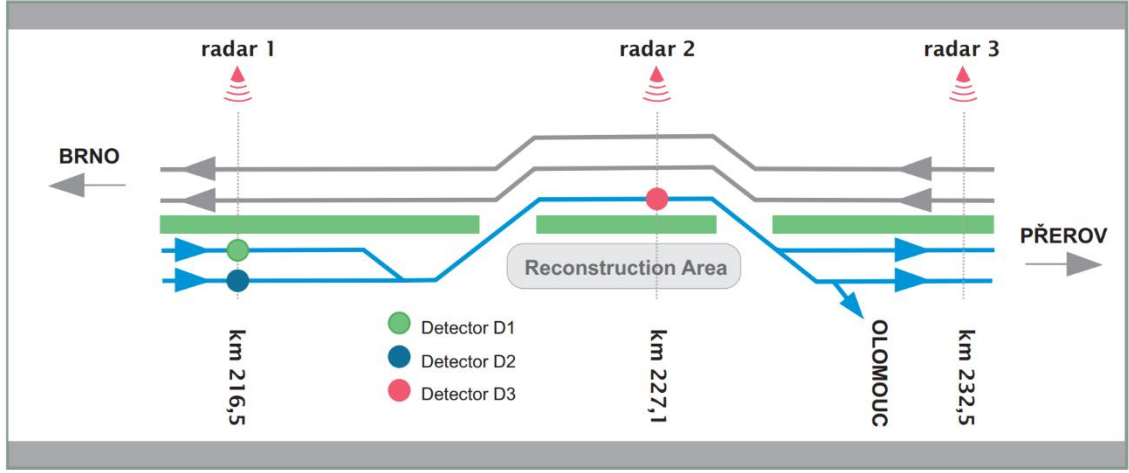
Research on zipping processes in vehicular traffic has been ongoing for a long time. Earlier works of Daganzo [122], Zheng [123], Hidas [124], Wang [125], and others have been trying to find an effective simulation tool for merging operations.

Roughly speaking, a general problem of these attempts is the fact that they all are neglecting the statistical nature of traffic flows and/or do not take into account different distributions of headways in various traffic regimes. Usually, the models consider traffic to be uniformly distributed. However, recent research shows [120], [126], [117], [127], [128], that this is by no means the case. Rather, different traffic regimes show different distributions each of which describes a certain specific case and a certain specific traffic regime. Therefore, when modelling traffic merging, one needs to look for an alternative approach.

5.2.2 Empirical observations of traffic merging and their statistical interpretations

5.2.2.1 Origin of the data

The data utilized for the follow up statistical analysis was measured during construction works on the Czech Highway D1 (notoriously famous for its everlasting construction works and resulting traffic congestions) from June to August 2016 on a 16km long road segment. The segment was chosen because it contains an area, where a two-line traffic flow merges (because of the roadworks) into one line (see picture 73 for a schematic description). Three sets of radar detectors (Wavetronics SmartSensor HD, with an accuracy of 0.1s for time measurements and 0.1km/h for velocity measurements) were put into three critical locations. The first and second detector (D1 and D2) have been placed in front of the merging area (localization: 216,5 km - one for the left line, one for the right line), the third detector (D3) has been placed directly inside the construction area (localization: 227,1 km). The last radar (localization: 232,5 km) was put behind the construction work exit area, where the flow can utilize two lines again. Unfortunately, data from this radar was not finally used (no detector was placed) for the analysis, because of the exit towards Olomouc (situated directly after the construction site). The exit disrupted the traffic flow far too much to make any statistical analysis reasonable.



Picture 73. Schematic representation of the D1 highway segment where the measurements were made. The chosen segment is 16km long.

The collected data (3.22 million events in total) has the following structure. The sets

$$T^{(in)} = \{\tau_{j,k}^{(in)} : j = 1, 2, \dots, N \wedge k = 1, 2, \dots, M\} \quad (6)$$

$$T^{(out)} = \{\tau_{j,k}^{(out)} : j = 1, 2, \dots, N \wedge k = 1, 2, \dots, M\} \quad (7)$$

contain chronologically ordered time-stamps, each time stamp representing a k th car from the j th sample. The set $T^{(in)}$ contains the timestamps captured during entering the detector line, whereas the set $T^{(out)}$ contains the timestamps captured when the vehicle left the detector line. Constants M and N represent the sampling size and the total number of samples. In a similar way,

$$V = \{v_{j,k} : j = 1, 2, \dots, N \wedge k = 1, 2, \dots, M\} \quad (8)$$

is the set of vehicular velocities. For each sub-sample j , it is possible to calculate the local traffic intensity

$$I_j = \frac{M}{\tau_{j,M}^{(in)} - \tau_{j,1}^{(out)}} \quad (9)$$

and local average velocity

$$\bar{v}_j = \frac{\sum_{k=1}^M v_{j,k}}{M} \quad (10)$$

based on these quantities a good approximation of the local traffic density can be obtained [127], [103]:

$$\rho_j = \frac{I_j}{\bar{v}_j} \quad (11)$$

Individual (re-scaled) time-clearances are then calculated as follows:

$$x_{j,k} = \frac{M(\tau_{j,k}^{(in)} - \tau_{j,k-1}^{(out)})}{\sum_{i=1}^M \tau_{j,i}^{(in)} - \sum_{i=1}^M \tau_{j,i-1}^{(out)}} \quad (12)$$

which ensures for all sample means that

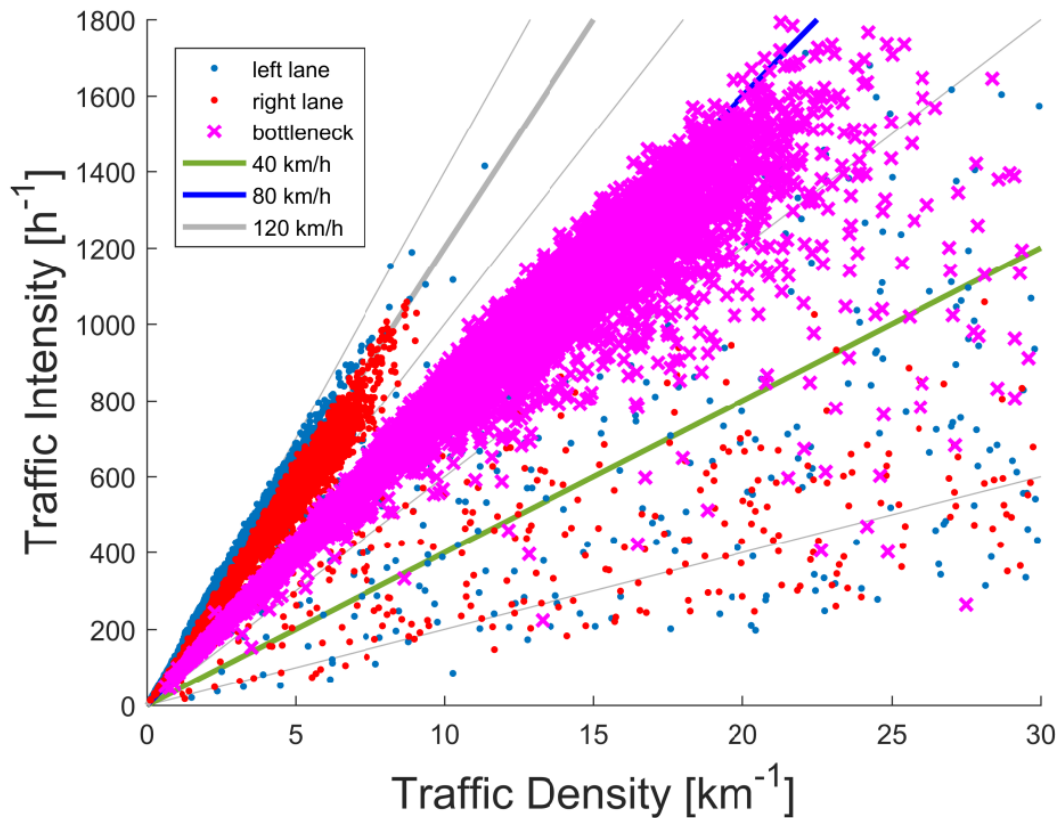
$$\bar{x}_j = \frac{\sum_{k=1}^M x_{j,k}}{M} = 1 \quad (13)$$

It is well known [129], [128], [126], [130], [131] that such a re-scaling procedure brings a considerable advantage when investigating relations in many types of systems, including economic, physical, biological, socio-physical or purely mathematical systems.

5.2.2.2 Macroscopic characteristics of a traffic merging systems

The macroscopic variables I_j , ρ_j and \bar{v}_j characterize the macroscopic state of the j th sample. To understand what traffic regime the explored sample is experiencing, one needs to check its position on the so-called *Intensity-Density plane* (ID-plane, also called fundamental diagram). The position of the sample on the plane is defined by its ID coordinates ρ_j, I_j . and helps to identify what traffic regime

vehicles from this sample are experiencing. Usually, a driver from a sample far right to the bottom of the ID plane (high traffic density, low traffic intensity) experiences congested traffic, whereas a driver from a sample with lower traffic density and higher traffic intensity most probably experiences free flow. What is essential before moving to any sort of statistical analysis is to assure that only a homogenous data sample will be analyzed. Because traffic, in general, is not uniform, when observing a larger sample of successive vehicles, it is clearly visible that each part of a larger sample has a different microstructure. Indeed, it is well known, that traffic dynamics exhibits many surprising patterns like traffic jams, stop-and-go waves propagating through the traffic sample, transitions to and from congested traffic states, local instabilities or meta-stabilities of traffic flow, scattering, platoon formation or traffic synchronization. Therefore, a larger sample of traffic data is difficult to be described with a single probability distribution, and is rather a mix of several different distributions, as it is a mix of several different traffic states at the same point in time. To avoid analyzing a non-homogenous data sample, consequently only samples from a limited region of the ID plane, that contain samples of similar statistical properties and traffic microstructure were subject of the analysis.



Picture 74. Fundamental diagram showing data from the D1, D2 and D3 detectors. Blue and red dots highlight data from detector D1 and D2 (left line and right line) which captured data before the vehicles entered the road work merging area. Purple marks show data from the D3 detector directly from the construction area where the flow has been merged. Strait lines highlight vehicles within the fundamental diagram, which move with the same velocity. It is immediately visible, that by merging of the two lines (which exhibit free traffic flow states), the mean velocity dropped dramatically from 120 km/h to roughly 80 km/h. This is a result of a traffic phase change induced by the zipping area, in which traffic suddenly swings from free flow to synchronized flow [132].

5.2.2.3 Microscopic characteristics of a traffic merging systems

As discussed, standard traffic flow without any merging can be very well described by the generalized inverse gaussian distribution (GIG distribution) [133], [134]. We have investigated if this is true also for the area directly after zipping occurs (data captured by the D3 detector), and if the same general principles apply also

for a merged traffic stream. The aim was to investigate, whether the merging process had some fundamental impact on the microscopic nature of traffic. To be more specific, we wanted to know, if the probability density function

$$f(x) = A\Phi(x)x^\alpha e^{-\frac{\beta}{x}}e^{-Dx} \quad (14)$$

where $\Phi(x)$ is the Heaviside step function, and where A and D are scaling and normalization constants:

$$A^{-1} = \frac{1}{A} = \begin{cases} 2 \left(\frac{\beta}{D}\right)^{\frac{\alpha+1}{2}} K_{\alpha+1}(2\sqrt{\beta D}) & \beta \neq 0, \alpha \in \mathbf{R} \\ \frac{\Gamma(\alpha+1)}{(\alpha+1)^{\alpha+1}} & \beta = 1, \alpha > -1 \end{cases} \quad (15)$$

$$D = \alpha + \beta + \frac{3 - e^{-2\sqrt{\frac{\beta}{4+\alpha}}}}{2} \quad (16)$$

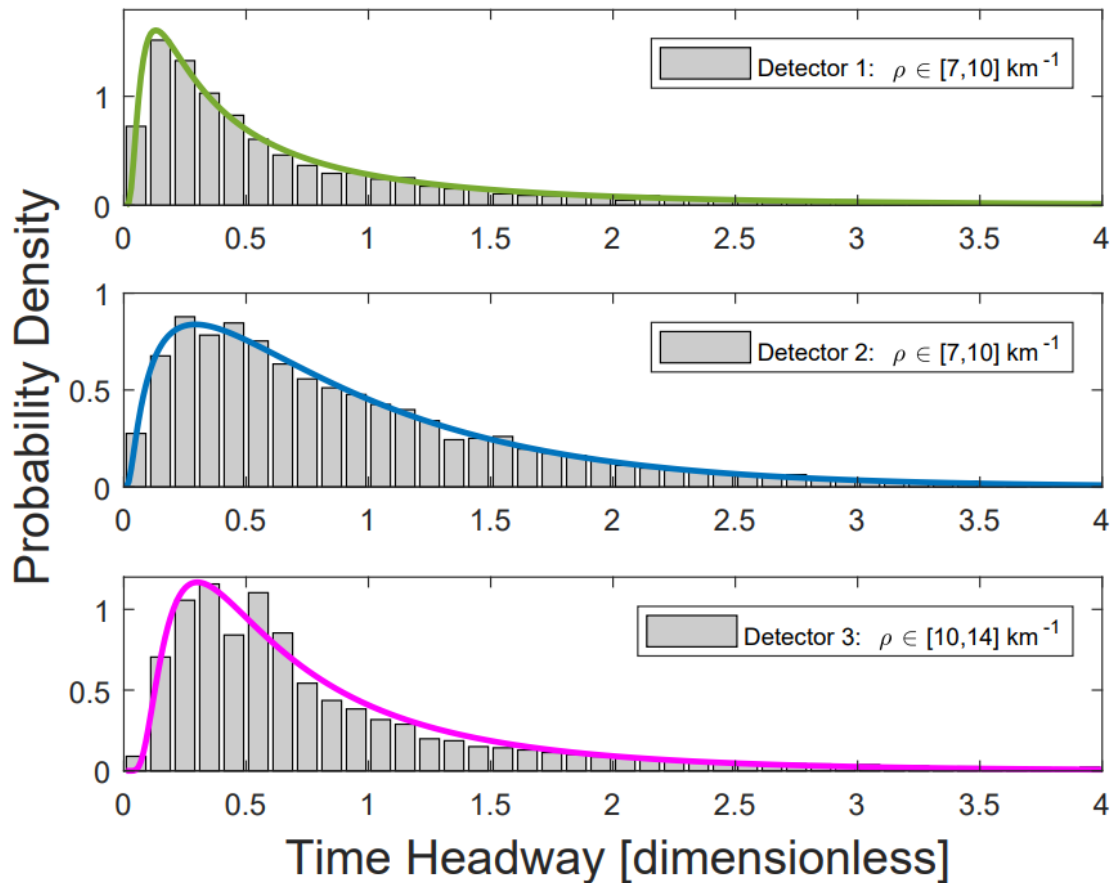
where $K_{\alpha+1}(x)$ represents a modified Bessel function of the second kind, and Γ represents the gamma function, could accurately describe not only bot streams before merging, but also the final merged traffic stream.

A crucial statistical quantity is the *stochastic resistivity* $\beta \geq 0$, which describes the systems resistance to stochastic influences. When referring to traffic, it can be understood as a parameter reflecting on the mental strain the driver is experiencing and acts as an indicator of repulsive forces in the system. Lower values of β correspond to a system being close to a Poissonian system of random non-correlated events and suggest no interaction between individual particles/elements/agents. In contrary, extremely high values if $\beta \rightarrow \infty$ lead to an equidistant arrangement of particles, which corresponds to a deterministic system. Therefore, a particular value of the resistivity (detected in vehicular systems) reveals an extent to which interaction forces (i.e. socio-dynamical impulses influencing driver's decisions and maneuvering) are damped by stochastic

fluctuations. Higher values of β indicate stronger mental strain of the driver, and stronger interactions between individual drivers. As an illustration of how well the generalized inverse gaussian distribution can describe the traffic data, please see picture 75. The parameters α and β of the associated GIG distribution were estimated based on the measured time headways by the Minimum Distance Estimation method (MDE), where the distance to be minimized can be described by the following metrics:

$$\mu = \left(\int_0^{\infty} |H(x) - f(x)|^2 dx \right)^{\frac{1}{2}} \quad (17)$$

where $H(x)$ represents the histogram of scaled time headways, and $f(x)$ represents the GIG probability density function.



Picture 75. Measured time headway distribution (histogram) with its corresponding estimated GIG distribution (green, blue and purple line). The picture shows how two traffic streams (measured by the D1 and D2 detectors) having an equal density between 7 and 10 vehicles per kilometer merge into one stream having a density between 10 and 14 vehicles per kilometer. As can be seen, the statistical model very accurately reproduces the empirical distributions both for each individual line before merging (green and blue line), as well as the final merged flow (purple line).



Picture 76. Estimated stochastic resistivity parameter β for each line in relation to traffic density. As can be seen, for lower densities, less than 7 vehicles per kilometer, the mental strain parameter β is pretty low, indicating that in low density traffic, there is not much mental pressure exerted on the driver (this is in correspondence to our everyday experience during driving). However, once the traffic density increases, the pressure the driver is experiencing also increases. For the merged stream (because of the just undergone zipping procedure and because of the narrower driving line related to the surrounding construction work), the mental strain level rises already at densities around 8 vehicles per kilometer as the driver needs to evaluate more information in a short time. Especially interesting is the evolution of the mental strain parameter for the fast line (the line that is being merged). For densities up to 15 vehicles per kilometer, drivers in both lines experience roughly the same amount of stress. However, for densities beyond that, there is a very sharp increase in the stress level the drivers experience in the fast line. This is because the merging procedure is about to start and there is far too low space in front of the driver resulting in a higher repulsive force acting on the driver (drivers in the fast line are forced to slow down because of many other cars

in front of them did slow down as they prepare for the zipping maneuver). Interesting is, that this is in no way the case for the slow line. There (at least at the location measured by the detector) seems to be no dramatic increase in the stress level experienced by the driver.

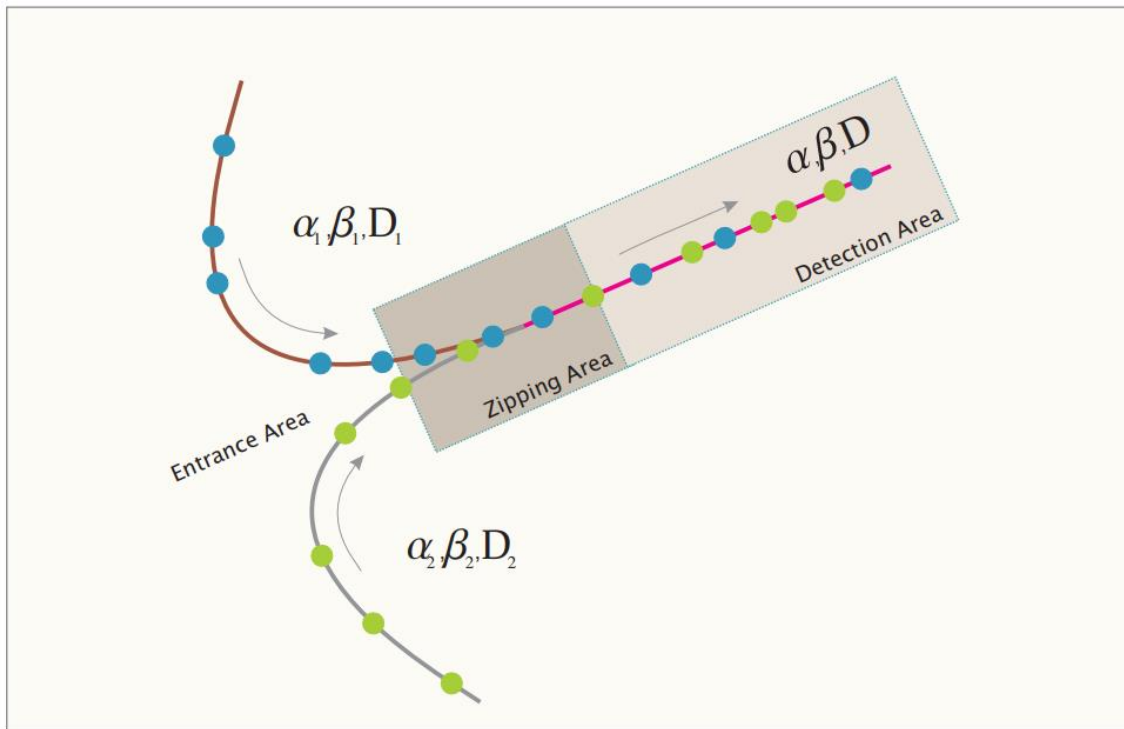
5.2.2.4 Modeling traffic merging by utilizing a cellular automaton

In the previous chapter, empirical data from a traffic merging procedure were studied in detail together with a statistical model based on the generalized inverse gaussian distribution. It could be shown, that the mentioned distribution can very accurately model the assessed situation. In this chapter, a traffic flow merging simulation based on a simple thermodynamic gas (traffic gas) cellular automaton will be presented. In many ways, it is very similar to the simple gas model described in the previous chapters, however it has been extended to incorporate the zipping procedure. The automaton consists of two one-dimensional thermal-like gases whose particles are attracted/repulsed by a combined and η -parametrized potential

$$\varphi = \eta \ln x + \frac{1}{x} \quad (\eta > 0) \quad (18)$$

and controlled by a fixed value of the stochastic resistivity $\beta \geq 0$. For such a gas, analytical solutions of associated steady-state distributions are well known [104] and lead to headways that are GIG distributed. Moreover, it is shown in [135] and discussed in [127] that a general system with asymmetric, forwardly-directed interactions and driving terms (which is a typical variant of traffic models) can be very reliably approximated by the many particle thermodynamic system like this. Above that, it is well known that the above-mentioned thermal-like gas generates GIG-distributed headways also in far-from-equilibrium states, which represents a great benefit for modelling of merging traffic. The model has random initial conditions (location of particles in each stream) and fixed parameters β_1 and β_2 assigned to the individual to-about-to-be-merged streams, and consists of three segments (see picture 77). The first segment contains the two traffic streams, that

are going to be merged. The second segment contains the merging area, and the third segment contains the merged stream together with a detection area. All these segments change their states according to below described rules, but each segment has different values of configuration parameters. In the third segment, particles are captured by a virtual detector (much like vehicles were captured by a real radar detector in the real road example given above) and related headway distributions were acquired also in the same way (MDE).



Picture 77. Schematic example of the merging automaton. Two separate traffic streams (brown and grey curves, containing blue and green particles) merge into one stream according to fixed merging rules. A detection area after the merging are captures information about passing particles.

Consider an ensemble of N point like particles at positions $x_1(t) > x_2(t) > \dots > x_N(t)$, where t is an integer value representing the time step of the automaton. The particle positions are updated by applying the following steps:

- 1) Timer t is increased by one

- 2) Potential energy of the particle ensemble is calculated based on the following formula:

$$U(t) = \eta \sum_{k=1}^{N-1} \ln(x_k(t) - x_{k+1}(t)) + \sum_{k=1}^{N-1} \frac{1}{x_k(t) - x_{k+1}(t)} \quad (19)$$

- 3) Pick a random particle-index $l \in \{1, 2, \dots, N\}$.
 4) A mean headway in the given segment is evaluated

$$w = \frac{1}{N-1} \sum_{k=1}^{N-1} (x_k(t) - x_{k+1}(t)) \quad (20)$$

- 5) Draw a random number δ uniformly distributed in the interval $(0, 1)$ and compute a new position for the l th particle: $x_l(t+1) = x_l(t) + \delta w$. Because the particles are prohibited to change their order, the new position is accepted only if $x_l(t+1) < x_{l-1}(t)$ otherwise the position is not updated and stays the same $x_l(t+1) = x_l(t)$ and the algorithm is skipped to step 9.
 6) The potential energy of the new particle configuration is evaluated

$$U' = U(t) + \eta \ln \left(\frac{x_{l-1}(t) - x_l(t+1)}{x_{l-1}(t) - x_l(t)} \right) + \frac{1}{x_{l-1}(t) - x_l(t+1)} - \frac{1}{x_{l-1}(t) - x_l(t)} \quad (21)$$

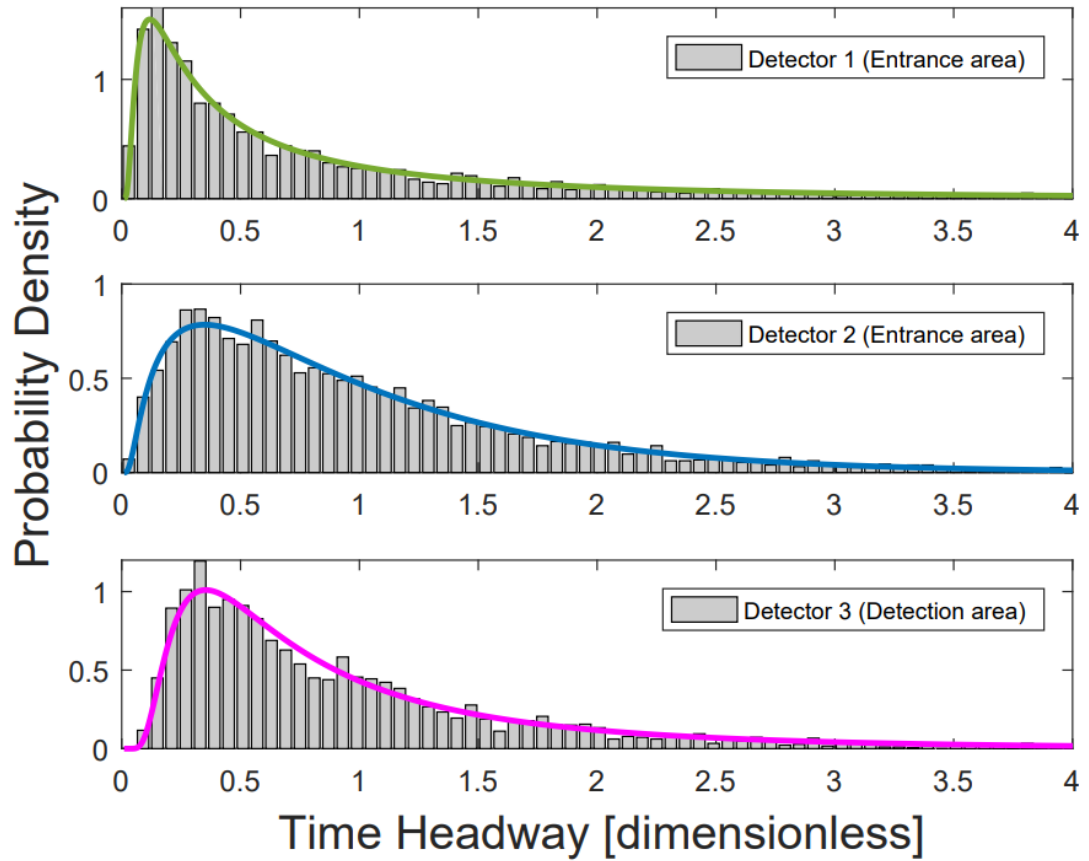
- 7) If $U' \leq U(t)$ then the l th particle takes on the new value $x_l(t+1)$
 8) If $U' > U(t)$ then the Boltzmann factor $h = e^{-\beta(U' - U(t))}$ is compared with another random number r uniformly distributed in the interval $(0, 1)$. If $h > r$ the l th particle takes on the new value $x_l(t+1)$ too. Otherwise, the original configuration remains unchanged and $x_l(t+1) = x_l(t)$.
 9) For every $k \neq l$ we set $x_k(t+1) = x_k(t)$.

In this manner, particles positions from the first and second segment, where the coefficients of resistivity (required in step 8) are specified at the beginning of a

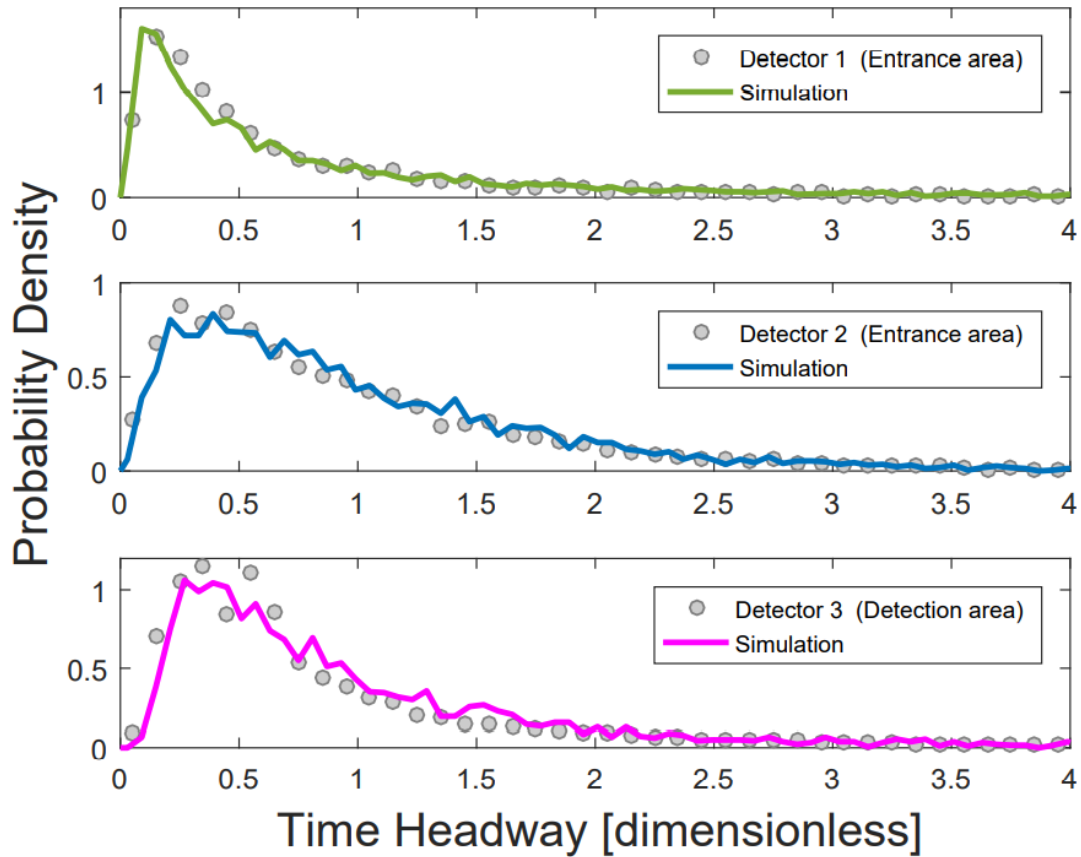
simulation procedure, are updated periodically before they enter the zipping area. Here they are merged into one one-dimensional ensemble (keeping the order in which particles entered the segment), that is described by a potential energy respective to the zipping area. An effective value of resistivity in the zipping area is then calculated as an average resistivity of all particles lying within this area:

$$\beta = \sum_{l=1}^N \left(\frac{\beta_l}{N} \right) \quad (22)$$

Where β_l is either β_1 or β_2 in dependence from which line the particle entered the merging area. This represents an implicit merging rule reflecting an empirical behavior of drivers moving in the vicinity of a merging point. After the particles pass through the zipping area to the detection area, their headways are recorded and statistically evaluated. It needs to be mentioned, that in the zipping area itself, the particle positions are updated in the very same way like they are in the two lines prior the merging, with the only difference being the β parameter utilized in step 8, which is calculated as a merged parameter from β_1 or β_2 in dependence on the particle configuration within the merging area. The above-mentioned algorithm is executed individually for both lines and the zipping area until the each of the segments reaches its individual thermal equilibrium and their headway distributions are statistically stable in time. The models output can be seen in picture 78. A comparison of the models output and real road merging data is displayed in picture 79.



Picture 78. The histogram shows the headway distribution for individual lines as well as the merging are acquired by relaxing the merging particle gas cellular automaton model into its thermal equilibrium. Green, blue and purple curves represent an associated GIG probability density function. As can be seen, the GIG also very accurately fits the data generated by the automaton merging model.



Picture 79. Comparison between real road headway probability distribution and simulation result distribution. As can be seen, the headway distribution acquired by the model very accurately matches the real road equivalent. The initial configuration parameters of the model were chosen based on estimated parameters from the real road merging.

Based on stochastic analysis of original vehicle-by-vehicle data measured in the vicinity of the zipping area it is clearly visible, that regardless of the detector position, all the time-clearance distributions belong to the family of the generalized inverse Gaussian distributions. The estimation procedure based on MDE however reveals significant differences in the stochastic resistivity of in-flow and out-flow streams. It confirms an intuitive opinion that streams in the left (fast) and right (slow) lanes (before the zipping area) are not statistically equivalent, despite the fact that they can have the same or similar macroscopic properties. Evolution of the stochastic resistivity (for evolving traffic density), which is one of the fundamental description quantities in physics of traffic, clearly shows that driver strategies (decision rules and maneuvering) are different in the fast and slow

entrance-lanes and are also different inside the construction area. It is also very interesting, that a simple cellular automaton model, which follows only basic intuitive rules can generate output remarkably similar to the real road situation. Both real road data, as well as the automaton model output highlight, that the merging procedure amplifies synchronization among cars. In other words, drivers experiencing a merging situation in real road traffic are more likely to adapt their driving behavior based on the behavior of surrounding cars to avoid collision. This is a result of increased mental strain experienced during the merging procedure, which in many aspects challenges the driver, and it is of no surprise that such a driver will adjust its driving behavior accordingly.

5.3 Super-chaotic statistics in traffic flow

In the previous chapter, traffic merging was investigated in detail. Analysis of data from a real road construction site showed, that there is a significant difference in statistical properties between the fast (left) and slow (right) line, and that imposing some restriction area on the common resource (road) can lead to a dramatic change in the driver's behavior and traffic flow in general. But is this the case also for unrestricted traffic? We have investigated the nature and level of correlation among vehicles in real road two-lane traffic data, and found out that there is a remarkable difference in the driver's behavior between the two driving lines, even when there is no apparent external influence or traffic restriction imposed on the system.

5.3.1 Origin of the data

The data we base our investigation on was measured by a set of inductive dual-loop traffic detectors, located on the D0 motorway in Prague (also commonly known as the Prague Ring). The advantage of using a dual-loop detector system is that it can capture both the vehicle speed as well as its length with a good precision. To illustrate how the system works, please refer to picture 80. The measurement system consists of two separate loops, the M_{loop} and the S_{loop} , both

with the same loop length and a fixed distance between them. When one of the loops detects a vehicle, a timer is started, and when the vehicle is detected by the second loop, the timer is stopped. The time at which the vehicle arrives at the M_{loop} - t_{m-on} and the time at which the vehicle arrives at the S_{loop} - t_{s-on} , can be used to calculate the vehicle speed [136]:

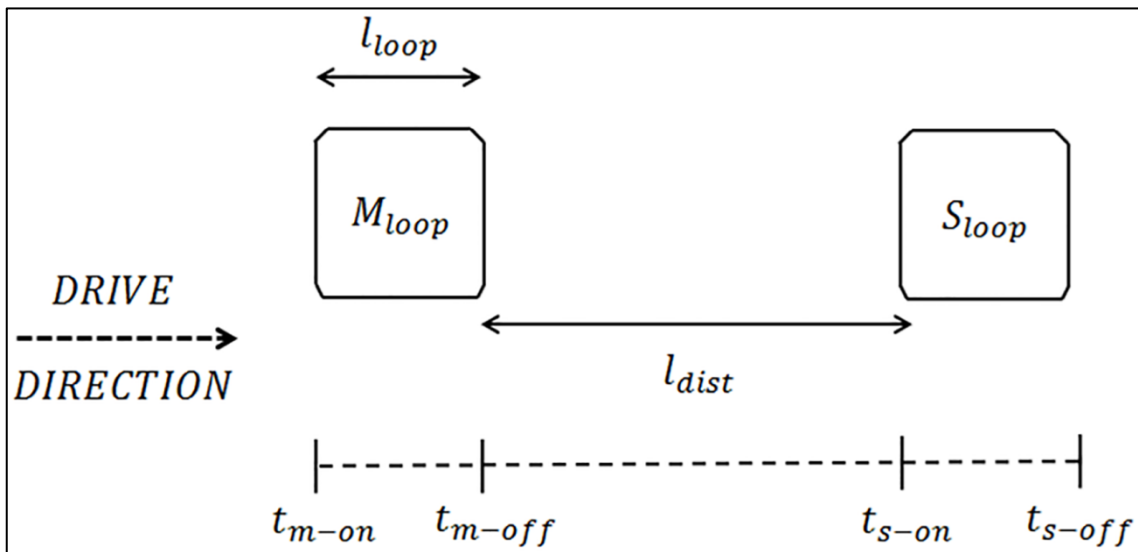
$$speed = \frac{l_{dist} + l_{loop}}{(t_{s-on} - t_{m-on})} \quad (23)$$

Where: l_{loop} = Loop length in meters

l_{dist} = Distance between the two loops in meters

t_{s-on} = Vehicle entry time at the first loop

t_{m-on} = Vehicle entry time at the second loop



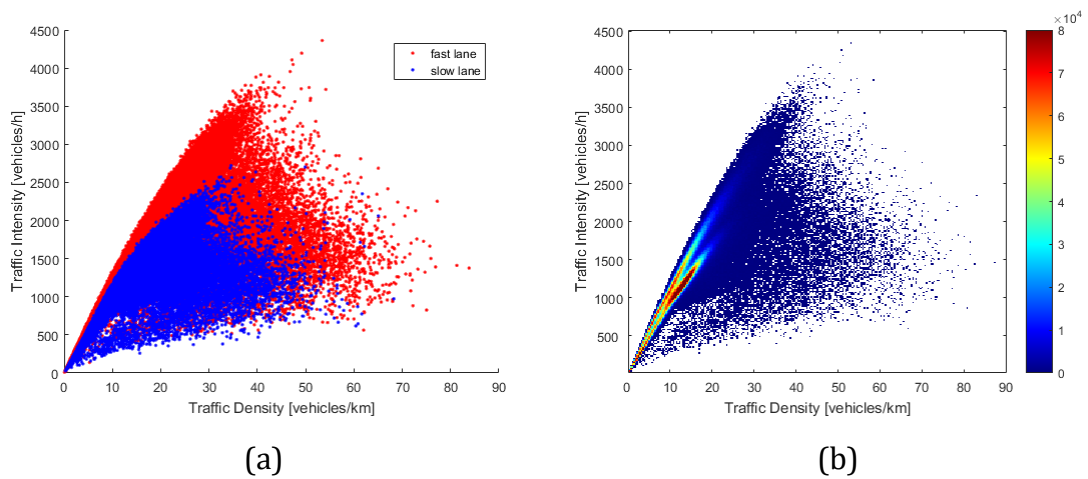
Picture 80. A schematic diagram of an inductive dual-loop traffic detector [136].

Based on the vehicle speed, and based on the On_{time} - the time the vehicle spends moving across the detector, the vehicle length can be obtained by:

$$L_{vehicle} = \left[speed \left(\frac{On_{time-M} + On_{time-S}}{2} \right) \right] - l_{loop} \quad (24)$$

Where: $speed$ is the Vehicle speed, l_{loop} is the Loop length in meters, On_{time-M} is the time the vehicle moves across the first loop and On_{time-S} is the time the vehicle moves across the second loop.

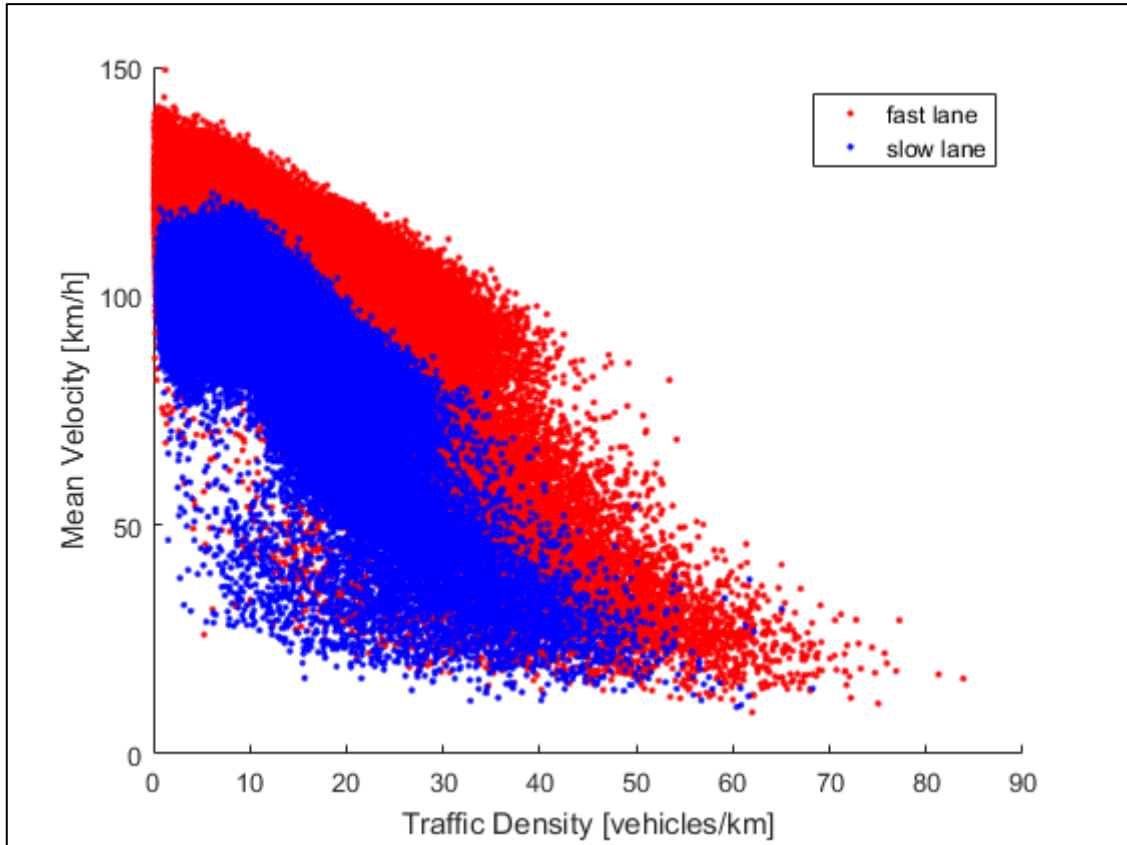
In a similar way, other important macroscopic and microscopic quantities can be extracted out of the data. Especially important are the time and distance headways (the time or the distance between two vehicles passing a detector), traffic density (the number of vehicles in a fixed road length), traffic intensity (the number of vehicles passing a point in a fixed time) and mean velocity (sum of velocities of fixed number of vehicles, divided by the number of vehicles). Also, similar to the assessment of the real road merging data explained in the previous chapter, a unification procedure had to be done for the data, to avoid analyzing a non-homogenous data sample. We have split the data into small samples each containing only a limited number of entries. Then, for each of the individual sample sets, the random variables describing the data (like for example time headways, or distance headways) were re-scaled to have a mean value of one. Finally, for each of the individual sample sets, local traffic density and traffic intensity was calculated, in order to understand at what position this sample set is located in the fundamental diagram. Only limited regions of the fundamental diagram, containing samples of similar statistical properties and traffic microstructure were subject of evaluation. Picture 81 shows the resulting fundamental diagram of the acquired data. Left, the fast and slow lane is represented by different colors, showing a difference in shape of the fundamental diagram. The heat map representation of the fundamental diagram (see picture 81 right) shows the number of vehicles belonging to the same region of the fundamental diagram. The heat is proportional to the number of vehicles. The two separate heat-center lines visible on the figure are the fast and the slow lane. The slow lane has a bigger heat-center as it contains in general more vehicles. The data in picture 81 represents 52 billion vehicles captured by 8 different detectors during a period of one year.



Picture 81. Fundamental diagram representation of the measured data.

5.3.2 The difference between the fast and the slow lane

As can be seen on the heat map representation of the fundamental diagram in picture 81, already on macroscopic level both lanes display differences. For the same traffic densities, the fast lane exhibits a sharper increase in traffic intensity, and is able to maintain this increase even in more dense traffic before finally entering saturation and congested traffic. The comparison of mean velocities, displayed in picture 82 confirms this observation. While both lanes contain a similar region of slow-movers for low densities < 20 vehicles/km, the faster moving vehicles show different properties in the mean velocity trend. For the slow lane, the maximum mean velocity seems to slightly grow for densities below 10 vehicles/km, and then enters a bound regime, experiencing a linear decrease in mean velocity, until reaching the threshold value at density 35 vehicles/km, followed by a sharp breakdown in mean velocity which signalizes that the traffic has entered congestion. For the fast lane however, there seems to be a bound regime from the very beginning, displaying as well a decrease in mean velocity, but with a milder slope. Also, vehicle in the fast lane seem to enter the congestion related breakdown in mean velocity later, at density 40-45 vehicles/km.



Picture 82. Mean velocity comparison of the fast and slow lane.

To understand the differences in the microscopic structure, we have once again utilized the generalized inverse gaussian distribution to assess the distribution of the random variables describing the time headways between vehicles. As discussed in the previous chapter, the GIG distribution is perfect for such an assessment, as it not only very accurately describes time headways between vehicles in real road traffic, but can also describe a general many particle systems in far-from-equilibrium state. (Interesting is to mention that the GIG distribution is known to accurately describe not only traffic data, but also for example the intervals between failures of air-conditioning equipment, intervals between pulses along nerve fibers, fracture toughness of MIG welds and has a close connection to the hazard functions and lifetime modelling in general [134]). For the purpose of investigating the micro structure of unrestricted two-lane traffic flow, we introduce the probability density function:

$$f(x) = A\Phi(x)x^\alpha e^{-\frac{\beta}{x}} e^{-Dx} \quad (25)$$

where $\Phi(x)$ is the Heaviside step function, and

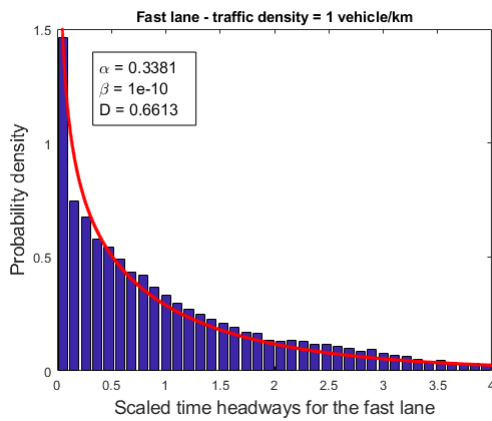
$$A = \frac{1}{2 \left(\frac{\beta}{D}\right)^{\frac{\alpha+1}{2}} K_{\alpha+1}(2(\alpha+1)\sqrt{D\beta})} \quad (26)$$

where $K_{\alpha+1}(x)$ represents a modified Bessel function of the second kind, and $\beta > 0, D > 0$ and α are real parameters (compared to the previous notion of the GIG from the traffic merging model, we didn't express D to be a function of α and β so the current function is a three-parameter function rather than a two parameter one from the previous chapter). Similar to the previous example, the β parameter indicates the systems entropy. It represents the amount of chaos in the system and when referring to traffic, it can be understood as a parameter reflecting on the mental strain the driver is experiencing and acts as an indicator of repulsive forces in the system. As can be seen in picture 84 (b), the stress parameter β is heavily influenced by traffic density. When traffic density is low, the driver experiences low stress levels, as there is no necessity to respond to the local traffic (no repulsive forces slowing down vehicles). The probability distribution is reduced to the Poisson distribution - see picture 83 (b). However, with increasing traffic density, the driver is forced more and more to respond to its surrounding and the driver needs to evaluate more and more information in a short time, increasing the stress level consistently. The correlation between individual drivers rises, and the data can no longer be described by the Poisson distribution. Once the stress level is unbearable, the driver slows down. If this happens in a larger scale, the system enters a congested state and the mean velocity and traffic intensity decreases dramatically, sometimes even halting the whole traffic flow. Note the difference in β parameter dependence on traffic density for the fast and slow lane in picture 84 (b).

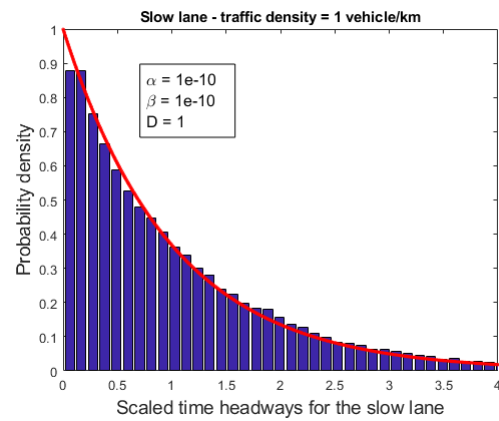
The α parameter on the other hand represents attractive forces in the system. It represents the desire of the driver to follow or catch upon a vehicle. In short range interaction, the repulsive forces always prevail, reflecting on the instinct for self-preservation, however when the distance between the drivers gets sufficient, attractive interaction gains more and more ground. Note the difference in α

parameter dependence on traffic density for the fast and slow lane in picture 84 (a).

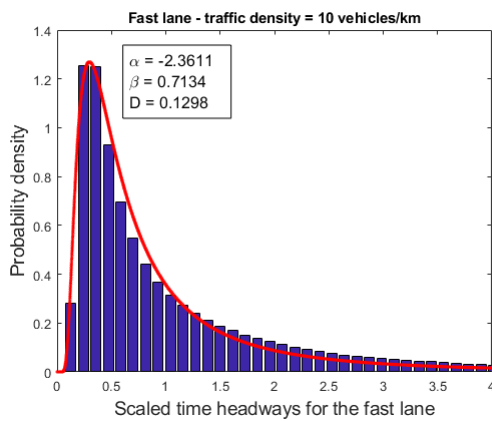
The interaction of the driver with other vehicles is defined by a ratio between the stress parameter β and the attraction parameter α . Both are dependent on traffic density (larger densities result in larger value for both of the parameters). Let us therefore introduce the force ratio $\kappa = -\frac{\alpha}{\beta}$, which represents the level of attractive force presence in the system. As can be seen in picture 83 (a-f), the generalized inverse Gaussian distribution can very accurately describe situations in both the fast and the slow lane, for low and high densities.



(a)



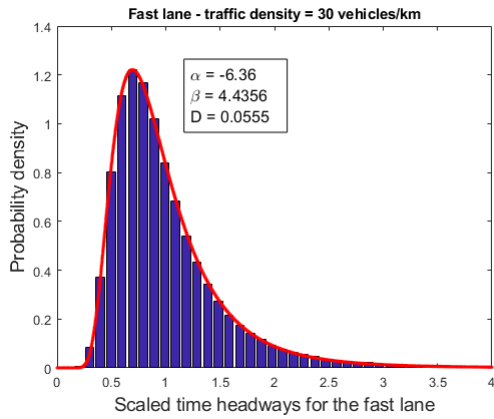
(b)



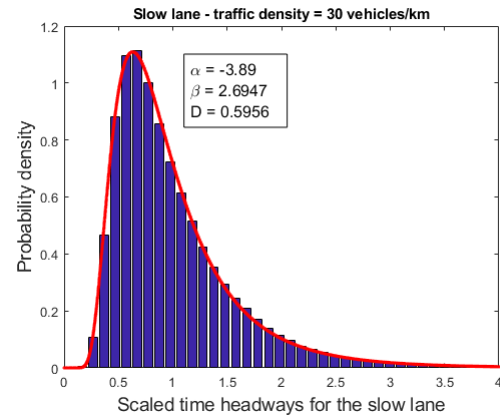
(c)



(d)

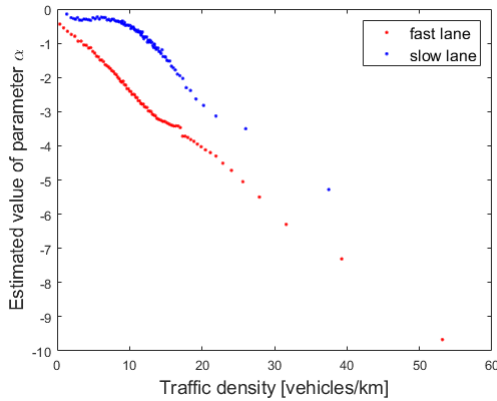


(e)

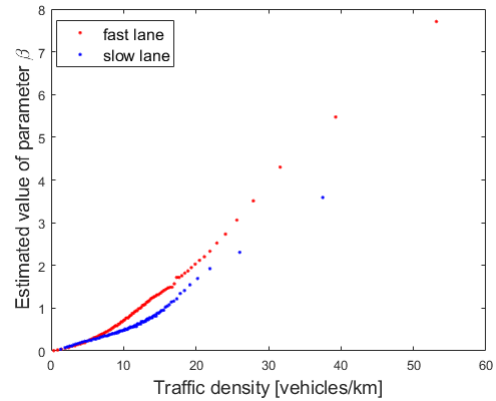


(f)

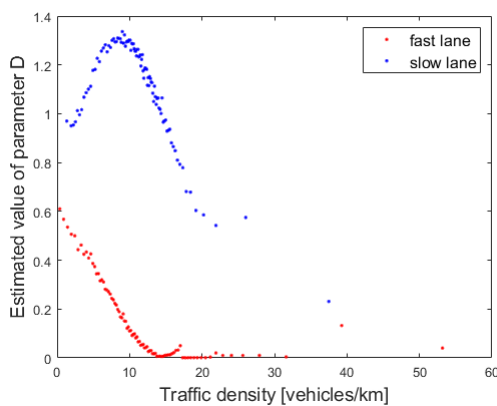
Picture 83. Inter-vehicle time headway statistics. Bars represent the probability density for real traffic data. The red curve represents the GIG distribution



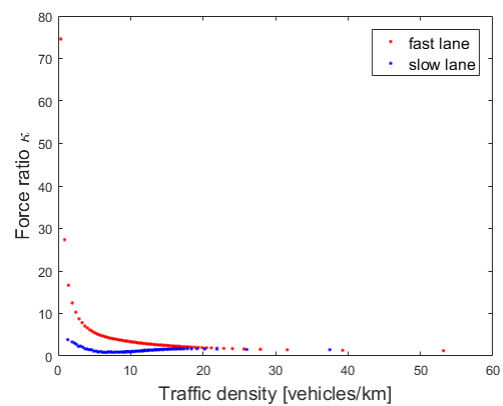
(a)



(b)



(c)

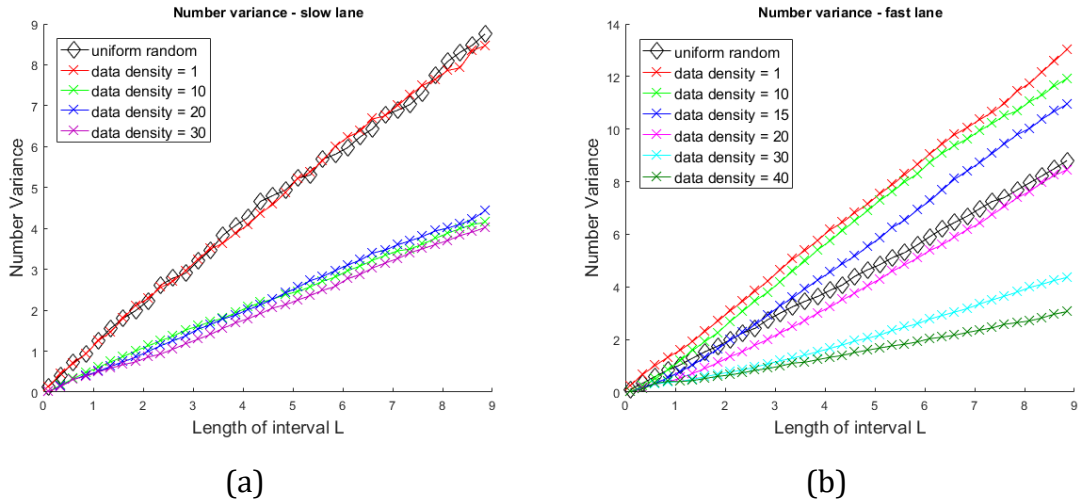


(d)

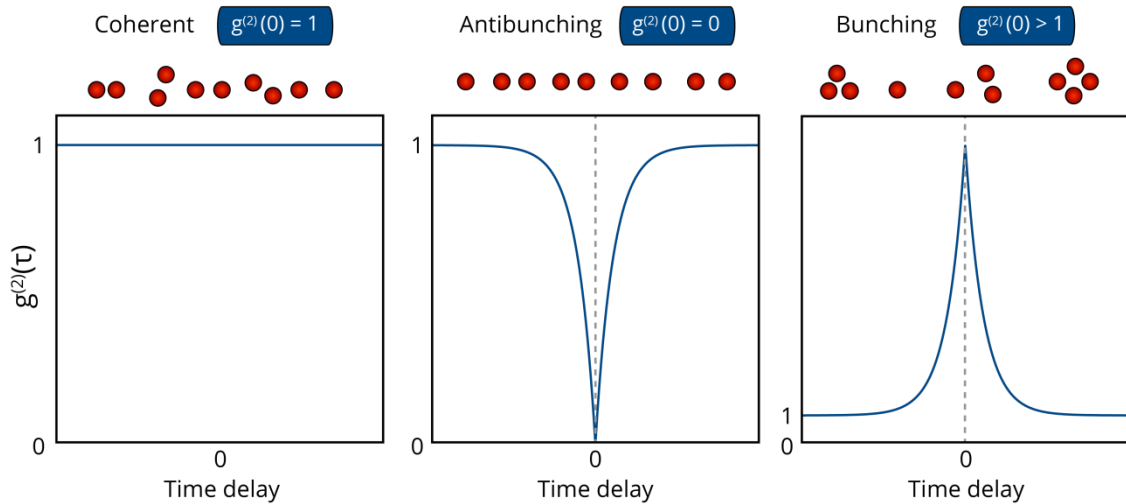
Picture 84. Evolution of fit parameters α , β and D in relation to traffic density, together with the force ratio κ .

5.3.3 Number variance of traffic flow

Finally, to assess the nature of inter-vehicle interaction, and the character of difference between the slow and the fast lane, we have used the number variance distribution (which detailed description was delivered in chapter 7.1.2.2). For this purpose, the entire fundamental diagram was sliced into 100 pieces, each piece representing a small traffic density region. Consecutively, applying the formula (4), the number variance distribution for both fast and slow lane was calculated for each of these density regions separately. Consistent with the observations made utilizing the fundamental diagram view and the GIG density estimation (for which the fast and the slow lane showed major differences) also the statistical properties of the number variance distribution differ lane to lane considerably. While the number variance distribution of the data from the slow lane - see picture 85 (a) - confirms the expectation that there is no correlation between vehicles for ultra-low densities (the red curve matches exactly the curve for independent events), and that higher traffic densities (green, blue and purple line) show increasing correlation with increasing traffic density, the number variance of the fast lane shows a completely different (and extremely unexpected) behavior. Indeed, against the expectation, the number variance distribution obtained for the fast lane - see picture 85 (b), shows for lower densities a gradient higher than 1, making this distribution super-Poissonian and not matching the distribution for independent events at all - see the red, green and blue curve in picture 85 (b). Similar super-Poissonian distributions can be found for example in photon counting experiments and statistics of light, in quantum optics [137], [138], [139], [140]. In these experiments, thermal light (for example sun light) shows intensity fluctuations as its inherent aspect and as a result, there is a statistical tendency for photons to arrive simultaneously at a detector, resulting in so called "photon bunching" (this phenomenon can be in general attributed to the wave-particle duality of photons and is in physics known as the Hanbury Brown and Twiss effect [141]). The related probability distribution of photon arrival time at the detector is super-Poissonian.



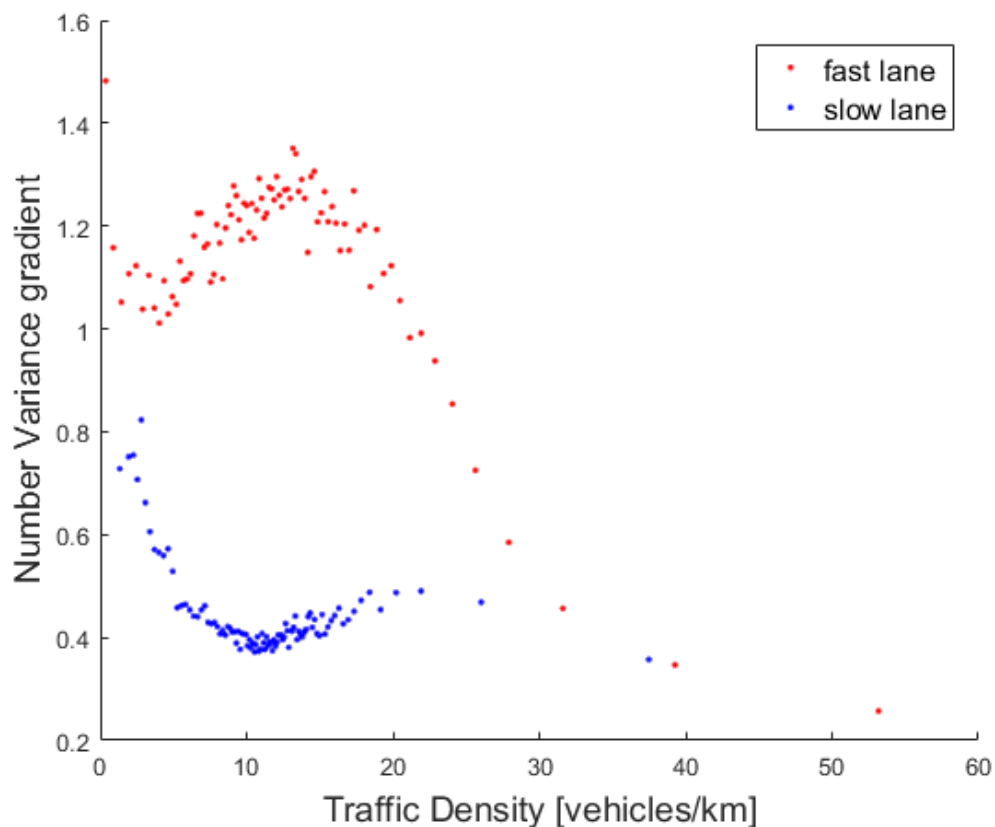
Picture 85. Number variance distribution for data from the slow lane (left) and from the fast lane (right).



Picture 86. Photon spacing for coherent light (laser), anti-bunched light and bunched (thermal) light [142]. Note the spacings for the bunching case.

For fast lane traffic data, the super-Poissonian character of the number variance distribution might be attributed to a similar effect, which we call “vehicle bunching” in order to keep the analogy with thermal light and quantum optics. However, the source of the bunching is different. It originates in the driver’s lane-changing behavior. Imagine a common traffic situation experienced on freeways. A driver in the slow lane wants to overtake a slower moving vehicle and decides to change to the fast lane. When there is a vehicle moving in the fast lane, it might need to slow down in order to avoid collision with the lane-changing vehicle from

the slow lane. When there are more vehicles moving in the fast lane, they are slowed as well, forming a bunch of vehicles moving within a close distance, not unlike bunched photons - see picture 86. Not many of such overtaking maneuvers originating in the slow lane are necessary to block the fast lane locally, which results in traffic intensity fluctuations in the fast lane. As a result, the fast lane exhibits super-Poissonian like statistics for traffic densities as far as 20 vehicles/km. Also note that the probability distribution of time headways for the fast lane for ultra-low densities shown in picture 83 is not exactly a Poisson distribution as the probability of having very small time-headways is much larger than it should be for an uncorrelated sample. This is because it captures the small time-headways between individual vehicles which form a vehicle bunch in the fast lane.



Picture 87. The gradient of Number Variance (statistical compressibility) in relation to traffic density. A gradient of 1 indicates independent events.

Interesting is also to review the evolution of the number variance gradient (also called *statistical compressibility*) with traffic density. As can be seen in picture 87, for the slow lane the gradient decreases with increasing traffic density, indicating an increase in correlation among the vehicles. This trend continues until reaching a local minimum in statistical compressibility (local correlation maximum) at densities approximately 10 vehicles/km. Note that this is exactly the density, where the estimated parameter D reaches its maximum value - see picture 84 (c). For the fast lane, the statistical compressibility starts already at values larger than 1, indicating positive correlation and “vehicle bunching”. Beginning at traffic density of about 5 vehicles/km, the vehicle bunching effect starts to increase. At the same time, the compressibility decrease in the slow lane starts to slow down, as more and more vehicles perform a lane-change, exiting the slow lane (increasing entropy) and feeding the vehicle bunching effect at the fast lane. Also, the estimated parameter β (i.e. the mental strain parameter) starts to separate at this density, showing different values for the slow lane and the fast lane (β in the fast lane increases faster, because some of the vehicles in the slow lane are doing the lane change maneuver, increasing stress level for drivers in the fast lane). This effect culminates in traffic densities approximately 15 vehicles/km. From this density onwards, fewer and fewer vehicles from the slow lane try to perform a lane-change maneuver, as the fast lane is simply too occupied to do the maneuver safely, and the willingness to start such a maneuver decreases. As a result, the number of vehicle-bunching situations decreases, intensity fluctuations dissipate, and the slow lanes β parameters run perpendicular to the fast lane β parameter, indicating that the mental stress level increases with traffic density in the same manner for both slow and fast lane. Starting at traffic densities 20 vehicles/km onwards, the statistical compressibility for the fast lane falls below 1, and the system transits from its super-Poissonian regime to the standard sub-Poissonian regime seen in the slow lane, until finally reaching a congested state for both lanes, indicated by a similar compressibility for both of the lanes – this happens at traffic density approximately 30 vehicles/km. Note, that this is exactly the density where there is a break down in mean velocity for the slow-lane - see picture 82.

Conclusion

The aim of this thesis was to deliver a complete and comprehensive overview of cellular automata and their potential in didactics of physics. The concept itself was based on the ability of cellular automata to exhibit even the most complex dynamics, while being in fact generated only by a set of very simple rules. This remarkable ability of cellular automata to describe a system just by describing these underlying simple rules was proven to be advantageous in didactics of physics, because it permits to study even the most complex systems from an educational perspective without having to rely on complex mathematical rigor. This is especially important in education of first grade and second grade students, where the education in mathematics just started and where students do not have enough mathematical understanding to be able to comprehend complex systems. However, it is these systems which exhibit a variety of very interesting dynamics, which often borders on several subject, and which, if sufficiently explained to students would promote synergy between individual school subject. It was shown, that cellular automata can deliver an easy way how to describe these systems, and make their study possible in first grade and second grade school environments, where a standard mathematical description approach would not be possible because of the related requirements for mathematical simplicity. This concept was not only shown to be applicable to already well understood systems which border on several school subjects, but also to systems that are not yet fully understood, and which are currently subject to scientific research. It establishes an interdisciplinary approach to teaching, and promotes synergy between science and education. The student is not simply expected to just memorize content through a repetitive learning ritual, which often results in development of a database-like understanding of physics through memorizing simple equations, without having deeper understanding of the highly abstract concept and relations defined by these equations. In contrary, the student is expected to put its own hands on the subject, study the underlying rules and their impact on the dynamics of the studied system. It challenges the student not only to memorize, but also to think. And a student who can think should be the contribution of our educational system to our society.

Bibliography

1	WOLFRAM, Stephen. Statistical mechanics of cellular automata. <i>Reviews of Modern Physics</i> [online]. 1983, 55 (3), 601-644 [cit. 2021-03-19]. ISSN 0034-6861. Accessible at: doi:10.1103/RevModPhys.55.601
2	DAS, Debasis. A Survey on Cellular Automata and Its Applications. <i>Global Trends in Computing and Communication Systems - 4th International Conference, ObCom 2011, Vellore, TN, India, 2011</i> . ISBN 978-3-642-29219-4
3	WOLFRAM, Stephen. <i>A new kind of science</i> . Champaign, IL: Wolfram Media, c2002. ISBN 1-57955-008-8.
4	MACRAE, Norman. <i>John von Neumann: the scientific genius who pioneered the modern computer, game theory, nuclear deterrence, and much more</i> . [Providence, RI]: American Mathematical Society, 1999. ISBN 978-0821820643.
5	VON NEUMANN, J. The general and logical theory of automata. In: L. A. Jeffress (Ed.), <i>Cerebral mechanisms in behavior; the Hixon Symposium</i> (p. 1-41). 1951, Wiley.
6	TURING, A. M. On Computable Numbers, with an Application to the Entscheidungsproblem. <i>Proceedings of the London Mathematical Society</i> [online]. 1937, s2-42 (1), 230-265 [cit. 2021-03-19]. ISSN 00246115. Accessible at: doi:10.1112/plms/s2-42.1.230
7	RUCKER, Rudy. The Origins of Cellular Automata. <i>psoup.math.wisc.edu</i> [online]. [cit. 2021-03-19]. Accessible at: http://psoup.math.wisc.edu/491/CAorigins.htm
8	VON NEUMANN, J. <i>Theory Of Self Reproducing Automata</i> . University of Illinois Press, 1966, ISBN 9780252727337.
9	John Von Neumann [photo]. In: <i>atomicheritage.org</i> [online]. [cit. 2021-03-19]. Accessible at: www.atomicheritage.org/sites/default/files/John_von_Neumann_ID_badge.png
10	Stanislaw Ulam [photo]. In: <i>atomicheritage.org</i> [online]. [cit. 2021-03-19].

	<p>Accessible at: www.atomicheritage.org/sites/default/files/John_von_Neumann_ID_badge.png</p>
11	<p>PESAVENTO, Umberto. An Implementation of von Neumann's Self-Reproducing Machine. <i>Artificial Life</i> [online]. 1995, 2(4), 337-354 [cit. 2021-03-19]. ISSN 1064-5462. Accessible at: doi:10.1162/artl.1995.2.337</p>
12	<p>HEDLUND, G. A. Endomorphisms and automorphisms of the shift dynamical system. <i>Mathematical Systems Theory</i> [online]. 1969, 3(4), 320-375 [cit. 2021-03-19]. ISSN 0025-5661. Accessible at: doi:10.1007/BF01691062</p>
13	<p>GARDENER, Martin. Mathematical Games: The fantastic combinations of John Conway's new solitaire game "life". <i>Scientific American</i>. 1970, 223, 120-123.</p>
14	<p>IGBLAN. IgbLAN - Life Universal Computer. igblan.free-online.co.uk [online]. [cit. 2021-03-19]. Accessible at: http://www.igblan.free-online.co.uk/igblan/ca/</p>
15	<p>RENDELL, Paul. A Turing Machine in Conway's Game of Life, extendable to a Universal Turing Machine. <i>rendell-attic.org</i> [online]. [cit. 2021-03-19]. Accessible at: http://rendell-attic.org/gol/tm.htm</p>
16	<p>COBAN. Programmable computer. In: <i>Forums for Conway's Game of Life</i>. <i>ConwayLife.com</i> [online]. [cit. 2021-03-19]. Accessible at: https://conwaylife.com/forums/viewtopic.php?f=2&t=2561#p37428.</p>
17	<p>Build a working game of Tetris in Conway's Game of Life. In: <i>Code Golf and coding challenges</i>. <i>codegolf.stackexchange.com</i> [online]. [cit. 2021-03-19]. Accessible at: https://codegolf.stackexchange.com/questions/11880/build-a-working-game-of-tetris-in-conways-game-of-life/142673#142673</p>
18	<p>Game of Life. <i>Creative Tinkering</i>. <i>tinkering.ee</i>. [online]. [cit. 2021-03-19]. Accessible at: http://tinkering.ee/webgl/game-of-life/.</p>
19	<p>ZUSE, Konrad. Rechnender Raum. <i>Bad Hersfeld : Elektronische Datenverarbeitung</i>. Vol. 8. 1967. Accessible at: ftp://ftp.idsia.ch/pub/juergen/zuse67scan.pdf</p>

20	ZUSE, Konrad. Calculating Space (Rechnender Raum). ZENIL, Hector. <i>A Computable Universe</i> [online]. WORLD SCIENTIFIC, 2012, 2012-12-18, s. 729-786 [cit. 2021-03-19]. ISBN 978-981-4374-29-3. Accessible at: doi:10.1142/9789814374309_0036
21	MAINZER, Klaus and Leon CHUA. <i>The Universe as Automaton</i> [online]. Berlin, Heidelberg: Springer Berlin Heidelberg, 2012 [cit. 2021-03-19]. SpringerBriefs in Complexity. ISBN 978-3-642-23476-7. Accessible at: doi:10.1007/978-3-642-23477-4
22	FREDKIN, Edward. An informational process based on reversible universal cellular automata. <i>Physica D: Nonlinear Phenomena</i> [online]. 1990, 45 (1-3), 254-270 [cit. 2021-03-19]. ISSN 01672789. Accessible at: doi:10.1016/0167-2789(90)90186-S
23	MÜLLER, Vincent C. Pancomputationalism: Theory or Metaphor? In: Ruth Hagengruber and Uwe Riss (eds.), <i>Philosophy, computing and information science</i> (History and philosophy of technoscience; London: Pickering & Chattoo), 213-21. ISBN 9781138710764.
24	CABALLERO-GIL, Pino, Amparo FÚSTER-SABATER and Oscar DELGADO-MOHATAR. Linear Cellular Automata as Discrete Models for Generating Cryptographic Sequences. <i>Journal of Research and Practice in Information Technology</i> [online]. 2008, 40 , 254-270 [cit. 2021-03-19]. arXiv:1005.0086. Accessible at: https://arxiv.org/abs/1005.0086
25	MANNING. An Approach to Highly Integrated, Computer-Maintained Cellular Arrays. <i>IEEE Transactions on Computers</i> [online]. 1977, C-26 (6), 536-552 [cit. 2021-03-21]. ISSN 0018-9340. Accessible at: doi:10.1109/TC.1977.1674879
26	NANDI, S., B. K. KAR and P. Pal CHAUDHURI. Theory and Applications of Cellular Automata. <i>IEEE Transactions on Computers</i> [online]. 1995, Vol. 26 , No. 6 [cit. 2021-03-19]. DOI: 10.1109/TC.1977.1674879. Accessible at: https://dl.acm.org/doi/10.1109/TC.1977.1674879
27	SIKDAR, Biplab K., Debesh K. DAS, Vamsi BOPPANA, Cliff YANG, Sobhan MUKHERJEE and P. Pal CHAUDHURI. Cellular automata as a built in self test structure. In: <i>Proceedings of the 2001 conference on Asia South Pacific</i>

	<i>design automation - ASP-DAC '01</i> [online]. New York, New York, USA: ACM Press, 2001, 2001, s. 319-324 [cit. 2021-03-21]. ISBN 0780366344. Accessible at: doi:10.1145/370155.370367
28	QADIR, Fasel. A Few Applications of Digital Image Processing Based on Two-Dimensional Cellular Automata. <i>INTERNATIONAL JOURNAL OF CREATIVE RESEARCH THOUGHTS</i> [online]. 2017, 5(1) [cit. 2021-03-19]. ISSN: 2320-2882. Accessible at: https://www.ijcrt.org/papers/IJCRT1133029.pdf
29	ANGHELESCU, Petre, Silviu IONITA and Emil SOFRON. Block Encryption Using Hybrid Additive Cellular Automata. In: <i>7th International Conference on Hybrid Intelligent Systems (HIS 2007)</i> [online]. IEEE, 2007, 2007, s. 132-137 [cit. 2021-03-21]. ISBN 0-7695-2946-1. Accessible at: doi:10.1109/HIS.2007.23
30	KUNDU, Anirban, Alok Ranjan PAL, Tanay SARKAR, Moutan BANERJEE, Sutirtha Kr. GUHA and Debajyoti MUKHOPADHYAY. Comparative study on Null Boundary and Periodic Boundary 3-neighborhood Multiple Attractor Cellular Automata for classification. In: <i>2008 Third International Conference on Digital Information Management</i> [online]. IEEE, 2008, 2008, s. 204-209 [cit. 2021-03-21]. ISBN 978-1-4244-2916-5. Accessible at: doi:10.1109/ICDIM.2008.4746805
31	SEREDYNSKI, Marcin and Pascal BOUVRY. Block cipher based on reversible cellular automata. <i>New Generation Computing</i> [online]. 2005, 23(3), 245-258 [cit. 2021-03-21]. ISSN 0288-3635. Accessible at: doi:10.1007/BF03037658
32	MRAZ, M., N. ZIMIC, I. LAPANJA and I. BAJEC. Fuzzy cellular automata: from theory to applications. In: <i>Proceedings 12th IEEE International Conference on Tools with Artificial Intelligence. ICTAI 2000</i> [online]. IEEE Comput. Soc, 2000, s. 320-323 [cit. 2021-03-21]. ISBN 0-7695-0909-6. Accessible at: doi:10.1109/TAI.2000.889889
33	GÖDEL, Kurt. Über formal unentscheidbare Sätze der Principia Mathematica und verwandter Systeme I. <i>Monatshefte für Mathematik und Physik</i> [online]. 1931, 38-38(1), 173-198 [cit. 2021-03-19]. ISSN 0026-

	9255. Accessible at: doi:10.1007/BF01700692
34	GU, Mile, Christian WEEDBROOK, Álvaro PERALES and Michael A. NIELSEN. More really is different. <i>Physica D: Nonlinear Phenomena</i> [online]. 2009, 238 (9-10), 835-839 [cit. 2021-03-21]. ISSN 01672789. Accessible at: doi:10.1016/j.physd.2008.12.016
35	BROWN, Robert. XXVII. A brief account of microscopical observations made in the months of June, July and August 1827, on the particles contained in the pollen of plants; and on the general existence of active molecules in organic and inorganic bodies. <i>The Philosophical Magazine</i> [online]. 2009, 4 (21), 161-173 [cit. 2021-03-21]. ISSN 1941-5850. Accessible at: doi:10.1080/14786442808674769
36	EINSTEIN, A. Über die von der molekularkinetischen Theorie der Wärme geforderte Bewegung von in ruhenden Flüssigkeiten suspendierten Teilchen. <i>Annalen der Physik</i> [online]. 1905, 322 (8), 549-560 [cit. 2021-03-21]. ISSN 00033804. Accessible at: doi:10.1002/andp.19053220806
37	SBALZARINI, I.F. and P. KOUMOUTSAKOS. Feature point tracking and trajectory analysis for video imaging in cell biology. <i>Journal of Structural Biology</i> [online]. 2005, 151 (2), 182-195 [cit. 2021-03-21]. ISSN 10478477. Accessible at: doi:10.1016/j.jsb.2005.06.002
38	AMITH, Michael J. de. <i>Statistical Analysis Handbook</i> . The Winchelsea Press, Drumlin Publications, Drumlin Security Ltd, UK, 2018. ISBN: 1912556073.
39	LORENZ, Edward N. Deterministic Nonperiodic Flow. <i>Journal of Atmospheric Sciences</i> [online]. 1963, 20 (2), 130-148 [cit. 2021-03-21]. Accessible at: 10.1175/1520-0469(1963)020<0130:DNF>2.0.CO;2
40	BOUCHER, Chris. Wolfram Demonstrations Project. <i>Using Rule 30 to Generate Pseudorandom Real Numbers</i> . [Online] November 2007. Accessible at: https://demonstrations.wolfram.com/UsingRule30ToGeneratePseudorandomRealNumbers/
41	BOUCHER, Chris. Wolfram Demonstrations Project. <i>Comparing Rule 30 Pseudorandoms to a Uniform Distribution</i> . [Online] November 2007. Accessible at:

	http://demonstrations.wolfram.com/ComparingRule30PseudorandomsToAUniformDistribution/
42	CHAKRABORTY, Trina, Manik BANIK and Pinaki PATRA. Uncertainty principle guarantees genuine source of intrinsic randomness. <i>Quantum Information Processing</i> [online]. 2014, 13 (4), 839-848 [cit. 2021-03-21]. ISSN 1570-0755. Accessible at: doi:10.1007/s11128-013-0695-5
43	KIM, Minjun, Anak Agung JULIUS and U Kei CHEANG, ed. <i>Microbiorobotics: biologically inspired microscale robotic systems</i> . Second edition. Amsterdam: Elsevier, [2017]. Micro & nano technologies series. ISBN 978-0-323-42993-1.
44	BELKAID, Marwen, Elise BOUSSEYROL, Romain DURAND-DE CUTTOLI, et al. Mice adaptively generate choice variability in a deterministic task. <i>Communications Biology</i> [online]. 2020, 3 (1) [cit. 2021-03-21]. ISSN 2399-3642. Accessible at: doi:10.1038/s42003-020-0759-x
45	BRUNEAU, John. Artfail. <i>Video Game Art stuff</i> . [Online]. Accessible at: https://artfail.com/automata/#mech
46	GeologyCafe. <i>Introduction to geology - chapter 3 minerals</i> . [Online] 2015. Accessible at: https://www.geologycafe.com/class/chapter3.html
47	Pinterest. <i>Giant halite cubes! Rock salt, Salt crystal, Crystals</i> . [Online] 2018. Accessible at: https://www.pinterest.com/pin/515591857333831412/ .
48	Interestingengineering. <i>13 Best Reddits for Education, Lifestyle, and DIY</i> . [Online]. Accessible at: https://interestingengineering.com/13-best-reddits-for-education-lifestyle-and-diy .
49	FRANK, S. A. The common patterns of nature. <i>Journal of Evolutionary Biology</i> [online]. 2009, 22 (8), 1563-1585 [cit. 2021-03-21]. ISSN 1010-061X. Accessible at: doi:10.1111/j.1420-9101.2009.01775.x
50	National Academies of Sciences, Engineering, and Medicine. <i>Quantum Computing: Progress and Prospects</i> . The National Academies Press Washington, DC. 2019. ISBN: 978-0-309-47972-1
51	SHU, Jian-Jun. A new integrated symmetrical table for genetic codes. <i>Biosystems</i> [online]. 2017, 151 , 21-26 [cit. 2021-03-21]. ISSN 03032647. Accessible at: doi:10.1016/j.biosystems.2016.11.004

52	AKHLAGHPOUR, Hessameddin. An RNA-Based Theory of Natural Universal Computation. <i>Cornell University</i> [online]. 2020. [cit. 2021-03-19]. Accessible at: https://arxiv.org/abs/2008.08814v2
53	BASSETT, Danielle S. and Michael S. GAZZANIGA. Understanding complexity in the human brain. <i>Trends in Cognitive Sciences</i> [online]. 2011, 15 (5), 200-209 [cit. 2021-03-21]. ISSN 13646613. Accessible at: doi:10.1016/j.tics.2011.03.006
54	DUNN, Greg and Brian EDWARDS. KOTTKE. <i>Marvelous and super-detailed visualizations of the complex structure of the human brain.</i> [Online] 2017. Accessible at: https://kottke.org/17/04/marvelous-and-super-detailed-visualizations-of-the-complex-structure-of-the-human-brain
55	TEMAM, Roger. <i>Navier-Stokes Equations: Theory and Numerical Analysis.</i> AMS Chelsea Publishing, 2000. ISBN 9780821827376.
56	Navier–Stokes Equation. <i>claymath.org</i> [online]. [cit. 2021-03-19]. Accessible at: http://www.claymath.org/millennium-problems/navier%E2%80%93stokes-equation
57	FEFFERMAN, Charles L. EXISTENCE AND SMOOTHNESS OF THE NAVIER–STOKES EQUATION. <i>claymath.org</i> [online]. [cit. 2021-03-19]. Accessible at: https://www.claymath.org/sites/default/files/navierstokes.pdf
58	ANDERSON, John. <i>Computational Fluid Dynamics.</i> McGraw-Hill Education, 1995. ISBN 978-0-07-001685-9.
59	HALL, Nancy. Lift of Rotating Cylinder. <i>grc.nasa.gov.</i> [online]. [cit. 2021-03-19]. Accessible at: https://www.grc.nasa.gov/www/K-12/airplane/cyl.html
60	LANDAU, L. D. and E. M. Lifshitz. <i>Fluid Mechanics.</i> London: Pergamon. 1987. ISBN 0-08-033933-6.
61	MCDONOUGH, J. M. <i>Introductory Lectures on Turbulence – Physics, Mathematics, and Modeling.</i> London: Pergamon. 2004. Accessible at: http://web.engr.uky.edu/~acfd/lctr-notes634.pdf
62	KELLAY, H. Hydrodynamics experiments with soap films and soap bubbles: A short review of recent experiments. <i>Physics of Fluids</i> [online]. 2017, 29 (11) [cit. 2021-03-19]. ISSN 1070-6631. Accessible at:

	doi:10.1063/1.4986003
63	Karman vortex streets. <i>Science and Scientific Imaging</i> . <i>karlgaff.wordpress.com</i> . [online]. [cit. 2021-03-19]. Accessible at: https://karlgaff.wordpress.com/karman-vortex-streets/
64	MATLAB - MathWorks - MATLAB & Simulink. <i>mathworks.com</i> [online]. [cit. 2021-03-19]. Accessible at: https://www.mathworks.com/products/matlab.html
65	Microsoft Excel. <i>microsoft.com</i> [online]. [cit. 2021-03-19]. Accessible at: https://www.microsoft.com/en-us/microsoft-365/excel
66	Visual Basic 6.0 Documentation. <i>microsoft.com</i> [online]. [cit. 2021-03-19]. Accessible at: https://docs.microsoft.com/en-us/previous-versions/visualstudio/visual-basic-6/visual-basic-6.0-documentation?redirectedfrom=MSDN
67	WILSON, E. O. and B. HOLLOBLER. The rise of the ants: A phylogenetic and ecological explanation. <i>Proceedings of the National Academy of Sciences</i> [online]. 2005, 102 (21), 7411-7414 [cit. 2021-03-19]. ISSN 0027-8424. Accessible at: doi:10.1073/pnas.0502264102
68	CRESPI, Bernard J. and Douglas YANEGA. The definition of eusociality. <i>Behavioral Ecology</i> [online]. 1995, 6 (1), 109-115 [cit. 2021-03-19]. ISSN 1045-2249. Accessible at: doi:10.1093/beheco/6.1.109
69	WHEELER, William Morton. <i>Ants: Their Structure, Development And Behavior</i> . Columbia university press, 1910. ISBN 978-0-231-00121-2
70	Fantastic Ants - Did You Know? <i>National Geographic Magazine</i> [Online]. [cit. 2021-03-19]. Accessible at: https://web.archive.org/web/20080730071158/http://ngm.nationalgeographic.com/2007/08/ants/did-you-know-learn
71	How many ants are there for every one person on earth? <i>topics.info.com</i> [Online]. [cit. 2021-03-19]. Accessible at: https://web.archive.org/web/20130813234547/http://topics.info.com/How-many-ants-are-there-for-every-one-person-on-earth_452
72	WILSON, B. H. and Edward O. <i>The Ants</i> . Harward University Press, 1990. ISBN 9780674040755.

73	JACKSON, Duncan E. and Francis L.W. RATNIEKS. Communication in ants. <i>Current Biology</i> [online]. 2006, 16 (15), R570-R574 [cit. 2021-03-19]. ISSN 09609822. Accessible at: doi:10.1016/j.cub.2006.07.015
74	RAJABI-BAHAABADI, Mojtaba, Afshin SHARIAT-MOHAYMANY, Mohsen BABAEI and Chang Wook AHN. Multi-objective path finding in stochastic time-dependent road networks using non-dominated sorting genetic algorithm. <i>Expert Systems with Applications</i> [online]. 2015, 42 (12), 5056-5064 [cit. 2021-03-19]. ISSN 09574174. Accessible at: doi:10.1016/j.eswa.2015.02.046
75	SHARKEY, Amanda J. C. Robots, insects and swarm intelligence. <i>Artificial Intelligence Review</i> [online]. 2006, 26 (4), 255-268 [cit. 2021-03-19]. ISSN 0269-2821. Accessible at: doi:10.1007/s10462-007-9057-y
76	BOUFFANAIS, Roland. <i>Design and Control of Swarm Dynamics</i> [online]. Singapore: Springer Singapore, 2016 [cit. 2021-03-19]. SpringerBriefs in Complexity. ISBN 978-981-287-750-5. Accessible at: doi:10.1007/978-981-287-751-2
77	RAMASWAMY, Sriram. The Mechanics and Statistics of Active Matter. <i>Annual Review of Condensed Matter Physics</i> [online]. 2010, 1 (1), 323-345 [cit. 2021-03-19]. ISSN 1947-5454. Accessible at: doi:10.1146/annurev-conmatphys-070909-104101
78	MARCHETTI, M. C., J. F. JOANNY, S. RAMASWAMY, T. B. LIVERPOOL, J. PROST, Madan RAO and R. Aditi SIMHA. Hydrodynamics of soft active matter. <i>Reviews of Modern Physics</i> [online]. 2013, 85 (3), 1143-1189 [cit. 2021-03-19]. ISSN 0034-6861. Accessible at: doi:10.1103/RevModPhys.85.1143
79	HAUPT, Michael. Why Facebook/Cambridge Analytica's Data Scandal is Awesome News for Humanity. <i>bitcoininsider.org</i> [Online]. [cit. 2021-03-19]. Accessible at: https://www.bitcoininsider.org/article/21622/why-facebookcambridge-analyticas-data-scandal-awesome-news-humanity
80	PAPAGEORGIU, Markos. Some remarks on macroscopic traffic flow modelling. <i>Transportation Research Part A: Policy and Practice</i> , Elsevier. 1998. vol. 32 (5), 323-329.

81	DAGANZO, C. F. <i>Fundamentals of transportation and traffic operations</i> . Elsevier Science Ltd. 1997
82	LIGHTHILL, M. J. and Whitham, G. B. On Kinematic Waves. II. A Theory of Traffic. <i>Proceedings of the Royal Society of London</i> . 1955, Series A, vol. 299. pp. 317-345.
83	BUCHHOLTZ, VOLKHARD and THORSTEN PÖSCHEL. A VECTORIZED ALGORITHM FOR MOLECULAR DYNAMICS OF SHORT RANGE INTERACTING PARTICLES. <i>International Journal of Modern Physics C</i> [online]. 2011, 04 (05), 1049-1057 [cit. 2021-03-19]. ISSN 0129-1831. Accessible at: doi:10.1142/S0129183193000811
84	CHEN, Shiyi, Hudong CHEN, Daniel MARTNEZ and William MATTHAEUS. Lattice Boltzmann model for simulation of magnetohydrodynamics. <i>Physical Review Letters</i> [online]. 1991, 67 (27), 3776-3779 [cit. 2021-03-19]. ISSN 0031-9007. Accessible at: doi:10.1103/PhysRevLett.67.3776
85	NAGEL, Kai and Michael SCHRECKENBERG. A cellular automaton model for freeway traffic. <i>Journal de Physique I</i> [online]. 1992, 2 (12), 2221-2229 [cit. 2021-03-19]. ISSN 1155-4304. Accessible at: doi:10.1051/jp1:1992277
86	YANG, Qi. and D. Morgan. Hybrid Traffic Simulation Model. <i>Transportation Research Board 85th Annual Meeting</i> . Washington DC, United States. 2006.
87	BURGHOUT, Wilco, Haris N. KOUTSOPOULOS and Ingmar ANDRÉASSON. Hybrid Mesoscopic–Microscopic Traffic Simulation. <i>Transportation Research Record: Journal of the Transportation Research Board</i> [online]. 2005, 1934 (1), 218-225 [cit. 2021-03-19]. ISSN 0361-1981. Accessible at: doi:10.1177/0361198105193400123
88	POSCHINGER, A., KATES, R., and MEIER, J., The flow of data in coupled microscopic and macroscopic traffic simulation models. In: <i>World Congress on Intelligent Transportation Systems</i> , Torino, 2000.
89	EISENBLÄTTER, B., L. SANTEN, A. SCHADSCHNEIDER and M. SCHRECKENBERG. Jamming transition in a cellular automaton model for traffic flow. <i>Physical Review E</i> [online]. 1998, 57 (2), 1309-1314 [cit. 2021-03-19]. ISSN 1063-651X. Accessible at: doi:10.1103/PhysRevE.57.1309
90	SPINRAD, Bernard I. britannica.com. <i>Nuclear reactor</i> . [Online] 2019.

	Accessible at: https://www.britannica.com/technology/nuclear-reactor/Fissile-and-fertile-materials
91	Lightning Physics. [Online] 2014. Accessible at: http://ffden-2.phys.uaf.edu/212_fall2003.web.dir/kristina_smith/description.html
92	MARCEL, C., F. BONETTO and A. CLAUSSE. Simulation of boiling heat transfer in small heaters by a coupled cellular and geometrical automata. <i>Heat and Mass Transfer</i> [online]. 2011, 47 (1), 13-25 [cit. 2021-03-21]. ISSN 0947-7411. Dostupné z: doi:10.1007/s00231-010-0667-6
93	RUTTLEY, Tara. A Lab Aloft (International Space Station Research). <i>Boiling it down to the bubbles: It is about heat transfer</i> . [Online] 2011. Accessible at: https://blogs.nasa.gov/ISS_Science_Blog/2011/04/15/post_1301433765536/
94	HOW, Martin J. and Johannes M. ZANKER. Motion camouflage induced by zebra stripes. <i>Zoology</i> [online]. 2014, 117 (3), 163-170 [cit. 2021-03-21]. ISSN 09442006. Accessible at: doi:10.1016/j.zool.2013.10.004
95	STANKOWICH, Theodore, Tim CARO and Matthew COX. BOLD COLORATION AND THE EVOLUTION OF APOSEMATISM IN TERRESTRIAL CARNIVORES. <i>Evolution</i> [online]. 2011, 65 (11), 3090-3099 [cit. 2021-03-21]. ISSN 00143820. Accessible at: doi:10.1111/j.1558-5646.2011.01334.x
96	Pinterest. <i>Human and Animal Skin Leather Textures for Photoshop</i> . [Online] 2017. Accessible at: https://www.pinterest.com/pin/439804719852350356/
97	Tatasz. <i>Compound Cellular Automata</i> . [Online] 2019. Accessible at: https://tatasz.github.io/compound_ca2/
98	WITTEN, T. A. and L. M. SANDER. Diffusion-Limited Aggregation, a Kinetic Critical Phenomenon. <i>Physical Review Letters</i> [online]. 1981, 47 (19), 1400-1403 [cit. 2021-03-21]. ISSN 0031-9007. Accessible at: doi:10.1103/PhysRevLett.47.1400
99	MARTINEAU, Sébastien. Directed Diffusion-Limited Aggregation. <i>Latin American Journal of Probability and Mathematical Statistics</i> [online]. 2017,

	14(1) [cit. 2021-03-21]. ISSN 1980-0436. Accessible at: doi:10.30757/ALEA.v14-15
100	JLC Online. <i>Lichtenberg Figure Burning</i> . [Online]. Accessible at: https://www.jlconline.com/products-tools/hand-tools/real-deal-review-conestoga-works-lichtenberg-figure-wood-burner_o .
101	WÖHLKE, Thomas. <i>Diffusion-limited aggregation..</i> [Online] 2016. Accessible at: https://thomas-woehlke.blogspot.com/2016/01/diffusion-limited-aggregation.html
102	Criticalthinking. <i>criticalthinking.org</i> . [Online]. [cit. 2021-03-19]. Accessible at: http://www.criticalthinking.org/data/pages/29/159e33cd3add1bb75c1f848a06a80d37519cf2e476776.pdf
103	HELBING, Dirk. Traffic and related self-driven many-particle systems. <i>Reviews of Modern Physics</i> [online]. 2001, 73(4), 1067-1141 [cit. 2021-03-19]. ISSN 0034-6861. Accessible at: doi:10.1103/RevModPhys.73.1067
104	KRBÁLEK, Milan. Equilibrium distributions in a thermodynamical traffic gas. <i>Journal of Physics A: Mathematical and Theoretical</i> , Volume 40, Number 22, Pages 5813–5821, 2007.
105	KRBÁLEK, Milan. Quantitative analysis of interaction range in vehicular flows. <i>Transportation Research Procedia</i> , Volume 25, Pages 1268–1275, 2017.
106	METROPOLIS, Nicholas, Arianna W. ROSENBLUTH, Marshall N. ROSENBLUTH, Augusta H. TELLER and Edward TELLER. Equation of State Calculations by Fast Computing Machines. <i>The Journal of Chemical Physics</i> [online]. 1953, 21(6), 1087-1092 [cit. 2021-03-19]. ISSN 0021-9606. Accessible at: doi:10.1063/1.1699114
107	KRBÁLEK, Milan. Inter-vehicle gap statistics on signal-controlled crossroads. <i>Journal of Physics A: Mathematical and Theoretical</i> [online]. 2008, 41(20) [cit. 2021-03-19]. ISSN 1751-8113. Accessible at: doi:10.1088/1751-8113/41/20/205004
108	KRBÁLEK, Milan. Discrete thermodynamical modelling of traffic streams. <i>12th World Conference on Trade Research Society</i> , July 11–15, Lisbon –

	Portugal, 2010.
109	WEISSTEIN, E. W. Correlation coefficient. <i>mathworld.wolfram.com</i> [Online]. [cit. 2021-03-19]. Accessible at: https://mathworld.wolfram.com/CorrelationCoefficient.html
110	SZÉKELY, Gábor J., Maria L. RIZZO and Nail K. BAKIROV. Measuring and testing dependence by correlation of distances. <i>The Annals of Statistics</i> [online]. 2007, 35 (6), 2769-2794 [cit. 2021-03-19]. ISSN 0090-5364. Accessible at: doi:10.1214/009053607000000505
111	ZENG, Guoping. A Unified Definition of Mutual Information with Applications in Machine Learning. <i>Mathematical Problems in Engineering</i> [online]. 2015, 2015 , 1-12 [cit. 2021-03-19]. ISSN 1024-123X. Accessible at: doi:10.1155/2015/201874
112	FUKUMIZU, K., A. Gretton, X. Sun, B. Schölkopf. Kernel Measures of Conditional Dependence. <i>21st Annual Conference on Neural Information Processing Systems</i> , September 2007, Pages 489–496.
113	AGARWAL, R., P. Sacre, S. V. Sarma. Mutual Dependence: A Novel Method for Computing Dependencies Between Random Variables. <i>Cornel University Library</i> , Volume 2015, 2015.
114	GUHR, Thomas, Axel MÜLLER-GROELING and Hans A. WEIDENMÜLLER. Random-matrix theories in quantum physics: common concepts. <i>Physics Reports</i> [online]. 1998, 299 (4-6), 189-425 [cit. 2021-03-19]. ISSN 03701573. Accessible at: doi:10.1016/S0370-1573(97)00088-4
115	HELBING, Dirk. From microscopic to macroscopic traffic models. PARISI, Jürgen, Stefan C. MÜLLER and Walter ZIMMERMANN, ed. <i>A Perspective Look at Nonlinear Media</i> [online]. Springer Berlin Heidelberg, 1998, s. 122-139 [cit. 2021-03-19]. Lecture Notes in Physics. ISBN 978-3-540-63995-4. Accessible at: doi:10.1007/BFb0104959
116	LI, Xiaopeng and Yanfeng OUYANG. Characterization of traffic oscillation propagation under nonlinear car-following laws. <i>Transportation Research Part B: Methodological</i> [online]. 2011, 45 (9), 1346-1361 [cit. 2021-03-19]. ISSN 01912615. Accessible at: doi:10.1016/j.trb.2011.05.010
117	KRBÁLEK, Milan and Petr ŠEBA. Spectral rigidity of vehicular streams

	(random matrix theory approach). <i>Journal of Physics A: Mathematical and Theoretical</i> [online]. 2009, 42 (34) [cit. 2021-03-19]. ISSN 1751-8113. Accessible at: doi:10.1088/1751-8113/42/34/345001
118	SCHARF, R and F M IZRAILEV. Dyson's Coulomb gas on a circle and intermediate eigenvalue statistics. <i>Journal of Physics A: Mathematical and General</i> [online]. 1990, 23 (6), 963-977 [cit. 2021-03-19]. ISSN 0305-4470. Accessible at: doi:10.1088/0305-4470/23/6/018
119	LECLERCQ, Ludovic, Victor L. KNOOP, Florian MARCZAK and Serge P. HOOGENDOORN. Capacity drops at merges: New analytical investigations. <i>Transportation Research Part C: Emerging Technologies</i> [online]. 2016, 62 , 171-181 [cit. 2021-03-19]. ISSN 0968090X. Accessible at: doi:10.1016/j.trc.2015.06.025
120	KRBALEK, Milan and Dirk HELBING. Determination of interaction potentials in freeway traffic from steady-state statistics. <i>Physica A: Statistical Mechanics and its Applications</i> [online]. 2004, 333 , 370-378 [cit. 2021-03-19]. ISSN 03784371. Accessible at: doi:10.1016/j.physa.2003.10.059
121	KRBALEK, Milan, Apeltauer, J., Apeltauer, T., Szabová, Z., 2018. Three methods for estimating a range of vehicular interactions, <i>Physica A</i> 491, 112-126.
122	DAGANZO, Carlos F. The cell transmission model, part II: Network traffic. <i>Transportation Research Part B: Methodological</i> [online]. 1995, 29 (2), 79-93 [cit. 2021-03-19]. ISSN 01912615. Accessible at: doi:10.1016/0191-2615(94)00022-R
123	ZHENG, P. Microscopic Simulation Model of Merging Operation at Motorway On-Ramps, <i>PhD thesis</i> , University of Southampton, UK, 2002
124	HIDAS, P. Modelling vehicle interactions in microscopic simulation of merging and weaving. <i>Transportation Research Part C: Emerging Technologies</i> [online]. 2005, 13 (1), 37-62 [cit. 2021-03-19]. ISSN: 0968-090X. Accessible at: https://www.worldcat.org/title/transportation-research-an-international-journal-part-c-emerging-technologies/oclc/642927975

125	WANG, Jiao, Ronghui LIU and Frank MONTGOMERY. A Simulation Model for Motorway Merging Behaviour. <i>Transportation and Traffic Theory</i> [online]. Elsevier, 2005, 2005, s. 281-301 [cit. 2021-03-19]. ISBN 9780080446806. Accessible at: doi:10.1016/B978-008044680-6/50017-9
126	KRBÁLEK, Milan. Analytical derivation of time spectral rigidity for thermodynamic traffic gas. <i>Kybernetika</i> [online]. 2010, 46 (6), 1108. [cit. 2021-03-19]. Accessible at: https://www.researchgate.net/publication/228847790_Analytical_derivation_of_time_spectral_rigidity_for_thermodynamic_traffic_gas
127	KRBÁLEK, Milan. Theoretical predictions for vehicular headways and their clusters. <i>Journal of Physics A: Mathematical and Theoretical</i> [online]. 2013, 46 (44) [cit. 2021-03-19]. ISSN 1751-8113. Accessible at: doi:10.1088/1751-8113/46/44/445101
128	KRBÁLEK, Milan and Tomáš HOBZA. Inner structure of vehicular ensembles and random matrix theory. <i>Physics Letters A</i> [online]. 2016, 380 (21), 1839-1847 [cit. 2021-03-19]. ISSN 03759601. Accessible at: doi:10.1016/j.physleta.2016.03.037
129	MEHTA, M. L. <i>Random matrices (Third Edition)</i> . New York: Academic Press, 2004. ISBN: 1483299899.
130	SARKAR, Camellia and Sarika JALAN. Social patterns revealed through random matrix theory. <i>EPL (Europhysics Letters)</i> [online]. 2014, 108 (4) [cit. 2021-03-19]. ISSN 0295-5075. Accessible at: doi:10.1209/0295-5075/108/48003
131	PLEROU, Vasiliki, Parameswaran GOPIKRISHNAN, Bernd ROSENOW, Luís A. Nunes AMARAL, Thomas GUHR and H. Eugene STANLEY. Random matrix approach to cross correlations in financial data. <i>Physical Review E</i> [online]. 2002, 65 (6) [cit. 2021-03-19]. ISSN 1063-651X. Accessible at: doi:10.1103/PhysRevE.65.066126
132	KERNER, B. S. <i>The Physics of Traffic</i> . New York: Springer-Verlag, 2004. ISBN 978-3-540-40986-1.
133	JOHNSON, N. L., Kotz, S., Balakrishnan, N. <i>Continuous Univariate Distributions, Vol. 1</i> . John Wiley & Sons, 1994. ISBN: 978-0471584957

134	JÜRGENSEN, B. <i>Statistical Properties of the Generalized Inverse Gaussian Distribution, Lecture Notes in Statistics</i> . Heidelberg: Springer, 1982. ISBN 978-1-4612-5698-4.
135	TREIBER, M. and D. HELBING. Hamilton-like statistics in onedimensional driven dissipative many-particle systems. <i>The European Physical Journal B</i> [online]. 2009, 68 (4), 607-618 [cit. 2021-03-19]. ISSN 1434-6028. Accessible at: doi:10.1140/epjb/e2009-00121-8
136	MOCHOLÍ BELENGUER, Ferran, Antonio MOCHOLÍ SALCEDO, Antonio GUILL IBAÑEZ, Victor MILIÁN SÁNCHEZ and Yachin IVRY. Advantages offered by the double magnetic loops versus the conventional single ones. <i>PLOS ONE</i> [online]. 2019, 14 (2) [cit. 2021-03-19]. ISSN 1932-6203. Accessible at: doi:10.1371/journal.pone.0211626
137	TEICH, Malvin C. and Bahaa E.A. SALEH. <i>Photon Bunching and Antibunching</i> [online]. Elsevier, 1988, 1988, s. 1-104 [cit. 2021-03-19]. Progress in Optics. ISBN 9780444870964. Accessible at: doi:10.1016/S0079-6638(08)70174-4
138	MORGAN, B. L. and L. MANDEL. Measurement of Photon Bunching in a Thermal Light Beam. <i>Physical Review Letters</i> [online]. 1966, 16 (22), 1012-1015 [cit. 2021-03-19]. ISSN 0031-9007. Accessible at: doi:10.1103/PhysRevLett.16.1012
139	NAKAYAMA, Kazuyuki, Yutaka YOSHIKAWA, Hisatoshi MATSUMOTO, Yoshio TORII and Takahiro KUGA. Precise intensity correlation measurement for atomic resonance fluorescence from optical molasses. <i>Optics Express</i> [online]. 2010, 18 (7) [cit. 2021-03-19]. ISSN 1094-4087. Accessible at: doi:10.1364/OE.18.006604
140	PARK, Jiho, Taek JEONG and Han Seb MOON. Temporal intensity correlation of bunched light from a warm atomic vapor with a ladder-type two-photon transition. <i>Scientific Reports</i> [online]. 2018, 8 (1) [cit. 2021-03-19]. ISSN 2045-2322. Accessible at: doi:10.1038/s41598-018-29340-7
141	HANBURY BROWN, R., TWISS, R. Q., Interferometry of the intensity fluctuations in light. I. Basic theory: the correlation between photons in coherent beams of radiation. <i>Proceedings of the Royal Society A</i> . 1957, 242

	(1230), pp. 300–324. [cit. 2021-03-19]. Accessible at: http://123.physics.ucdavis.edu/week_6_files/hanbury_brown_et_twiss.pdf
142	Measuring time dynamics with time-resolved cathodoluminescence. <i>DELMIC</i> [Online]. [cit. 2021-03-19]. Accessible at: https://blog.delmic.com/time-resolved-cathodoluminescence .